Active Fault Tolerant Control of an Electro-Hydraulic Driven Elevator Based on Robust Adaptive Observers

by

ZHAO ZHONGYU

A Thesis
in the
Department of
Mechanical and Industrial Engineering

Presented in partial fulfillment of the requirements
for the degree of Doctor of Philosophy at
Concordia University
Montreal, Quebec, Canada

September 2010

Your file Votre référence
ISBN: 978-0-494-71152-1
Our file Notre référence
ISBN: 978-0-494-71152-1

ABSTRACT

Active Fault Tolerant Control of an Electro-Hydraulic Driven Elevator Based on Robust Adaptive Observers

Zhao Zhongyu, Ph.D.

Concordia University, 2010

Faults are minor malfunctions that deteriorate the performance of a system. In a safety critical situation such as the control of an airplane, compounding faults may cascade into a catastrophic event if not properly compensated. Active Fault Tolerant Control (AFTC) addresses the fault accommodation problem – the reliability and robustness of the system in faults – beyond the conventional stability and performance requirements for a normally operating plant.

This thesis studies the AFTC of an electro-hydraulic driven elevator, which serves as a primary control surface of an airplane. The proposed AFTC system consists of three components:

A Fault Detection and Estimation (FDE) component is designed based on two robust adaptive observers. (1). Adaptive Unknown Input Observer: a disturbance decoupled observer utilizing the geometry property and measurement redundancy of the system; (2). $H_\infty/H\_$ adaptive observer: an optimization based observer to maximize the system's response to faults and minimize that to disturbances. The $H_\infty/H\_$ adaptive observer is constructed with the technique of Unitary System, which is defined as a linear system whose singular values of transfer matrix are equal.

A fuzzy Proportional-Integral (PI) controller is designed based on the fuzzy Tagaki-Sugeno (TS) model of a nonlinear system, which consists of different linear models at different operating points.

The reconfiguration is carried out based on the fault information available from FDE. To reduce the time needed for the online computation, multiple controllers are designed offline for different faults scenarios. A new controller is constructed online as a fuzzy combination of these controllers to meet the post-fault stability and performance requirements.

Simulation results show that, with the proposed AFTC, occurring faults are detected promptly and estimated accurately with the FDE component. The performance of the post-fault elevator is quickly restored after the reconfiguration.

ACKNOWLEDGEMENT

I would like to express my sincere thanks to my supervisors, Dr. Wenfang Xie and Dr. Henry Hong, for their guidance, supervision, and support throughout my studies. Their help, suggestions and encouragement are invaluable to the completion of this thesis.

I would like to thank Dr. Chen Xiang from University of Windsor for being the external examiner.

I also thank other members of my PhD committee, Dr. John Xiupu Zhang, Dr. Zhang Youmin, and Dr. Brandon Gordon, for their suggestions and help in the past few years.

I would like to dedicate this thesis to my father, my mother and my little sister: thank you, with all my heart, for your support and love.

Table of Content

LIST OF FIGURES

LIST OF TABLES

NOMENCLATURE

A	System matrix in a state space representation of linear system
B	Input matrix for control signals
E	Input matrix for disturbance signals
F	Input matrix for faults
x	State vector of a system
$\hat{x}$	The estimation of x
$\tilde{x}$	Estimation error of x
θ	Unknown fault parameters
$\hat{\theta}$	Estimation of θ
$\tilde{\theta}$	Estimation error of θ
d	Vector of disturbances
f	Vector of faults
ϕ	Known input signal matrix for fault parameters
H_∞	H_∞ norm of a system

H_-	H_- index of a system
k_v	Gain of the Electro-Hydraulic Servo Valve
K_{ps}	Joint stiffness of the elevator
K_s	Spring Stiffness of a subsystem of the elevator
H_m	Hinge stiffness of the elevator
C_{12}	Internal leaking coefficient of the hydraulic cylinder
C_1	Leaking to environment from the active chamber of cylinder
C_2	Leaking to environment from the passive chamber of cylinder
$\|\bullet\|$	Norm of $\bullet$
n_r	Number of rules in the fuzzy TS model of fault-free elevator
n_θ	Number of rules in the fuzzy TS model of the elevator with faults
$G(s)$	A transfer matrix
$G^T(s)$	Transpose of $G(s)$
$G^\sim(s)$	Conjugate transpose of $G(s)$: $G^\sim(s) = G^T(\bar{s})$

ABBREVIATIONS

AFTC	Active Fault Tolerant Control
AUIO	Approximate Unknown Input Observer
AUIO	Adaptive Unknown Input Observer
EA	Eigenstructure Assignment
EHSV	Electro-Hydraulic Servo Valve
FDE	Fault Detection and Estimation
FDI	Fault Detection and Isolation
FTC	Fault Tolerant Control
ILMI	Iterative Linear Matrix Inequality
LMI	Linear Matrix Inequality
LPV	Linear Parameter-Varying
LTI	Linear Time-Invariant
LTV	Linear Time-Varying
MIMO	Multiple-Input Multiple-Output

PFTC	Passive Fault Tolerant Control
PI	Proportional-Integral
SISO	Single-Input Single-Output
SVD	Singular Value Decomposition
TS	Tagaki-Sugeno
UIO	Unknown Input Observer

CHAPTER 1

INTRODUCTION

1.1 Motivations and Objectives

Faults, according to [1], are "deviation of at least one characteristic property or parameter of the system from the acceptable/usual/standard condition." Unlike a failure, which suggests a "permanent interruption" of a system, an occurring fault usually appears as unexpected but tolerable performance deterioration. If not properly compensated, however, faults will eventually develop into failures. In a safety critical situation, compounding faults may even cascade into a catastrophic event as shown in the following accident, which is adopted from the aircraft accident report [2] of National Transportation Safety Board (NTSB) USA.

"On January 8, 2003, about 08:47:28 eastern standard time, Air Midwest (doing business as US Airways Express) flight 5481, a Raytheon (Beechcraft) 1900D, N233YV, crashed shortly after takeoff from runway 18R at Charlotte-Douglas International Airport, Charlotte, North Carolina. The 2 flight crewmembers and 19 passengers aboard the airplane were killed, 1 person on the ground received minor injuries, and the airplane was destroyed by impact forces and a postcrash fire."

After an investigation of one year, NTSB determined that "the probable cause of this accident was the airplane's loss of pitch control during takeoff." The main reason of the control loss was accounted as "the incorrect rigging of the elevator control system"

after a maintenance, which resulted in a discrepancy between the position of control column and the real position of the elevator. The controlled movement of the elevator was then limited to the range of -7° to 14°, which was -15° to 22° before the maintenance. The fatal accident, however, could be avoided if not for the second reason: the overload of the airplane and the miscalculation of center of gravity, which led the airplane to an angle of attack that was unrecoverable with the limited elevator.

Although routines of maintenance and overhaul can reduce the chance of faults occurring, the risk of faults cannot be eliminated completely due to, partially, the existence of human errors. The accident above, for example, was the result of a series of such errors that started when some important steps in the maintenance were skipped. Since faults are inevitable, constructing a system that functions properly even in the case of faults is therefore of the same importance as preventing faults.

Fault Tolerant Control (FTC) addresses the fault accommodation problem – the reliability and robustness of the systems in faults - beyond the conventional stability and performance requirements for a normally operating plant. Depending on how faults are handled, FTC can be classified into two categories [3]: Passive FTC (PFTC) and Active FTC (AFTC).

In PFTC, faults are treated as structured model uncertainties or disturbances. Robust controllers are designed such that the stability and performance of the closed-loop system can be maintained even when faults occur. The fault information is neither known nor estimated when the system is in operation, which results in some disadvantages of PFTC such as limited fault types, less satisfactory performances, and more conservative

controllers. Moreover, when operating without proper knowledge of the occurring faults, the system might be further damaged.

AFTC, on the other hand, reselects or reconfigures the applied controller based on the fault information, which is estimated online with the Fault Detection and Isolation (FDI) component. In the reselection case, multiple controllers are designed offline - one for the normal fault-free circumstance and others for different fault situations. In the case of a fault occurring, the controller for the particular fault, which is identified based on the result of FDI, is switched on to replace the fault-free controller. Since all controllers are designed offline, this approach responds faster to the faults and uses less fault information compared to the reconfiguration method. One disadvantage is that the accommodated faults are limited to the pre-defined ones.

In the reconfiguration approach, a single controller is designed and applied to the fault-free system. Occurring faults are evaluated through the FDI process. The model of the post-fault system is rebuilt based on the fault information. The controller is then reconfigured or redesigned online based on the post-fault model.

AFTC requires more information compared to PFTC as it involves the process of FDI. This complexity is necessary in situations where the safety is of the first priority. In the aforementioned accident, for example, the airplane had nine safe flights with the faulty elevator after the maintenance. The discrepancy between the control column and the elevator was recorded by the Flight Data Recorder (FDR) in all of the nine flights. Due to the lack of proper FDI process, however, the fault never appeared to the flight crew.

This thesis studies the Active Fault Tolerant Control of an electro-hydraulic driven elevator. As a primary control surface, the elevator is attached to the tail (usually the horizontal stabilizer) of an airplane. The position (angle) variation of the elevator changes the aerodynamic torque acting on the airplane, which consequently alters the pose (angle of attack) and the elevation of the airplane. The proper functioning of the elevator is critical to the safety of the airplane as it is the control surface that provides the most elevation capability.

The objective of the research is to develop an AFTC system with the following features:

1. The prompt detection and accurate estimation of faults: Faults in this thesis are modeled as unexpected abrupt changes of parameters from their nominal values. An occurring fault needs to be detected promptly and estimated accurately when the system is subject to disturbances and other existing faults.

2. The stability and performance of the fault-free system: A controller needs to be designed to meet the performance requirement for the fault-free closed-loop system;

3. The stability and performance of the post-fault system: A reconfiguration mechanism needs to be designed; if the performance requirement cannot be satisfied due to the loss of capability of the post-fault system, the requirement can be relaxed to prioritize the stability. In either case, the foremost priority is to reduce the possibility of further damage to the system.

1.2 Content of the Research

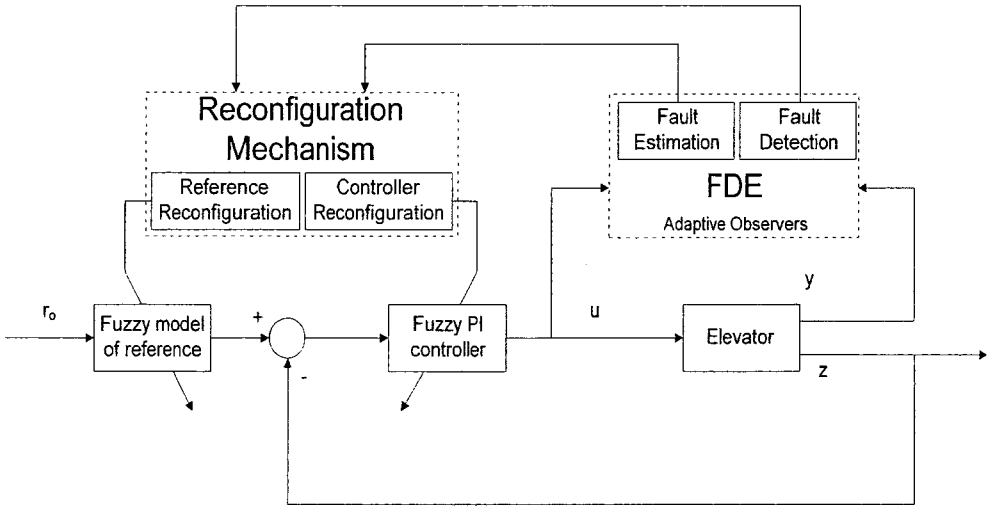

Figure 1.1 Structure of the AFTC system

In this thesis, an active fault tolerant control system is constructed as shown in Figure 1.1, where in the figure, r_o is the reference signal for the elevator to follow, u is the control signal, y is the measurement for the purpose of fault diagnosis, and z is the controlled output that tracks r_o. The AFTC system has the following features:

1. Fault Detection and Estimation (FDE) based on robust adaptive observers: Adaptive observers are constructed for the purpose of faults evaluation. The deviation from zeros of the output estimation errors – the residuals – is taken as the indicator of faults; the magnitudes of the occurring faults are then estimated with the parameter estimation component of the adaptive observer. To enhance the robustness to disturbance and more importantly to reduce the interacting among

different faults, two types of robust adaptive observer, Adaptive Unknown Input Observer and $H_\infty/H\_$ adaptive observer, are designed;

2. Fuzzy PI controller and Reconfiguration: A fuzzy Proportional-Integral (PI) controller is designed based on the fuzzy Tagaki-Sugeno (TS) model of the fault-free elevator so that the stability and performance of the fault-free system can be guaranteed. Multiple controllers are designed offline for different faults scenarios. A fuzzy model of the reference signal is also developed so that the faulty elevator will not be forced to follow a reference signal that exceeds its capability. With the fault information available from FDE, the reconfiguration is carried out so that the post-fault controller and the reference signal are constructed with the fuzzy inference technique.

The main contributions of the thesis are summarized as follows:

1. Adaptive Unknown Input Observer is constructed so that, if certain measurement redundancy requirement is satisfied, the estimation of fault is not affected by the disturbance and other occurring faults;

2. Unitary System is defined as a system whose singular values of transfer function matrix are all equal. A method of constructing a closed-loop unitary system is developed. The benefit of a unitary system is that, for a fault detection system whose inputs are faults and outputs are residuals, all faults will appear in the residuals with the same intensity since, for different inputs with the same magnitude, the magnitude of the outputs is the same for a unitary system.

3. An H_∞/H_- adaptive observer is constructed to reduce the effect of disturbance and meanwhile maintain the sensitivity to faults. The H_∞/H_- adaptive observer is built with the technique of Unitary System;

4. A reconfigurable fuzzy PI controller is constructed based on the fuzzy TS model of the elevator where the dynamics of the elevator - at different operating points and different fault scenarios - is modeled as linear models in the fuzzy rules. The stability and performance requirement is enforced in the form of matrix inequalities with the explicit consideration of performance degradation [4];

5. A reconfiguration mechanism is developed with fuzzy inference technique. The new controller can be reconfigured as the fuzzy blending of the pre-designed controllers. The reference signal of tracking is also reconfigured with fuzzy inference.

1.3 Thesis Outline

The researches in the area of Active Fault Tolerant Control are introduced in Chapter 2. FDI methods based on parameter estimation, output observer and adaptive observer are introduced with the focus on robust residual generation techniques. Fault tolerant controller design and reconfiguration methods are reviewed thereafter.

The structure of the electronic-hydraulic driven elevator is introduced in Chapter 3. The nonlinear mathematic model of the elevator is built for the purpose of simulation. Faults in the elevator are modeled as the abrupt change of different parameters. A linear model, which is used to construct the fuzzy model of the elevator, is presented.

In Chapter 4, the Adaptive Unknown Input Observer is developed for the purpose of disturbance-decoupled estimation. The observer integrates the technique of adaptive observer and unknown input observer so that, if certain requirements on the measurement redundancy are satisfied, both the estimation of states and parameters converge to the real values respectively.

In Chapter 5, Unitary System is defined as a linear time-invariant system whose singular values of transfer matrix are equal. The method of building a closed-loop unitary system in a weighted observer form is introduced.

In Chapter 6, H_∞/H_- observer, which has balanced robustness to disturbances and sensitivity to faults, is designed with the technique of Unitary System. An H_∞/H_- adaptive observer is then constructed so that the estimation of parameters is optimized for disturbance rejection.

In Chapter 7, a fuzzy PI controller is constructed for a nonlinear system with the consideration of parameter fault. Performance degradation is modeled into the controller design procedure as a decay rate constraint. The reconfiguration method for both controller and reference signal is developed based on fuzzy inference technique. An Active Fault Tolerant Control system is then constructed and applied to the elevator.

The thesis is completed in Chapter 8 with conclusions and recommendations of future works.

CHAPTER 2

ACTIVE FAULT TOLERANT CONTROL: RELEVANT BACKGROUND

An AFTC system usually contains three components [3]: Fault Detection and Isolation (FDI), a fault-free controller and a reconfiguration mechanism. In the normal situation, the system operates under the control of the fault-free controller. The health of the system is monitored by the FDI. If any occurring fault is identified by the FDI, the reconfiguration mechanism replaces the fault-free controller with a new one to restore the performance and prevent further damage of the system. This chapter introduces the relevant researches with regard to these three components.

2.1 Fault Detection and Isolation

Fault Detection and Isolation (which is also referred as FDD – Fault Detection and Diagnosis- or FDE – Fault Detection and Estimation – if the magnitude of faults is estimated) techniques can be classified into three general categories according to [5]: quantitative model based methods [6], qualitative model based methods, and history data based methods [7]. Although all three techniques have successful applications, the FDI research in FTC mainly focuses on the quantitative model based methods, which are also referred to as model-based FDI, for their closeness to the control theories such as linear system, dynamics, modeling and identification [90].

In the model-based FDI, the fault information is extracted from residuals, which are the artificial signals describing the difference between the real system (with or without faults) and the mathematical model. For a fault-free system, the magnitude of residuals is zero or, more practically, smaller than certain threshold value. An occurring fault can be announced if the difference is larger than the threshold value. According to the statistics in [8], three popular FDI methods are output observer, parameters estimation and adaptive observer.

2.1.1 Methods for FDI

Output Observer [8-14]

An output observer for FDI utilizes the output estimation errors - the difference between the outputs of the observer and the real system - for fault detection and isolation. The Kalman filter and the Luenberger observer are the two most used state estimation methods that are applied as output observers in FDI.

The Kalman filter is an optimal states estimator of linear stochastic process where disturbances are modeled as zero mean noises with known distribution (covariance). The estimated states in the Kalman filter are optimized so that the sensitivity of the estimation error to the modeled disturbances is minimized. With the Extended Kalman filter or other variations of the Kalman filter [9-11], simultaneous states and parameters estimation can also be accomplished. In [10] for example, an Extended Kalman filter is applied to evaluate the leaking fault of a hydraulic actuator.

The Luenberger observer is a state observer for deterministic linear systems. In the output observer method based on the Luenberger observer [8], FDI has two separate steps which are fault detection and fault isolation. Different requirements are applied to the residual signals in these two steps. In the fault detection, a single residual is required to respond to all faults. The residual stays zero or almost zero for the healthy system. In the case of any fault happening, the residual deviates from zero noticeably. In the fault isolation, multiple residuals are generated. Each residual responds to only one fault. The location of the fault then can be identified by analyzing the values of all residuals. Fundamental problems such as the possibility of constructing such residual signals are discussed in [12] for linear systems with unknown disturbances.

The FDI method based on output observers is capable of fast fault detection. However, multiple observers are required for the purpose of fault isolation and the magnitude of occurring fault is not estimated.

Parameters Estimation [15, 16]

In parameters estimation methods, the faults are modeled as functions of parameters. These parameters are estimated online based on the input-output model of a system. The differences between the nominal values and the estimated values of fault functions are taken as the indicators of faults.

The advantage of parameter-estimation-based FDI is that the method gives accurate post-fault information such as the location and magnitude of faults. In addition, multiple faults can be diagnosed and evaluated at the same time. The fault information,

however, is not available until all estimations converge. The time required for fault evaluation is thus longer than that for the output-observer-based method.

Adaptive Observer [17-22]

The study of adaptive observers is traced back to the joint state-parameter estimation for adaptive control systems [23, 24]. On one hand, the unmeasured states are evaluated for the purpose of state feedback control; on the other hand, the unknown parameters are estimated online so that the controller can be updated accordingly. When certain persistent excitation requirements are satisfied, the estimated states and parameters converge to their real values simultaneously. With the increasing reliability requirements on control systems, adaptive observers have also been applied to the fault diagnosis and evaluation, where faults are modeled as the changes of parameters from their nominal values and then estimated using the convergence capability of adaptive observers.

The FDI method based on adaptive observers integrates the technique of output observers and parameter estimation so that the occurring faults can be detected quickly and estimated accurately. The output estimation error can be taken as the indicator of fault as that in the output-observer-based method while multiple faults can be located and evaluated at the same time as in the parameter-estimation-based method.

The robustness to disturbance, however, needs further investigations for adaptive observers. For faults detection and estimation, the disturbance rejection capability of an adaptive observer is especially important since it is necessary to minimize, or even eliminate if possible, the influence of non-targeted faults, which are usually taken as the

disturbances to the estimation of targeted faults. Otherwise, the false estimation of one fault will spoil the estimations of all others.

In [25, 26], the performance of adaptive observers is discussed for the noise corrupted systems. It is stated in [26] that the expectation of the estimation errors is bounded if the magnitude of noises is bounded. Furthermore, for systems with independent noises of zero means, the expectation of estimation errors converges to zero. Therefore, an adaptive observer is at least Bounded-Input Bounded-Output stable to unknown external signals.

For a Multiple-Input Multiple-Output system (MIMO), the robustness to structured disturbances can be further enhanced for an adaptive observer by utilizing the measurement redundancy of the system. With proper measurements, the influence of disturbances can be eliminated in the estimation errors. One technique is to incorporate with the Unknown Input Observer (UIO) [8, 27], which is a disturbance-decoupled observer for the accurate state estimation. In [22], an adaptive UIO has been designed to estimate the faulty parameters of an aircraft actuator. The approach, however, needs full states (n independent) measurements, which reduces the necessity of states estimation.

2.1.2 Robustness in FDI: disturbance-decoupled residual generation

A robust residual insensitive to disturbances has to be built if the disturbances compromise the fault detection. Robust residuals are also necessary for the fault isolation with multiple residuals, where, for each residual, all non-targeted faults are considered as disturbances.

Eigenvector Assignment (EA) [28-30] and Unknown Input Observer (UIO) [8, 27, 31] are two disturbance-decoupled residual generation methods. In EA, the closed-loop system matrix *(A+LC)* of the observer is constructed so that the distribution matrix E of disturbances is a part of the eigenvectors matrix of *(A+LC)*, where A, C and L are respectively the open-loop system matrix, the output matrix and the feedback gain of the observer. With a properly selected weighted matrix W, the transfer matrix from the disturbances to the residual thus satisfies $G_d(s) = WC(sI - A - LC)^{-1}E = 0$. In UIO, a coordinate transformation of states is applied to the observer so that, by utilizing the geometry property of the system, the estimation error $H\tilde{y}$ is free of disturbances, where $\tilde{y}$ is the output estimation error and H is the matrix that describes the coordinate transformation.

These two methods make use of the analytical redundancy of a system to decouple disturbances (including model uncertainties) from the residual so that the response to disturbance in the residual is eliminated. One requirement for building an AFTC system is the redundancy in actuators and sensors. With redundant actuators, it is possible to reconfigure the controller when actuator faults occur; with redundant sensors, it is possible to extract fault information from the measurements. The analytical redundancy is the redundancy based on physical principles and mathematical relations. Unlike the hardware redundancy which implies multiple hardware with the same function, the analytical redundancy uses different hardware for the similar functions.

Although robust residuals can be generated with the EA and UIO, one main restriction is that the measurement redundancy required for the disturbance decoupling is difficult to be satisfied.

2.1.3 Robustness in FDI: optimization-based residual generation

The Approximate Unknown Input Observer (AUIO) method [32] is an optimization-based robust residual generation technique. Instead of seeking a disturbance-decoupled residual, this approach tries to minimize the influence of disturbances on the residual. As this approach usually also reduces the sensitivity to faults, a trade-off is made between the robustness to disturbances and the sensitivity to faults. In AUIO, the robust residual generation is formulated into the optimization of a cost function so that, when it is optimized, the difference between the sensitivities of the residual to faults and to disturbances, is maximized. Different cost functions in general forms are introduced in [32]. Most research up to date [33-41] uses similar cost functions but with different sensitivity definitions.

In [33-36], the problem of residual generation is formulated into H_2 or H_∞ optimizations which can be solved with robust controller design methods such as loop shaping, LQR (Linear Quadratic Regulator) or LMI (Linear Matrix Inequality) optimization. In general, the residual has the form of:

$$r = G_{rd}(s)d + G_{rf}(s)f \tag{2.1}$$

where, $G_{rd}(s)$ is the transfer function matrix from the disturbances d to the residual r; $G_{rf}(s)$ is the transfer function matrix from the faults f to the residual r. To minimize the sensitivity of the residual signal to the disturbances, the norm of $G_{rd}(s)$ is used as the cost function and minimized as:

$$J = \| G_{rd}(s) \|. \tag{2.2}$$

To maximize the sensitivity of the residual to the faults f at the same time, the cost function can be changed to the form of:

$$J = \frac{\| G_{rd}(s) \|}{\| G_{rf}(s) \|} \tag{2.3}$$

or:

$$J = \| G_{rd}(s) \| - \| G_{rf}(s) \|. \tag{2.4}$$

In [37-41], the problem of residual generation is formulated into a multiple objective optimization with the cost function in the form of:

$$\min_{f} \max_{d} \max_{v} J = J_f - J_d - J_v \tag{2.5}$$

where f is the targeted faults to be detected; d is the disturbances to be decoupled (including the non-targeted faults to be separated from f); v includes other unwanted sources that may spoil the fault detection, such as the unknown initial states of the system. J_f, J_d and J_v are the sub-cost functions of the three signals f, d and v, which usually

have the form of quadratic functions. In [38] for example, the cost function has the form of:

$$J = \frac{1}{2}\int_{t_0}^{t} (\| f \|^2_{Q_1^{-1}} - \| d \|^2_{\gamma Q_2^{-1}} - \| \tilde{y} \|^2_{V^{-1}}) d\tau - \frac{1}{2} \| \tilde{x}_o \|^2_{\Pi^{-1}} \tag{2.6}$$

where, $\| \cdot \|$ stands for a weighted norm; $\tilde{y}$ is the output estimation error; $\tilde{x}_o$ is the initial state difference between the observer and the real system; the subscripts $Q_1, Q_2, V,$ and Π are design parameters of positive definite weight matrices; γ is a positive scalar parameter.

The multi-objective optimization in Equation (2.6) can be explained as maximizing the cost function for the system subject to unknown inputs of faults, disturbances and initial states, where $\int_{t_0}^{t} \| f \|^2_{Q_1^{-1}} d\tau$, $\int_{t_0}^{t} \| d \|^2_{\gamma Q_2^{-1}} d\tau$, and $\| \tilde{x}_o \|^2_{\Pi^{-1}}$ are taken as the residual's sensitivities to these three inputs respectively. $\int_{t_0}^{t} | \tilde{y} \|^2_{V^{-1}} d\tau$ is a constraint on the estimation error so that the optimization of (2.6) is solvable. When (2.6) is maximized, the difference between the residual's sensitivity to faults and its sensitivities to the other two inputs is also maximized.

A common feature of these optimizations is to find a balance between the robustness to disturbances and the sensitivity to faults, which makes them intrinsically all variations of the H_∞/H_- optimization [42].

2.1.4 Robustness and sensitivity in FDI: H_∞/H_- optimization

The H_∞/H_- optimization is initially defined in [30] and further explored in [32,37,41,43-49] with different forms but a common objective: maximizing the difference between the sensitivity of the residual to faults (H_-) and that to disturbances (H_∞).

In [44] and [45], the optimization is formulated into two H_∞ minimization problems: one for $G_{rd}(s)$, the closed-loop transfer matrix from the disturbances to the residual; the other for $I - G_{rf}(s)$, the complementary of the closed-loop transfer matrix from the faults to the residual. In [37] and [46], a weighting filter is used so that these two H_∞ minimizations emphasize different frequency ranges. These methods, similar to the approaches used in robust control [50] and robust estimation [51], are all based on the singular value property of constant matrices. With the consideration of frequency as in a transfer matrix, however, these methods are less satisfactory in finding the optimum.

In [47], the optimization is formulated into a multi-objective cost function in the frequency domain and solved with the genetic algorithm. In [48], the optimization is formulated as a constraint to a Lyapunov function. In [41], the problem is transformed into a multi-objective optimization in the time domain. The solutions of [41] and [48] are in the Linear Matrix Inequality (LMI) form. A general feature of the above methods is that they are all trade-off optimizations involving cost functions with weighted robustness and sensitivity. In [43], the solution to the H_∞/H_- optimization is given in the form of two matrix inequalities, which are solved approximately with an Iterative LMI (ILMI) method

as they cannot be solved in the framework of LMI optimization. For these numerical methods, however, the calculation time required to obtain the optimum is unknown. Besides, the inaccuracy of the optimization result - the distance from the optimum - is hard to evaluate.

The exact solutions to the H_∞/H_- optimization are given in [32] and [49] only for just-proper systems, where the optimization is tackled through transfer matrix factorization. In [49] the solution is an open-loop inverse filter and in [32] the solution is a Luenberger observer.

These two methods, however, are suitable to sensor faults detection since just-proper systems, where the direct feed-through D (as in the state space form) has full rank, are assumed. The H_∞/H_- optimization involves the singular values of two transfer matrices: from disturbances and faults to residuals. As shown in [32] and [49], the solution to this robustness and sensitivity problem is to transform one involved transfer matrix to a special form whose singular values are equal to the same constant at all frequencies. Therefore, H_∞ and H_- of the transfer matrix are also equal to the same constant. However, this solution is available only for a just-proper transfer matrix since the magnitude frequency response and the singular values of a strictly-proper transfer matrix always attenuate to zero as the frequency increases to infinity. Besides, for a strictly-proper system, this solution involves an improper inverse, which cannot be realized practically. For strictly-proper systems, the H_∞/H_- optimization is solvable only when the frequency range is considered since H_- is always zero in the whole frequency

range, which makes the optimization even complicated. The solution to the H_∞/H_- optimization of strictly-proper systems is still absent.

2.2 Controller Design and Reconfiguration Methods

In a PFTC system a single controller is designed to meet the stability and performance requirements under all circumstance, with or without faults. In an AFTC system, each controller only has to deal with the fault situation it is designed for. Many controller design methods have been applied to AFTC systems such as, to name a few, poles and eigenvectors placement [52], Linear Quadratic Regulator [53], robust control [54, 55], Quantitative Feedback Control (QFT) [56], model predictive control [57], and adaptive control [58, 59].

AFTC has its advantage of changing the parameters and even the structures of controller based on the FDI results. Therefore, the reconfiguration method is important for the performance of an AFTC system. Different strategies are applied in AFTC depending on different objectives of reconfiguration.

Pseudo-Inverse Method (PIM) [59]

PIM calculates the state feedback gain of the post-fault system based on the identified system dynamics so that the closed-loop system dynamics remains the same or almost the same. Mathematically, it is formulated to an optimization problem in the form of:

$$\min_{K_f} \| (A+BK) - (A_f + B_f K_f) \| \tag{2.7}$$

where, A, B and K are respectively the system matrix, input matrix and state feedback gain of the controller for the fault-free case; A_f, B_f, and K_f are their counterparts for the post-fault system. The objective of the optimization is to recalculate the post-fault feedback gain K_f so that the norm of the difference between the closed-loop system matrices is minimized. The solution to this optimization is:

$$K_f = B_f^{+}(A + BK - A_f), \tag{2.8}$$

where, B_f^{+} is the pseudo inverse of B_f.

One of the drawbacks of PIM is that the stability of the post-fault closed-loop system cannot be guaranteed if no extra constraints on the stability are imposed.

Eigenstructure Assignment Method [60, 61]

The Eigenstructure Assignment method minimizes the closed-loop performance difference between the pre- and post-fault systems instead of the difference between system matrices. The dynamic performance of a linear system depends largely on the eigenstructure – eigenvalues and eigenvectors - of its system matrix. The Eigenstructure Assignment method minimizes the eigenvectors differences between the two (pre- and post-fault) system matrices and keeps their significant eigenvalues the same. The stability of the closed-loop system then can be guaranteed by the same eigenvalues; meanwhile, the performance of the post-fault system can be recovered because of the similar eigenvectors. Mathematically, the Eigenstructure Assignment method for a system with a state feedback controller can be formulated into an optimization problem as follows:

$$\min_{K_f}(v_i^f - v_i)^T W(v_i^f - v_i) \tag{2.9}$$

subject to the constraints:

$$(A_f + B_f K_f)v_i^f = \lambda_i v_i^f$$

$$(A + BK)v_i = \lambda_i v_i . \tag{2.10}$$

where, λ_i, $i=1...n$, is the *ith* eigenvalue of the closed-loop system matrix (according to the poles placement control theory, all eigenvalues can be assigned arbitrarily with a state feedback controller if the system is controllable); v_i and v_i^f are the corresponding eigenvectors of the pre- and post-fault closed-loop system matrices; W is a constant weight matrix.

The advantage of the Eigenstructure Assignment method is the guaranteed stability and performance of the post-fault system. However, due to its poles placement nature, it is difficult for the method to deal with disturbances and uncertainties in the controller design.

Adaptive Control and Model Following [57, 58, 62]

Adaptive control can accommodate the faults in the form of parameters changing since it has the ability of automatically adapting to the changes of system parameters. One of the most used adaptive control methods in fault tolerant control is the model reference control or model following method. In the model following method, a reference model is selected first. The controller is designed so that the output of the closed-loop

system tracks that of the model. Depending on whether the fault parameters are estimated online or not, the method can be further classified into direct and indirect methods. In an indirect method, the fault parameters are estimated so that the model of the post-fault system can be built. The parameters of the controller are then tuned based on the post-fault system dynamics. In the direct method, the parameters of the controller are updated directly based on the tracking errors and performance of the system.

The disadvantage of adaptive control is that, because of its auto-adapting characteristic, it might take much time for the updated controller parameters to converge, which makes it suitable to deal with slow and small parameter variation faults.

Model Predictive Control [63, 64]

The model predictive control (MPC) is an online-optimization-based control algorithm. The performance requirements of the closed-loop system are formulated into an optimization problem. At every step, the optimization is carried out based on the system's current dynamics and the control signal is calculated with the optimization results. As discussed in [65], "the MPC architecture allows fault-tolerance to be embedded in a relatively easy way by: (a) redefining the constraints to represent certain faults (usually actuator faults), (b) changing the internal model, (c) changing the control objectives to reflect limitations due to the faulty mode of operation."

However, the heavy computational load, which is required for the optimization at every step, makes MPC only suitable for a slow process.

Multiple Models [63, 66]

The multiple models method is an integrated method considering both the FDI and the controller design. In this method, $q_f + 1$ observers are constructed. One fault-free observer is built with the model of the fault-free system; q_f observers are built with the models of the system with different faults (q_f faults in total). Similarly, $q_f + 1$ controllers are constructed: one controller is designed for the fault-free system; q_f controllers are designed for the system with different faults. The status of the system is monitored online based on the difference between the outputs of the system and the fault-free observer. Once a fault is detected, q_f observers for different faults start to run and their outputs are analyzed to determine the occurring possibility of each fault. The possibility of each fault is assigned to the corresponding controller, which is designed for that particular fault, as the effectiveness coefficient. These q_f controllers for different faults are then combined based on their effectiveness.

The Multiple Models method integrates the process of fault evaluation and fault tolerant control. However, as the magnitude of occurring fault is not estimated, the method is suitable to deal with the pre-defined faults with known magnitudes.

Fuzzy Control [63, 67-69]

A fuzzy logic system [70, 71] is a valuable tool for the AFTC of the parameter faults situation since:

1. A fuzzy controller [72, 73] can be designed offline and recalculated online: a group of controllers addressing the faults of pre-defined magnitudes can be constructed

offline; a new controller addressing the occurring fault with particular magnitude can be constructed online as a fuzzy blending of the available pre-defined controllers.

2. The inherent rule-based inference capability makes a fuzzy system a valuable tool of decision making which is required for the reconfiguration.

The main advantage of fuzzy control method is that, since the reconfigured controller is constructed online as a fuzzy blending of the offline-designed controllers, the computation load required for the reconfiguration is light. The disadvantage is that the detailed and accurate information of occurring fault is required.

2.3 Summary

From the above literature reviews, it is still a challenge to design a complete Active Fault Tolerant Control system with the capabilities of:

1. Fast and accurate fault detection, isolation and estimation (FDE) which is robust to disturbances and other non-targeted occurring faults;

2. Quick and proper reconfiguration to restore the performance of the post-fault system and prevent the further damage.

The research in this thesis addresses this challenge by presenting several original contributions in the following directions:

1. Robust FDE methods based on robust adaptive observers including Adaptive Unknown Input Observer and $H_\infty/H\_$ adaptive observer;

2. Controller design and Reconfiguration method based on fuzzy inference technique.

CHAPTER 3

MATHEMATIC MODEL OF AN ELECTRO-HYDRAULIC DRIVEN ELEVATOR

An elevator is the primary control of pitch – the rotation of an airplane about its lateral axis- whereas an aileron and a rudder are the primary controls of roll and yaw – the rotations about longitudinal and vertical axes. An elevator is attached to the tail of an airplane, usually to the back edge of the horizontal stabilizer. An angle position variation of the elevator alters the camber of the tail airfoil, which consequently changes the torque on the lateral axis, and thus changes the angle of attack and finally the elevation of the airplane.

Traditionally, an elevator, as shown in Figure 3.1, is connected to a control column in the cockpit through a series of cables, levers and pulleys so that it can be controlled by the pilot manually and directly. Nowadays in a fly-by-wire airplane, these mechanical components between the elevator and the control column are replaced with flight control computers and a set of local actuators and sensors: on the one hand, the movements of the control column are measured and then transmitted as electronic signals to the computers, where the control commands are computed and sent to the actuators of the elevator; on the other hand, the movements of the elevator are measured and fed back to the computers, where commands are calculated and sent to the actuators on the control column to provide artificial feel to the pilot.

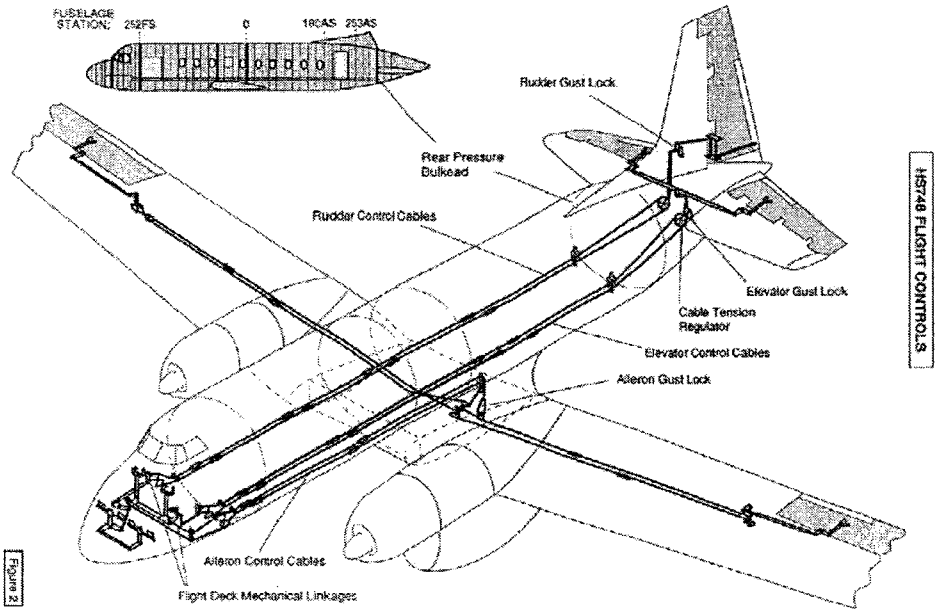

Figure 3.1 Flight control surface: elevator [1]

Although the fly-by-wire technique reduces the cost and increases the reliability of an airplane in the sense of hardware, it also reduces the pilot's control and supervision since the elevator becomes an autonomous system. Any occurring fault related to the elevator now needs to be addressed by the flight control computers. Therefore, the fly-by-wire technique enables as well as necessitates the fault tolerant control.

For the purpose of the active fault tolerant control, this chapter presents the mathematical models of the elevator including:

[1] The figure is adopted from the accident report of AAIB (Aircraft Accident Investigation Board of United Kingdom): http://www.aaib.gov.uk/cms_resources/1%2D99%20G%20ATMI%20Appendices%2Epdf

1. The nonlinear model of the fault-free elevator – for the purpose of simulation;

2. The model with faults – for faults simulation and fault detection and estimation;

3. The linear model of the elevator – for the constructing of the fuzzy Tagaki-Sugeno (TS) model (for the controller design).

3.1 The Nonlinear Model of the Elevator

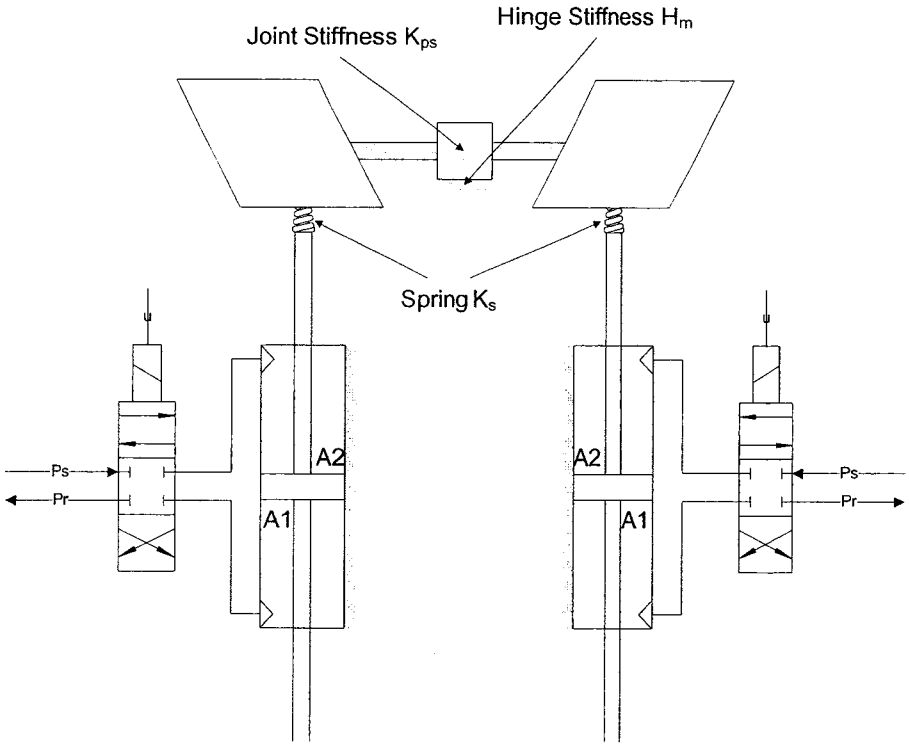

Figure 3.2 Structure of the elevator

The elevator studied in this research is shown in the simplified illustration of Figure 3.2. The elevator is adopted from [74], which is developed by Thales Canada for the demonstration of a Fly-By-Wire (FBW) Flight Control System (FCS) targeting

regional aircrafts. The elevator consists of two subsystems, the left and the right one. Each subsystem has a panel, a hydraulic cylinder and an Electro-Hydraulic Servo-Valve (EHSV). The panel of each subsystem, which is fixed to a shaft, is driven by the EHSV controlled hydraulic cylinder through a spring connection. The two shafts are connected through a joint so that the two panels will move synchronously. The joint is connected to the tail of the airplane through a hinge. The control commands u to the servo valves come from a flight control unit. The hydraulic fluid is supplied by a hydraulic pump station.

A commercial airplane is a highly redundant system. Boeing 767, for example, has three sets of the system shown in Figure 3.2. These three systems are controlled by different flight control units and powered with different pump stations [75]. This research, however, will focus on only one system. The mathematical model of the elevator can be derived as shown in (3.1) with the principles of mechanics and hydraulics [76].

$$\dot{x}_{1L} = x_{2L}$$

$$\dot{x}_{2L} = \frac{1}{m_L}\left[A_1 x_{3L} - A_2 x_{4L} - b x_{2L} - K_{sL}\left(x_{1L} - l x_{7L}\right)\right]$$

$$\dot{x}_{3L} = \frac{\beta\left[C_V w_L \sqrt{\frac{2}{\rho}} x_5 \sqrt{\left(P_s - x_{3L}\right)} - C_1 A_{1oL}\sqrt{\frac{2}{\rho}}\sqrt{x_{3L}} - C_{12} A_{12L}\left(x_{3L} - x_{4L}\right) - A_1 x_{2L}\right]}{V_1 + A_1 x_{1L}}$$

$$\dot{x}_{4L} = \frac{\beta\left[-C_V w_L \sqrt{\frac{2}{\rho}} x_5 \sqrt{x_{4L} - P_R} - C_2 A_{2oL}\sqrt{\frac{2}{\rho}}\sqrt{x_{4L}} + C_{12} A_{12L}\left(x_{3L} - x_{4L}\right) + A_2 x_{2L}\right]}{V_2 - A_2 x_{1L}}$$

$$\dot{x}_{5L} = x_{6L}$$

$$\dot{x}_{6L} = -\omega_{vL}{}^2 x_{5L} - 2\xi_{vL}\omega_{vL} x_{6L} + k_{vL} u_L$$

$$\dot{x}_{7L} = x_{8L}$$

$$\dot{x}_{8L} = \frac{1}{J_s}\left[K_{sL}\left(x_{1L} - l x_{7L}\right) - B_s x_{8L} - K_{Ps}\left(x_{7L} - x_{7R}\right) - 0.5 H_m\left(x_{7L} + x_{7R}\right)\right]$$

$$\dot{x}_{1R} = x_{2R}$$

$$\dot{x}_{2R} = \frac{1}{m_R}\left[A_1 x_{3R} - A_2 x_{4R} - b x_{2R} - K_{sR}\left(x_{1R} - l x_{7R}\right)\right]$$

$$\dot{x}_{3R} = \frac{\beta\left[C_V w_R \sqrt{\frac{2}{\rho}} x_{5R}\sqrt{P_S - x_{3R}} - C_1 A_{1oR}\sqrt{\frac{2}{\rho}}\sqrt{x_{3R}} - C_{12} A_{12R}\left(x_{3R} - x_{4R}\right) - A_1 x_{2R}\right]}{V_1 + A_1 x_{1R}}$$

$$\dot{x}_{4R} = \frac{\beta\left[-C_V w_R \sqrt{\frac{2}{\rho}} x_{5R}\sqrt{x_{4R} - P_R} - C_2 A_{2oR}\sqrt{\frac{2}{\rho}}\sqrt{x_{4R}} + C_{12} A_{12R}\left(x_{3R} - x_{4R}\right) + A_2 x_{2R}\right]}{V_2 - A_2 x_{1R}}$$

$$\dot{x}_{5R} = x_{6R}$$

$$\dot{x}_{6R} = -\omega_{vR}{}^2 x_{5R} - 2\xi_{vR}\omega_{vR} x_{6R} + k_{vR} u_R$$

$$\dot{x}_{7R} = x_{8R}$$

$$\dot{x}_{8R} = \frac{1}{J_s}\left[K_{sR}\left(x_{1R} - l x_{7R}\right) - B_s x_{8R} + K_{Ps}\left(x_{7L} - x_{7R}\right) - 0.5 H_m\left(x_{7L} + x_{7R}\right)\right] \qquad (3.1)$$

The available measurements are:

$$y = \begin{bmatrix} x_{1L} & x_{2L} & x_{3L} & x_{4L} & x_{5L} & x_{7L} & x_{1R} & x_{2R} & x_{3R} & x_{4R} & x_{5R} & x_{7R} \end{bmatrix}^T . \tag{3.2}$$

The physical meanings of the states and parameters (and their values) are given in Table 3.1 and 3.2.

The control objective is to move the two subsystems synchronously and follow the reference angle of the elevator which is given either by the pilot or the flight control units. Therefore, the controlled outputs of the elevator are taken as:

$$z = \begin{bmatrix} \dfrac{x_{7L} + x_{7R}}{2} \\ \dfrac{x_{7L} - x_{7R}}{2} \end{bmatrix},$$

or,

$$z = C_z x \tag{3.3}$$

where, x_{7L} and x_{7R} are the panel angels of the two subsystem; and

$$C_z = \begin{bmatrix} 0 & 0 & 0 & 0 & 0 & 0 & 0.5 & 0 & 0 & 0 & 0 & 0 & 0 & 0 & 0.5 & 0 \\ 0 & 0 & 0 & 0 & 0 & 0 & 0.5 & 0 & 0 & 0 & 0 & 0 & 0 & 0 & -0.5 & 0 \end{bmatrix}.$$

The first output is position of the elevator and the second output is the difference between the two subsystems. The control objective is thus mathematically formulated into:

$$z = \begin{bmatrix} \frac{x_{7L} + x_{7R}}{2} \\ \frac{x_{7L} - x_{7R}}{2} \end{bmatrix} = \begin{bmatrix} r \\ 0 \end{bmatrix} \tag{3.4}$$

where r is the elevator's angle reference.

Table 3.1 States of the elevator

Left system	Right system	Physical meanings
x_{1L}	x_{1R}	cylinder piston position
x_{2L}	x_{2R}	piston velocity
x_{3L}	x_{3R}	pressure in the active chamber of the cylinder
x_{4L}	x_{4R}	pressure in the passive chamber of the cylinder
x_{5L}	x_{5R}	EHSV spool position
x_{6L}	x_{6R}	EHSV spool velocity
x_{7L}	x_{7R}	panel angel
x_{8L}	x_{8R}	panel velocity
u_L	u_R	control current to EHSV

Table 3.2 Parameters of the elevator

Left system	Right system	Physical meanings	Values
m_L	m_R	piston mass	7.88×10^{-3} $(lb\text{-}s^2/in)$
A_1	A_1	active cylinder chamber area	3.6264 (in^2)
A_2	A_2	passive cylinder chamber area	3.6264 (in^2)
b	b	cylinder damping	9.27 $(lb/in/s)$
K_{sL}	K_{sR}	spring stiffness	2.5×10^5 (lbf/in)
l	l	arm length to the shaft	$2.924(in)$
β	β	the oil bulk modulus	1×10^5 (psi)
$C_V w_L\sqrt{\frac{2}{\rho}}$	$C_V w_R\sqrt{\frac{2}{\rho}}$	the flow rate gains of the EHSVs	$9.6571(in^2/psi^{1/2})$
P_S	P_S	the oil supply pressure	3000 (psi)
P_R	P_R	the oil reservoir pressure	50 (psi)
$C_{12}A_{12L}$	$C_{12}A_{12R}$	leaking coefficients between chambers	3.208×10^{-3} $(in^3/sec/psi)$

$C_1 A_{1oL}\sqrt{\frac{2}{\rho}}$	$C_1 A_{1oR}\sqrt{\frac{2}{\rho}}$	leaking coefficients in the active chambers	*0 ($in^2/psi^{1/2}$)*
$C_2 A_{2oL}\sqrt{\frac{2}{\rho}}$	$C_2 A_{2oR}\sqrt{\frac{2}{\rho}}$	leaking coefficients in the passive chambers	*0 ($in^2/psi^{1/2}$)*
V_1	V_1	Null volume of active chamber	*4.1 (in^3)*
ω_L	ω_R	EHSV natural frequency	*817 (rad/s)*
ξ_L	ξ_R	EHSV damping ratio	*0.8*
k_{vL}	k_{vR}	EHSV actuation gain	*0.00337(in/s^2/mA)*
B_s	B_s	shaft damping	*82(lbf-in-s/rad)*
J_s	J_s	equivalent inertia of the elevator surface	*7.5(lbf-in-s)*
K_{ps}		joint stiffness	*5×10^5 (lbf-in/rad)*
H_m		hinge stiffness	*8.6×10^3 (lbf-in/rad)*

3.2 The Model of Faults

Faults of an elevator can result in the loss of pitch control, which consequently reduces the elevation capability and thus endangers the performance, manoeuvrability,

and safety of an airplane. Two types of faults were considered in this thesis including the unsynchronized movement of panels and the gain loss of the elevator.

For the purpose of pitch control, the two panels of the elevator need to move synchronously. Unsynchronized movement of panels may lead to unexpected roll and yaw of the airplane. Moreover, the generated twisting torque on the joint may lead to the damage of elevator. For the two identical subsystems in Figure 3.2, which have the same structure and follow the same command (the current to the EHSVs), the fault of unsynchronized movement is normally the result of unexpected changes in one of the subsystem. In this thesis, this fault is modeled as the change of the following parameters:

1. k_{vL} and k_{vR} are the EHSV gains - a ratio of valve opening to its current command;

2. K_{sL} and K_{sR} are the stiffness of the springs;

3. $C_{1L} = C_1 A_{1oL}\sqrt{\frac{2}{\rho}}$ and $C_{1R} = C_1 A_{1oR}\sqrt{\frac{2}{\rho}}$ are the leaking of active chambers to environment;

4. $C_{2L} = C_2 A_{2oL}\sqrt{\frac{2}{\rho}}$ and $C_{2R} = C_2 A_{2oR}\sqrt{\frac{2}{\rho}}$ are the leaking of passive chambers to environment;

5. $C_{12L} = C_{12} A_{12L}$ and $C_{12R} = C_{12} A_{12R}$ are the leaking between the active and passive chambers.

The other fault considered in this research is the gain loss of the whole elevator, which means the elevator moves slower than it is expected. In the extreme case, the motion of the elevator may be restricted. In this thesis, such a fault is modeled as the increase of hinge stiffness H_m.

For the purpose of fault detection and evaluation, these faults are modeled into the state space representation of the elevator in the following form:

$$\dot{x} = Ax + Bu + \sum_{i=1}^{6} F_i \phi_i \theta_i \tag{3.5}$$

where

$$\dot{x} = Ax + Bu$$

is the dynamics of the system with normal parameters; x is the state vector, which is the same as that in Model (3.1); θ is the vector of fault parameters; ϕ is a matrix of known signals; F is the input matrix of $\phi\theta$.

According to the nonlinear model of (3.1), the parameter matrices in Model (3.5) are given as the followings:

$$A = \begin{bmatrix} & & & & & & 0 & 0 & 0 & 0 & 0 & 0 & 0 & 0 \\ & & & & & & 0 & 0 & 0 & 0 & 0 & 0 & 0 & 0 \\ & & & & & & 0 & 0 & 0 & 0 & 0 & 0 & 0 & 0 \\ & & & & & & 0 & 0 & 0 & 0 & 0 & 0 & 0 & 0 \\ & & & A_L & & & 0 & 0 & 0 & 0 & 0 & 0 & 0 & 0 \\ & & & & & & 0 & 0 & 0 & 0 & 0 & 0 & 0 & 0 \\ & & & & & & 0 & 0 & 0 & 0 & 0 & 0 & 0 & 0 \\ & & & & & & 0 & 0 & 0 & 0 & 0 & 0 & \frac{(K_{Ps}-0.5H_m)}{J_s} & 0 \\ 0 & 0 & 0 & 0 & 0 & 0 & 0 & 0 & & & & & & \\ 0 & 0 & 0 & 0 & 0 & 0 & 0 & 0 & & & & & & \\ 0 & 0 & 0 & 0 & 0 & 0 & 0 & 0 & & & & & & \\ 0 & 0 & 0 & 0 & 0 & 0 & 0 & 0 & & & & & & \\ 0 & 0 & 0 & 0 & 0 & 0 & 0 & 0 & & & A_R & & & \\ 0 & 0 & 0 & 0 & 0 & 0 & 0 & 0 & & & & & & \\ 0 & 0 & 0 & 0 & 0 & 0 & 0 & 0 & & & & & & \\ 0 & 0 & 0 & 0 & 0 & 0 & \frac{(K_{Ps}-0.5H_m)}{J_s} & 0 & & & & & & \end{bmatrix},$$

$$B = \begin{bmatrix} B_L & 0_{8\times1} \\ 0_{8\times1} & B_R \end{bmatrix},$$

where,

$$A_L = \begin{bmatrix} 0 & 1 & 0 & 0 & 0 & 0 & 0 & 0 \\ \frac{-K_{sL}}{m} & \frac{-b}{m} & \frac{A_p}{m} & -\frac{A_p}{m} & 0 & 0 & \frac{K_{sL}l}{m} & 0 \\ 0 & 0 & 0 & 0 & 0 & 0 & 0 & 0 \\ 0 & 0 & 0 & 0 & 0 & 0 & 0 & 0 \\ 0 & 0 & 0 & 0 & 0 & 1 & 0 & 0 \\ 0 & 0 & 0 & 0 & -\omega_v^{\,2} & -2\xi_v\omega_v & 0 & 0 \\ 0 & 0 & 0 & 0 & 0 & 0 & 0 & 0 \\ \frac{K_{sL}}{J_s} & 0 & 0 & 0 & 0 & 0 & \frac{-(K_{sL}l+K_{Ps}+0.5H_m)}{J_s} & \frac{-B_s}{J_s} \end{bmatrix},$$

$$A_R = \begin{bmatrix} 0 & 1 & 0 & 0 & 0 & 0 & 0 & 0 \\ \frac{-K_{sR}}{m} & \frac{-b}{m} & \frac{A_p}{m} & -\frac{A_p}{m} & 0 & 0 & \frac{K_{sR}l}{m} & 0 \\ 0 & 0 & 0 & 0 & 0 & 0 & 0 & 0 \\ 0 & 0 & 0 & 0 & 0 & 0 & 0 & 0 \\ 0 & 0 & 0 & 0 & 0 & 1 & 0 & 0 \\ 0 & 0 & 0 & 0 & -\omega_v^{\,2} & -2\xi_v\omega_v & 0 & 0 \\ 0 & 0 & 0 & 0 & 0 & 0 & 0 & 0 \\ \frac{K_{sR}}{J_s} & 0 & 0 & 0 & 0 & 0 & \frac{-(K_{sR}l + K_{Ps} + 0.5H_m)}{J_s} & \frac{-B_s}{J_s} \end{bmatrix}$$

$$B_L = B_R = \begin{bmatrix} 0 \\ 0 \\ 0 \\ 0 \\ 0 \\ k_v \\ 0 \\ 0 \end{bmatrix};$$

$$\theta_1 = \begin{bmatrix} \Delta k_{vL} \\ \Delta k_{vR} \end{bmatrix},\ \theta_2 = \begin{bmatrix} \Delta K_{sL} \\ \Delta K_{sR} \end{bmatrix}, \theta_3 = \Delta H_m\ , \theta_4 = \begin{bmatrix} C_{1L} \\ C_{2R} \end{bmatrix}, \theta_5 = \begin{bmatrix} C_{2L} \\ C_{2R} \end{bmatrix}, \theta_6 = \begin{bmatrix} C_{12L} \\ C_{12R} \end{bmatrix};$$

$$\phi_1 = \begin{bmatrix} u_L & 0 \\ 0 & u_R \end{bmatrix},\ \phi_2 = \begin{bmatrix} x_{1L} & 0 \\ x_{7L} & 0 \\ 0 & x_{1R} \\ 0 & x_{7R} \end{bmatrix},\ \phi_3 = \begin{bmatrix} x_{7L} \\ x_{7R} \end{bmatrix},\ \phi_4 = \begin{bmatrix} \frac{-\beta\sqrt{x_{3L}}}{V_1 + A_1 x_{1L}} & 0 \\ 0 & \frac{-\beta\sqrt{x_{3R}}}{V_1 + A_1 x_{1R}} \end{bmatrix},$$

$$\phi_5 = \begin{bmatrix} \dfrac{-\beta\sqrt{x_{3L}}}{V_2 - A_2 x_{1L}} & 0 \\ 0 & \dfrac{-\beta\sqrt{x_{3R}}}{V_2 - A_2 x_{1R}} \end{bmatrix},\ \phi_6 = \begin{bmatrix} \dfrac{-\beta(x_{3L} - x_{4L})}{V_1 + A_1 x_{1L}} & 0 \\ \dfrac{\beta(x_{3L} - x_{4L})}{V_2 - A_2 x_{1L}} & 0 \\ 0 & \dfrac{-\beta(x_{3R} - x_{4R})}{V_1 + A_1 x_{1R}} \\ 0 & \dfrac{\beta(x_{3R} - x_{4R})}{V_2 - A_2 x_{1R}} \end{bmatrix};$$

$$F_1 = \begin{bmatrix} 0 & 0 \\ 0 & 0 \\ 0 & 0 \\ 0 & 0 \\ 0 & 0 \\ 1 & 0 \\ 0 & 0 \\ 0 & 0 \\ 0 & 0 \\ 0 & 0 \\ 0 & 0 \\ 0 & 0 \\ 0 & 0 \\ 0 & 1 \\ 0 & 0 \\ 0 & 0 \end{bmatrix},\ F_2 = \begin{bmatrix} 0 & 0 & 0 & 0 \\ -\dfrac{1}{m} & \dfrac{l}{m} & 0 & 0 \\ 0 & 0 & 0 & 0 \\ 0 & 0 & 0 & 0 \\ 0 & 0 & 0 & 0 \\ 0 & 0 & 0 & 0 \\ 0 & 0 & 0 & 0 \\ \dfrac{1}{J_S} & -\dfrac{l}{J_S} & 0 & 0 \\ 0 & 0 & -\dfrac{1}{m} & \dfrac{l}{m} \\ 0 & 0 & 0 & 0 \\ 0 & 0 & 0 & 0 \\ 0 & 0 & 0 & 0 \\ 0 & 0 & 0 & 0 \\ 0 & 0 & 0 & 0 \\ 0 & 0 & \dfrac{1}{J_S} & -\dfrac{l}{J_S} \end{bmatrix},\ F_3 = \begin{bmatrix} 0 & 0 \\ 0 & 0 \\ 0 & 0 \\ 0 & 0 \\ 0 & 0 \\ 0 & 0 \\ 0 & 0 \\ -\dfrac{0.5}{J_S} & -\dfrac{0.5}{J_S} \\ 0 & 0 \\ 0 & 0 \\ 0 & 0 \\ 0 & 0 \\ 0 & 0 \\ 0 & 0 \\ 0 & 0 \\ -\dfrac{0.5}{J_S} & -\dfrac{0.5}{J_S} \end{bmatrix},$$

$$F_4 = \begin{bmatrix} 0 & 0 \\ 0 & 0 \\ 1 & 0 \\ 0 & 0 \\ 0 & 0 \\ 0 & 0 \\ 0 & 0 \\ 0 & 0 \\ 0 & 0 \\ 0 & 0 \\ 0 & 1 \\ 0 & 0 \\ 0 & 0 \\ 0 & 0 \\ 0 & 0 \\ 0 & 0 \end{bmatrix}, \quad F_5 = \begin{bmatrix} 0 & 0 \\ 0 & 0 \\ 0 & 0 \\ 1 & 0 \\ 0 & 0 \\ 0 & 0 \\ 0 & 0 \\ 0 & 0 \\ 0 & 0 \\ 0 & 0 \\ 0 & 1 \\ 0 & 0 \\ 0 & 0 \\ 0 & 0 \\ 0 & 0 \\ 0 & 0 \end{bmatrix}, \quad F_6 = \begin{bmatrix} 0 & 0 & 0 & 0 \\ 0 & 0 & 0 & 0 \\ 1 & 0 & 0 & 0 \\ 0 & 1 & 0 & 0 \\ 0 & 0 & 0 & 0 \\ 0 & 0 & 0 & 0 \\ 0 & 0 & 0 & 0 \\ 0 & 0 & 0 & 0 \\ 0 & 0 & 0 & 0 \\ 0 & 0 & 1 & 0 \\ 0 & 0 & 0 & 1 \\ 0 & 0 & 0 & 0 \\ 0 & 0 & 0 & 0 \\ 0 & 0 & 0 & 0 \\ 0 & 0 & 0 & 0 \end{bmatrix}.$$

3.3 The Linear Model of the Elevator

The mathematic model presented in Section 3.1 is a nonlinear model. In this section, a linear model of the elevator is developed. The linear model will be used to construct the fuzzy model of the elevator in the future for the purpose of controller design.

The nonlinear dynamics of the elevator only exists in the hydraulic cylinders in the form of:

$$\dot{x}_{3L} = \frac{\beta\left[C_V w_L \sqrt{\frac{2}{\rho}} x_5 \sqrt{(P_s - x_{3L})} - C_1 A_{1oL} \sqrt{\frac{2}{\rho}} \sqrt{x_{3L}} - C_{12} A_{12L}(x_{3L} - x_{4L}) - A_1 x_{2L}\right]}{V_1 + A_1 x_{1L}}$$

$$\dot{x}_{4L} = \frac{\beta\left[-C_V w_L\sqrt{\frac{2}{\rho}}x_5\sqrt{x_{4L}-P_R} - C_2 A_{2oL}\sqrt{\frac{2}{\rho}}\sqrt{x_{4L}} + C_{12}A_{12L}\left(x_{3L}-x_{4L}\right) + A_2 x_{2L}\right]}{V_2 - A_2 x_{1L}}$$

$$\dot{x}_{3R} = \frac{\beta\left[C_V w_R\sqrt{\frac{2}{\rho}}x_{5R}\sqrt{P_S - x_{3R}} - C_1 A_{1oR}\sqrt{\frac{2}{\rho}}\sqrt{x_{3R}} - C_{12}A_{12R}\left(x_{3R}-x_{4R}\right) - A_1 x_{2R}\right]}{V_1 + A_1 x_{1R}}$$

$$\dot{x}_{4R} = \frac{\beta\left[-C_V w_R\sqrt{\frac{2}{\rho}}x_{5R}\sqrt{x_{4R}-P_R} - C_2 A_{2oR}\sqrt{\frac{2}{\rho}}\sqrt{x_{4R}} + C_{12}A_{12R}\left(x_{3R}-x_{4R}\right) + A_2 x_{2R}\right]}{V_2 - A_2 x_{1R}}$$

where, x_{3L} and x_{4L} are the pressures in the active and passive chambers of the left cylinder; x_{3R} and x_{4R} are the pressures of the right cylinder.

One way of transforming the above nonlinear dynamics into a linear model is to expand all nonlinear functions locally at certain operating point using techniques such as Taylor series. For an accurate approximation with this method, however, the nonlinear model needs to be linearized at many operating points. Instead, the approximate transfer function [77] of a hydraulic cylinder is used, given in the form of:

$$X_p(s) = \frac{4\beta A_p K_f}{\left(ms^2 + bs + K_s\right)\left(Vs + 4\beta K_{tp}\right) + 4\beta A_p{}^2 s} X_v(s) + \frac{1}{ms^2 + bs + K_s} f(s), \qquad (3.6)$$

where, X_p is the position of the piston which is x_1 in the model of (3.1); X_v is the servo valve opening which is x_5 in (3.1); f is the load to the cylinder which is $K_s lx_7$ in (3.1); β, A_p, b, V, and K_s are respectively the oil volume modulus, the chamber's section area

(A_1 and A_2), the cylinder damping, the null volume of the chamber, and the spring stiffness as defined in Table 3.2. K_f and K_{tp} are defined as:

$$K_f = C_V w \sqrt{\frac{2}{\rho}} \sqrt{\frac{P_s - (P_1 - P_2)_o}{2}}$$

$$K_{tp} = \frac{C_V w \sqrt{\frac{2}{\rho}} x_{vo}}{4\sqrt{\frac{P_s - (P_1 - P_2)_o}{2}}} + C_{12} A_{12} \tag{3.7}$$

where, P_1 and P_2 are the pressures in the active and passive chambers respectively (x_3 and x_4); $(P_1 - P_2)_o$ and x_{vo} - or equivalently $(x_3 - x_4)_o$ and x_{so} - are the pressure difference and valve opening at the linearization point (it thus can be inferred that the transfer function is a local approximation of the cylinder dynamics at $(P_1 - P_2)_o$ and x_{vo}); $C_V w \sqrt{\frac{2}{\rho}}$, P_S, and $C_{12}A_{12}$ are defined in Table 3.2.

By replacing X_p, X_v, and f with x_1, x_5 and $K_s l x_7$, the transfer functions of the two cylinders in the elevator are now in the forms of:

$$x_{1L}(s) = \frac{4\beta A_1 K_f}{\left(ms^2 + bs + K_{sL}\right)\left(Vs + 4\beta K_{tp}\right) + 4\beta A_1^2 s} x_{5L}(s) + \frac{K_{sL} l}{ms^2 + bs + K_{sL}} x_{7L}(s) \tag{3.8}$$

$$x_{1R}(s) = \frac{4\beta A_1 K_f}{\left(ms^2 + bs + K_{sR}\right)\left(Vs + 4\beta K_{tp}\right) + 4\beta A_1^2 s} x_{5R}(s) + \frac{K_{sR} l}{ms^2 + bs + K_{sR}} x_{7R}(s). \tag{3.9}$$

By transforming the transfer functions back to the state space form, a linear model of the elevator in the state space form, which is linearized at $(x_{3L} - x_{4L},\ \ x_{5L})_o$ and $(x_{3R} - x_{4R},\ \ x_{5R})_o$, is obtained in the following form:

$$\dot{x} = A_o x + Bu. \tag{3.10}$$

By varying $(x_{3L} - x_{4L},\ \ x_{5L})_o$ and $(x_{3R} - x_{4R},\ \ x_{5R})_o$, different linear models can be obtained. The program of constructing the linear models at different operating points is given in Appendix C. The value of matrix A_o at

$$(x_{3L} - x_{4L},\ \ x_{5L}\ \ x_{3R} - x_{4R}\ \ x_{5R})_o = (100\ \ 0.01\ \ 100\ \ 0.01)$$

is also given in Appendix C. In this research, 16 linear models are constructed at 16 different operating points.

3.4 Summary

In this chapter, the nonlinear mathematic model of the elevator, which will be used to construct the simulation model, is presented. Faults of the elevator are discussed and modeled as abrupt changes of parameters. For the purpose of control, a local model of hydraulic cylinders, which is linearized at certain operating point, is constructed.

CHAPTER 4

ADAPTIVE UNKNOWN INPUT OBSERVER FOR FAULT DETECTION AND ESTIMATION

In Chapter 3, the mathematical model of the elevator is built and the faults have been modeled as unexpected parameter changes. In this chapter, an Adaptive Unknown Input Observer [78,79] that integrates the UIO with parameters estimation will be developed. A UIO is constructed for disturbance decoupling first; an auxiliary input is added to the UIO so that the stability of the observer and the exponential convergence of all estimations are guaranteed if the given requirements on the input signals are satisfied. The advantage of the proposed observer is that the estimations of both unknown states and unknown parameters are free of disturbance.

4.1 Problem Statement

The problem addressed in this chapter is the joint state-parameter estimation of a linear system with structural disturbances. The dynamics of the system is described by the following equations:

$$\dot{x} = Ax + Bu + Ed + \phi\theta$$

$$y = Cx \tag{4.1}$$

where, $A \in R^{n\times n}$, $B \in R^{n\times m}$ and $C \in R^{r\times n}$ are respectively the system, input and output matrices; $E \in R^{n\times p}$ is the known distribution matrix of disturbances; $d \in R^{p}$ is the vector

of unknown disturbances; $\phi \in R^{n \times k}$ is a matrix of known signals, which can be linear or nonlinear functions of the output y and input u; $\theta \in R^k$ is a vector of unknown parameters.

The objective is to build a robust adaptive observer to evaluate all unknown states x and parameters θ with the available input u, measurement y and signal matrix ϕ. The stability of the observer and the convergence of all estimations to real values need to be guaranteed.

4.2 The Adaptive Unknown Input Observer

The adaptive unknown input observer, with $\hat{x}$ and $\hat{\theta}$ as the estimated values of x and θ, has the form of:

$$\dot{z} = Nz + TBu + Ky + T\phi\hat{\theta} + \Gamma\dot{\hat{\theta}}$$

$$\dot{\hat{\theta}} = \Sigma\Gamma^T C^T (y - C\hat{x})$$

$$\dot{\Gamma} = N\Gamma + T\phi$$

$$\hat{x} = z + Hy \tag{4.2}$$

where, z is an intermediate states vector and the matrices (H, T, K, N and $\sum$) in the observer are selected as:

$$N + N^T < 0$$

$$(HC - I)E = 0$$

$$T = I - HC$$

$$A - HCA - K_1 C = N$$

$$NH = K_2$$

$$K = K_1 + K_2$$

$$\Sigma = \Sigma^T > 0 . \tag{4.3}$$

It is noted that the updates of $\hat{\theta}$ and $\hat{x}$ involve an evolving variable matrix of Γ, which makes the observer a Linear Time-Varying (LTV) system. To facilitate the proof of the stability and convergence of the proposed observer, two lemmas regarding the stability of an LTV system are presented first.

Lemma 4.1: An LTV system as shown in:

$$\dot{x} = A(t)x \tag{4.4}$$

with $A(t) = A(t)^T \leq 0$ is uniformly exponentially stable if there exist positive constants T_o and α so that for any t_o, the following inequality holds:

$$\int_{t_o}^{t_o+T_o} \underline{\sigma}(t)\, dt \geq \alpha > 0 \tag{4.5}$$

where, $\underline{\sigma}$ is the minimum singular value of $A(t)$.

Proof:

According to [80] (Theorem 8.2, page 132), the norm of the state vector in the autonomous system (4.4) satisfies the following inequality:

$$\|x(t)\| \le \|x_o\| e^{\frac{1}{2}\int_{t_o}^{t} \lambda_{\max}(\tau)d\tau}, \; t \ge t_o \tag{4.6}$$

where, $\lambda_{\max(t)}$ is the maximum eigenvalue of $A(t) + A(t)^T$. For a symmetric matrix $A(t) = A(t)^T \le 0$, its singular values satisfy:

$$\sigma(t) = -\lambda[A(t)] = -\frac{1}{2}\lambda\left[A(t) + A(t)^T\right]. \tag{4.7}$$

Then it is obvious that:

$$\lambda_{\max}(t) = -2\underline{\sigma}(t), \tag{4.8}$$

which means:

$$\|x(t)\| \le \|x_o\| e^{-\int_{t_o}^{t} \underline{\sigma}(\tau)d\tau}. \tag{4.9}$$

Since one has $\underline{\sigma}(t) \ge 0$ and for any t_o

$$\int_{t_o}^{t_o+T_o} \underline{\sigma}(t)dt \ge \alpha > 0, \tag{4.10}$$

the following inequality is obtained:

$$\int_{t_o}^{t} \underline{\sigma}(\tau)\,d\tau$$
$$= \int_{t_o}^{t_o+T_o} \underline{\sigma}(\tau)\,d\tau + \int_{t_o+T_o}^{t_o+2T_o} \underline{\sigma}(\tau)\,d\tau + \ldots + \int_{t_o+nT_o}^{t} \underline{\sigma}(\tau)\,d\tau \qquad (4.11)$$
$$\geq n\alpha \geq (\frac{t-t_o}{T_o} - 1)\alpha > (\frac{t-t_o}{T_o})\alpha > 0$$

where,

$$n = floor\left(\frac{t-t_o}{T_o}\right) \quad . \qquad (4.12)$$

Therefore the following inequality holds:

$$\|x(t)\| \leq \|x_o\| e^{-(\frac{t-t_o}{T_o}-1)\alpha} \leq \|x_o\| e^{\alpha} e^{-\frac{\alpha}{T_o}(t-t_o)}, \qquad (4.13)$$

which means the system in (4.4) is uniformly exponentially stable (following the definition 6.5 in [80], page 101).

Q. E. D.

Remark 4.1: Lemma 4.1 claims that, for an autonomous LTV system (4.4) with a semi-negative-definite system matrix, the exponentially stable condition is that, over some constant time period, the integral of the norm of the system matrix is lower bounded by a nonzero value.

Lemma 4.2: If the system:

$$\begin{bmatrix} \dot{x}_1 \\ \dot{x}_2 \end{bmatrix} = \begin{bmatrix} A_1(t) & 0 \\ 0 & A_2(t) \end{bmatrix} \begin{bmatrix} x_1 \\ x_2 \end{bmatrix} \qquad (4.14)$$

is uniformly exponentially stable, the following system:

$$\begin{bmatrix} \dot{z}_1 \\ \dot{z}_2 \end{bmatrix} = \begin{bmatrix} A_1(t) & A_{12}(t) \\ 0 & A_2(t) \end{bmatrix} \begin{bmatrix} z_1 \\ z_2 \end{bmatrix} \tag{4.15}$$

is also uniformly exponentially stable if $\|A_{12}(t)\| \le \bar{\sigma}$ is upper bounded , where $\|\bullet\|$ is the 2-norm of a matrix.

Proof:

The solution to differential equation (4.15) has the form:

$$\begin{bmatrix} z_1 \\ z_2 \end{bmatrix} = \begin{bmatrix} \Phi_1(t,t_o) & \Phi_{12}(t,t_o) \\ 0 & \Phi_2(t,t_o) \end{bmatrix} \begin{bmatrix} z_{10} \\ z_{20} \end{bmatrix}, \tag{4.16}$$

where, $\Phi_1(t,t_o)$ and $\Phi_2(t,t_o)$ are the state transition matrices associated with $A_1(t)$ and $A_2(t)$; $[z_{10} \quad z_{20}]^T$ is the initial states vector at time t_o. It is obvious that the states of System (4.14) are:

$$\begin{bmatrix} x_1 \\ x_2 \end{bmatrix} = \begin{bmatrix} \Phi_1(t,t_o) & 0 \\ 0 & \Phi_2(t,t_o) \end{bmatrix} \begin{bmatrix} x_{10} \\ x_{20} \end{bmatrix}. \tag{4.17}$$

Since System (4.14) is uniformly exponentially stable, there exist positive constants γ_1, λ_1 γ_2 and λ_2 such that, for all $t \ge t_o$:

$$\|\Phi_1(t,t_o)\| \le \gamma_1 e^{-\lambda_1(t-t_o)}$$

$$\|\Phi_2(t,t_o)\| \le \gamma_2 e^{-\lambda_2(t-t_o)}. \tag{4.18}$$

By taking z_2 in System (4.15) as an external input to the dynamics of z_1, it is derived that:

$$z_1 = \Phi_1(t,t_o)z_{10} + \int_{t_0}^{t} \Phi_1(t,\tau)A_{12}(\tau)\Phi_2(\tau,t_o)z_{20}d\tau\,, \tag{4.19}$$

or equivalently:

$$z_1 = \Phi_1(t,t_o)z_{10} + \left(\int_{t_0}^{t} \Phi_1(t,\tau)A_{12}(\tau)\Phi_2(\tau,t_o)d\tau\right)z_{20}\,. \tag{4.20}$$

From Equation (4.16) one has:

$$z_1 = \Phi_1(t,t_o)z_{10} + \Phi_{12}(t,t_o)z_{20}\,. \tag{4.21}$$

Matrix $\Phi_{12}(t,t_o)$ thus has the form of:

$$\Phi_{12}(t,t_o) = \int_{t_0}^{t} \Phi_1(t,\tau)A_{12}(\tau)\Phi_2(\tau,t_o)d\tau\,. \tag{4.22}$$

With the norm property of:

$$\left\|\Phi_{12}(t,t_o)\right\| \le \int_{t_0}^{t} \left\|\Phi_1(t,\tau)\right\|\left\|A_{12}(\tau)\right\|\left\|\Phi_2(\tau,t_o)\right\|d\tau\,, \tag{4.23}$$

it is derived that:

$$\left\|\Phi_{12}(t,t_o)\right\| \le \bar{\sigma}\gamma_1\gamma_2\int_{t_0}^{t} e^{-\lambda_1(t-\tau)}e^{-\lambda_2(\tau-t_o)}d\tau\,. \tag{4.24}$$

Inequality (4.24) is the same as:

$$\left\|\Phi_{12}(t,t_o)\right\| \le \bar{\sigma}\gamma_1\gamma_2\int_{t_0}^{t} e^{-\lambda(t-t_0)}d\tau = \bar{\sigma}\gamma_1\gamma_2 e^{-\lambda(t-t_0)} \tag{4.25}$$

with $\lambda = \min(\lambda_1, \lambda_2)$.

From the norm property:

$$\left\|\begin{matrix}\Phi_1(t,t_o) & \Phi_{12}(t,t_o)\\ 0 & \Phi_2(t,t_o)\end{matrix}\right\| \le \left\|\begin{matrix}\left\|\Phi_1(t,t_o)\right\| & \left\|\Phi_{12}(t,t_o)\right\|\\ 0 & \left\|\Phi_2(t,t_o)\right\|\end{matrix}\right\|, \tag{4.26}$$

it is obtained that:

$$\left\|\begin{matrix}\Phi_1(t,t_o) & \Phi_{12}(t,t_o)\\ 0 & \Phi_2(t,t_o)\end{matrix}\right\| \le \left\|\begin{matrix}\gamma_1 e^{-\lambda_1(t-t_o)} & \bar{\sigma}\gamma_1\gamma_2 e^{-\lambda(t-t_0)}\\ 0 & \gamma_2 e^{-\lambda_2(t-t_o)}\end{matrix}\right\|. \tag{4.27}$$

The following inequality thus holds:

$$\left\|\begin{matrix}z_1\\ z_2\end{matrix}\right\| \le \left\|\begin{matrix}\gamma_1 e^{-\lambda_1(t-t_o)} & \bar{\sigma}\gamma_1\gamma_2 e^{-\lambda(t-t_0)}\\ 0 & \gamma_2 e^{-\lambda_2(t-t_o)}\end{matrix}\right\| \bullet \left\|\begin{matrix}z_{10}\\ z_{20}\end{matrix}\right\|. \tag{4.28}$$

Since for a matrix $M \in R^{m\times n}$, the following norm property holds:

$$\left\|M\right\| \le \sqrt{mn}\left|\bar{M}_{ij}\right|, \tag{4.29}$$

the following inequality is derived:

$$\left\|\begin{matrix}z_1\\ z_2\end{matrix}\right\| \le \gamma e^{-\lambda_o(t-t_o)}\left\|\begin{matrix}z_{10}\\ z_{20}\end{matrix}\right\|, \tag{4.30}$$

where, $|\bar{M}_{ij}|$ is the maximal absolute of all elements M_{ij} in M so that $|\bar{M}_{ij}| = \max|M_{ij}|$; $\gamma e^{-\lambda_0(t-t_0)}$ is the maximum element in the matrix. It thus follows that System (4.16) is uniformly exponentially stable.

Q. E. D.

Remark 4.2: The 2-norm of a matrix is an induced norm [82]. For a matrix G and two vectors a and b that satisfy:

$$b = Ga,$$

the 2-norm of G is defined as:

$$\|G\| = \max \frac{\|b\|_2}{\|a\|_2},$$

with

$$\|a\|_2 = \sqrt{\Sigma a_i^2}$$

$$\|b\|_2 = \sqrt{\Sigma b_i^2},$$

where a_i and b_i are the ith element of a and b respectively.

Remark 4.3: The 2-norm of $\|A_{12}(t)\|$ satisfies [82]:

$$\|A_{12}(t)\| = \bar{\sigma}[A_{12}(t)].$$

Therefore, the requirement on $A_{12}(t) \leq \bar{\sigma}$ is equivalently to:

$$\bar{\sigma}\left[A_{12}(t)\right] \leq \bar{\sigma},$$

which means the time-varying $\bar{\sigma}\left[A_{12}(t)\right]$ is upper bounded by $\bar{\sigma}$, where $\bar{\sigma}$ is any positive constant.

With the above two lemmas, the stability and convergence of the observer are summarized in the following theorem.

Theorem 4.1: For the system:

$$\dot{x} = Ax + Bu + Ed + \phi\theta$$

$$y = Cx \tag{4.31}$$

with unknown disturbances d and unknown parameters θ, a robust adaptive observer can be designed in the following form:

$$\dot{z} = Nz + TBu + Ky + T\phi\hat{\theta} + \Gamma\dot{\hat{\theta}}$$

$$\dot{\hat{\theta}} = \Sigma^{-1}\Gamma^{T}C^{T}(y - C\hat{x})$$

$$\dot{\Gamma} = N\Gamma + T\phi$$

$$\hat{x} = z + Hy \tag{4.32}$$

where, z is an intermediate states vector and the matrices (H, T, K, N and $\sum$) in the observer are selected as:

$$N + N^T < 0$$

$$(HC - I)E = 0$$

$$T = I - HC$$

$$A - HCA - K_1 C = N$$

$$NH = K_2$$

$$K = K_1 + K_2$$

$$\Sigma = \Sigma^T > 0 \quad . \tag{4.33}$$

The adaptive observer is uniformly exponentially stable and the estimated states and parameters converge to the real values in an exponential rate if the following conditions are satisfied:

1. $Rank(CE) = Rank(E)$;

2. $(A - HCA, C)$ is an observable pair;

3. $\int_{t_o}^{t_o+T_o} \underline{\sigma}\left(-\Sigma^{-1}\Gamma^T C^T C\Gamma\right) dt \geq \alpha > 0$, where α is any positive constant;

4. $\left\|\Sigma^{-1}\Gamma^T C^T C\right\| \leq \beta$, where β is any positive constant .

Proof:

The estimation error has the form of:

$$\begin{aligned}\dot{\tilde{x}} = Ax + Bu + Ed + \phi\theta - [Nz + TBu + KCx + T\phi\hat{\theta} + \Gamma\dot{\hat{\theta}}] \\ - HC(Ax + Bu + Ed + \phi\theta)\end{aligned}, \tag{4.34}$$

where $\tilde{x} = x - \hat{x}$.

After manipulations, Equation (4.34) can be written as:

$$\begin{aligned}\dot{\tilde{x}} = (A - HCA - KC)x + (I - HC - T)Bu + (I - HC)Ed \\ + (I - HC)\phi\theta - T\phi\hat{\theta} - Nz - \Gamma\dot{\hat{\theta}}\end{aligned}. \tag{4.35}$$

With $K = K_1 + K_2$, the above equation therefore becomes:

$$\begin{aligned}\dot{\tilde{x}} = (A - HCA - K_1C)x + (I - HC - T)Bu + (I - HC)Ed \\ + (I - HC)\phi\theta - T\phi\hat{\theta} - (Nz + K_2Cx) - \Gamma\dot{\hat{\theta}}\end{aligned}. \tag{4.36}$$

With the parameters selected as in (4.33) and:

$$\dot{\theta} = 0$$

$$\tilde{\theta} = \theta - \hat{\theta}, \tag{4.37}$$

Equation (4.36) is written as:

$$\dot{\tilde{x}} = Nx + T\phi\tilde{\theta} - (N\bar{x}) - \Gamma\dot{\hat{\theta}} = N\tilde{x} + T\phi\tilde{\theta} + \Gamma\dot{\tilde{\theta}}. \tag{4.38}$$

From (4.32), one has:

$$\dot{\Gamma} = N\Gamma + T\phi . \tag{4.39}$$

With:

$$\left(\tilde{x} - \dot{\Gamma}\tilde{\theta}\right) = \dot{\tilde{x}} - \dot{\Gamma}\tilde{\theta} - \Gamma\dot{\tilde{\theta}}, \tag{4.40}$$

it is derived that:

$$\left(\tilde{x} - \dot{\Gamma}\tilde{\theta}\right) = N\left(\tilde{x} - \Gamma\tilde{\theta}\right). \tag{4.41}$$

With the updating law of the estimated parameters as:

$$\dot{\tilde{\theta}} = \Sigma^{-1}\Gamma^T C^T (y - C\hat{x}) , \tag{4.42}$$

the dynamics of parameter errors is derived as:

$$\dot{\tilde{\theta}} = -\Sigma^{-1}\Gamma^T C^T C\tilde{x} \tag{4.43}$$

or equivalently:

$$\dot{\tilde{\theta}} = -\Sigma^{-1}\Gamma^T C^T C\left(\tilde{x} - \Gamma\tilde{\theta}\right) - \Sigma^{-1}\Gamma^T C^T C\Gamma\tilde{\theta} . \tag{4.44}$$

The dynamics of the adaptive observer is then changed to the form of:

$$\begin{bmatrix} \dot{\tilde{\theta}} \\ \left(\tilde{x} - \dot{\Gamma}\tilde{\theta}\right) \end{bmatrix} = \begin{bmatrix} -\Sigma^{-1}\Gamma^T C^T C\Gamma & -\Sigma^{-1}\Gamma^T C^T C \\ 0 & N \end{bmatrix} \begin{bmatrix} \tilde{\theta} \\ \left(\tilde{x} - \Gamma\tilde{\theta}\right) \end{bmatrix} . \tag{4.45}$$

Since $N+N^T<0$ and the condition 3 are satisfied, with Lemma 4.1, the following system:

$$\begin{bmatrix} \dot{\tilde{\theta}} \\ \dot{\left(\tilde{x}-\Gamma\tilde{\theta}\right)} \end{bmatrix} = \begin{bmatrix} -\Sigma^{-1}\Gamma^T C^T C\Gamma & 0 \\ 0 & N \end{bmatrix} \begin{bmatrix} \tilde{\theta} \\ \left(\tilde{x}-\Gamma\tilde{\theta}\right) \end{bmatrix} \tag{4.46}$$

is uniformly exponentially stable.

With condition 4 that $\left\|\Sigma^{-1}\Gamma^T C^T C\right\|$ is upper bounded, System (4.45) is also uniformly exponentially stable following Lemma 4.2. This implies that $\tilde{\theta}\to 0$ and $\left(\tilde{x}-\Gamma\tilde{\theta}\right)\to 0$ in an exponential rate.

Q. E. D.

Remark 4.4: The four conditions in the theorem above can be explained as follows:

Condition 1 is required as the measurement redundancy. Disturbances can be decoupled only when there are enough independent measurements in the system so that $(HC-I)E=0$ is solvable;

Condition 2 is required so that the poles of the observer, which are the eigenvalues of N, can be assigned freely with the feedback gain K_I;

Condition 3 is the persistent excitation requirement on the richness of signals matrix ϕ, which states that the filtered output Γ of ϕ must have enough energy in all channels;

Condition 4 is the requirement on the size of ϕ. Since the output matrix C and the selected parameter $\sum$ are all known, the upper boundedness of $\|\Sigma\Gamma^T C^T C\|$ implies the norm of ϕ is bounded.

4.3 Simulation Results for Fault Estimation

The proposed Adaptive Unknown Input Observer in the former section is applied to the fault estimation of the elevator. Three types of parameter faults are considered: the loss of the EHSV gains, the stiffness change of the springs and the hinge. The dynamics and the faults of the hydraulic system are taken as disturbance to the system. The mathematical model of the elevator and all faults was shown in Equation (3.5) of Chapter 3. According to (3.5), the parameter θ and its estimate are defined as:

$$\theta = \begin{bmatrix} \theta_1 \\ \theta_2 \\ \theta_3 \end{bmatrix}, \ \hat{\theta} = \begin{bmatrix} \hat{\theta}_1 \\ \hat{\theta}_2 \\ \hat{\theta}_3 \end{bmatrix};$$

the signal matrix ϕ is defined as:

$$\phi = \begin{bmatrix} F_1\phi_1 & F_2\phi_2 & F_3\phi_3 \end{bmatrix}.$$

In the simulations, the EHSV gain loss is modeled as the change of parameter k_v to 0.5 of its original value ($0.00337\ in/sec^2/mA$) for the left EHSV and to 0.4 for the right. The stiffness change of the spring for each cylinder is modeled as the change of parameter K_s to 5 times of its original value ($2.5\times10^5\ lbf/in$) for the left and to 3 times of its original value ($2.5\times10^5\ lbf/in$) for the right. The stiffness change of the hinge is

modeled as the change of parameter H_m to 10 times of its original value (8.594×10^3 *lbf-in/rad*). All faulty parameters change simultaneously at 1 second. To simulate the noise corrupted system, white noises are added to the measurements. The size of the noise added to each channel is 5 percent of that specific measurement. The simulation results of parameter estimations are shown in Figures 4.1 to 4.3. In each figure, the actual change of each parameter is shown as the dashed curve; the estimated parameter change is shown as the solid curve. The results of states estimation errors for x_1 to x_8 are shown in Figure 4.4, where, in each sub-figure, the solid curve is the state estimation of the left system and the dashed curve is the estimation of the right system.

From the results, it can be seen that the residuals –output estimation errors of the observer – response to the occurring faults instantaneously, which guarantees the prompt faults detection. The locations and magnitudes of the occurring faults are then evaluated quickly and accurately, even when the pressure dynamics and the faults of the hydraulic system are taken as unknown disturbances to the observer.

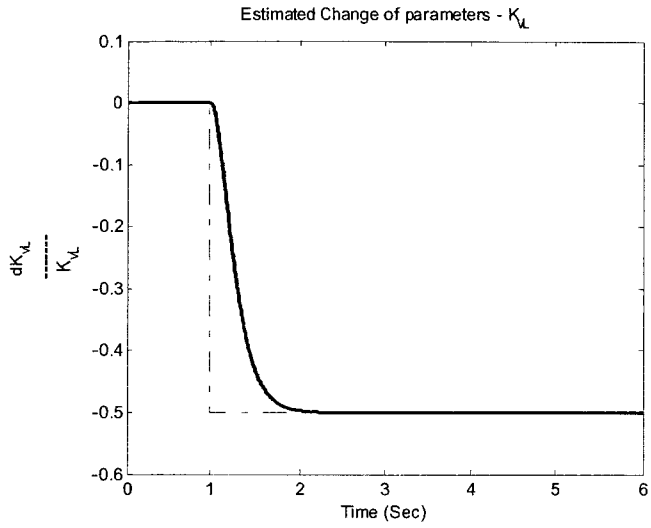

(a)

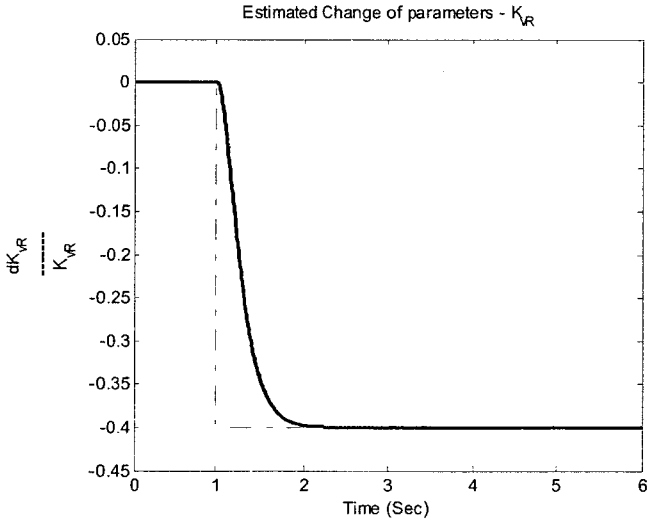

(b)

Figure 4.1 Estimation of k_v

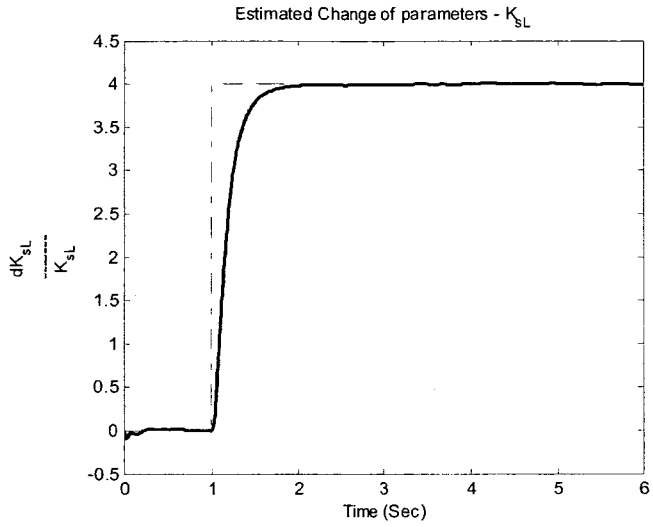

(a)

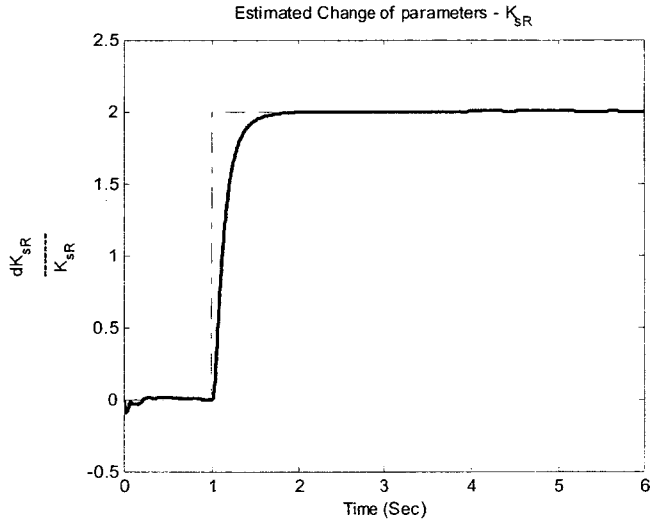

(b)

Figure 4.2 Estimation of K_s

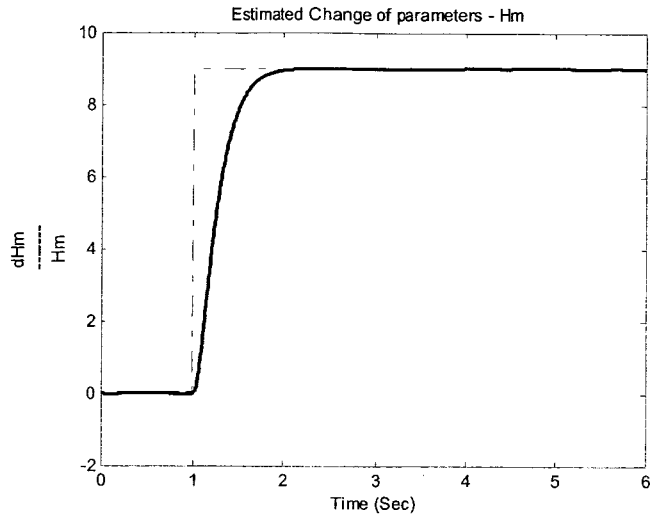

Figure 4.3 Estimation of H_m

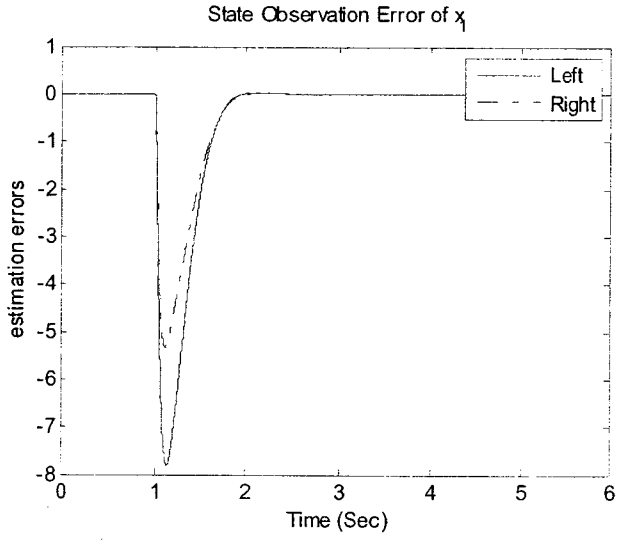

(a)

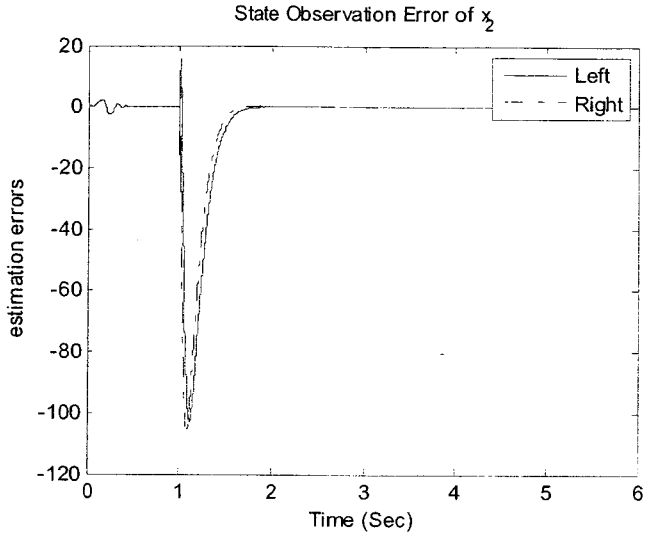
State Observation Error of x2
20
0
-20
-40
-60
-80
-100
-120
estimation errors
0
1
2
3
4
5
6
Time (Sec)
Left
Right

(b)

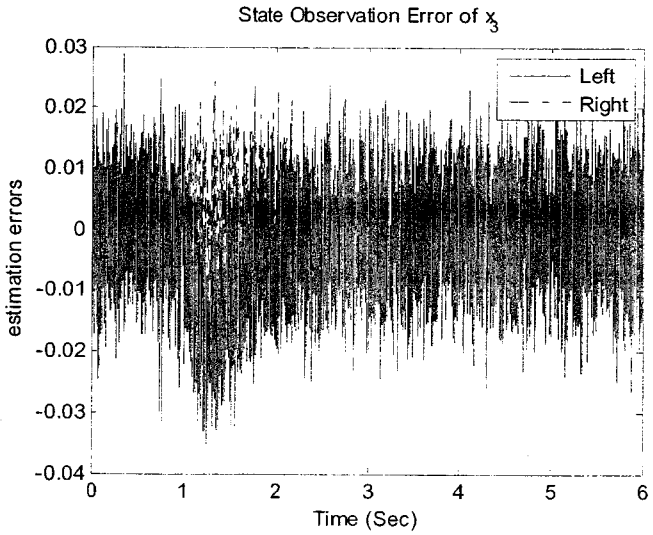
State Observation Error of x3
0.03
0.02
0.01
0
-0.01
-0.02
-0.03
-0.04
estimation errors
0
1
2
3
4
5
6
Time (Sec)
Left
Right

(c)

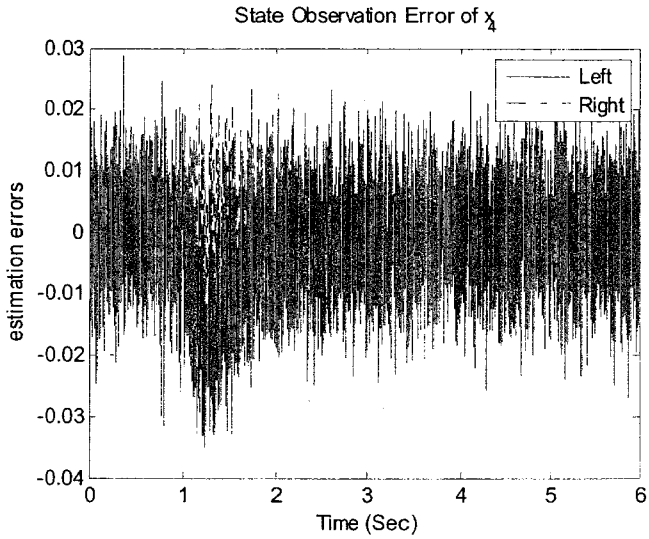
State Observation Error of x4
Left
Right
estimation errors
Time (Sec)
0.03
0.02
0.01
0
-0.01
-0.02
-0.03
-0.04
0
1
2
3
4
5
6

(d)

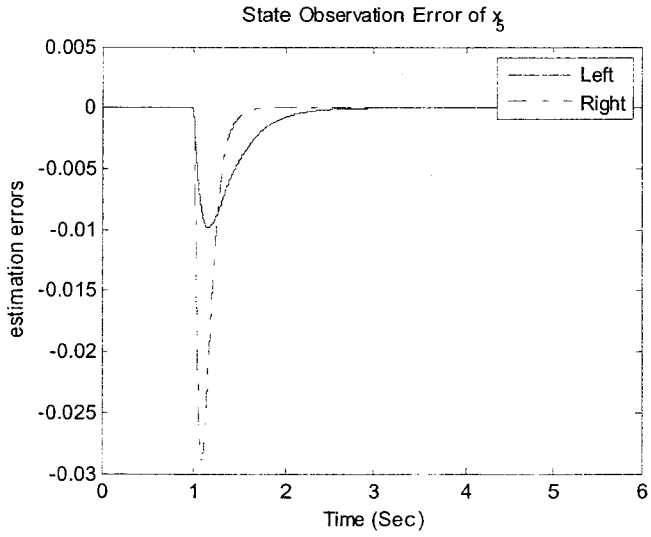
State Observation Error of x5
Left
Right
estimation errors
Time (Sec)
0.005
0
-0.005
-0.01
-0.015
-0.02
-0.025
-0.03
0
1
2
3
4
5
6

(e)

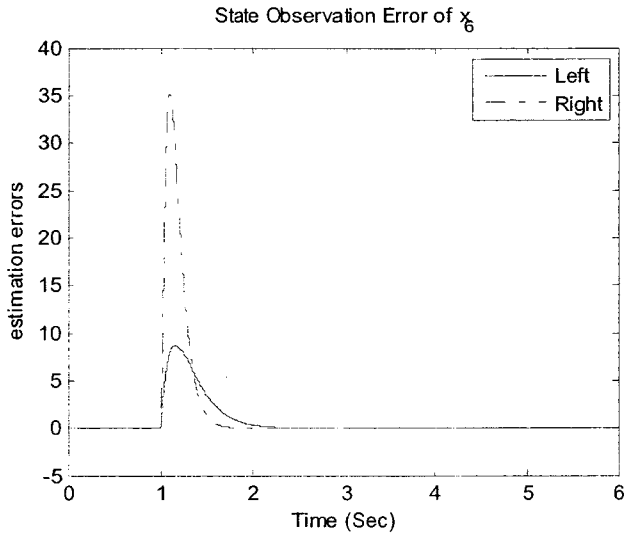
State Observation Error of x6
Left
Right
estimation errors
Time (Sec)
40
35
30
25
20
15
10
5
0
-5
0
1
2
3
4
5
6

(f)

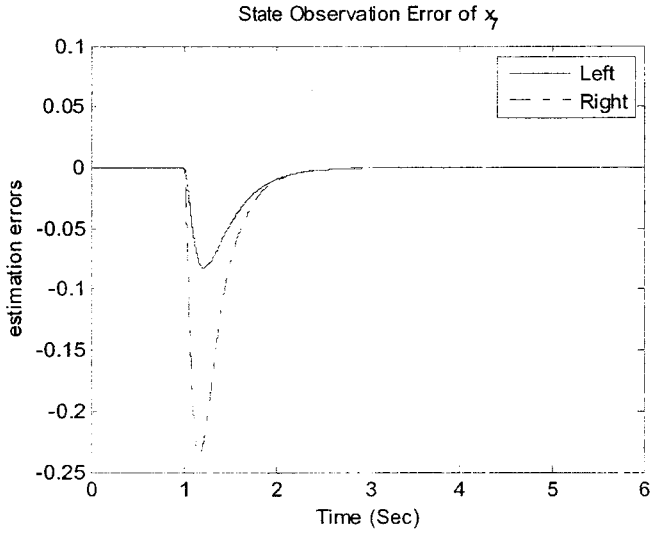
State Observation Error of x7
Left
Right
estimation errors
Time (Sec)
0.1
0.05
0
-0.05
-0.1
-0.15
-0.2
-0.25
0
1
2
3
4
5
6

(g)

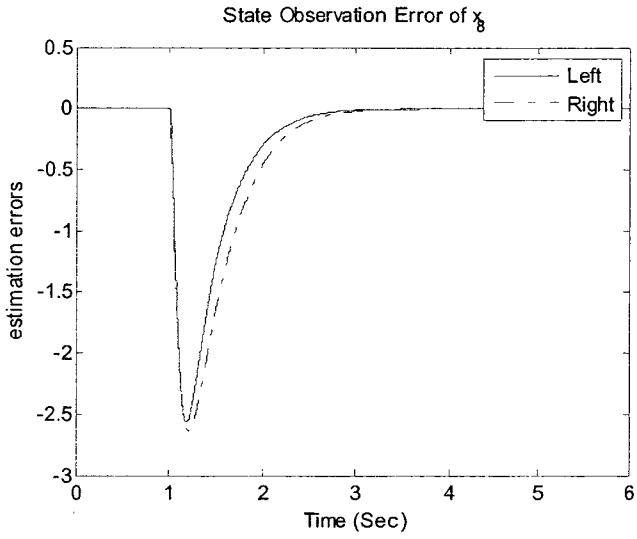

(h)

Figure 4.4 States estimation errors

4.4 Summary

In this chapter, an adaptive unknown input observer with the capability of disturbance rejection has been designed for the fault detection and estimation. The exponential stability of the observer and the exponential convergence of all estimations to the real values have been proved. The observer is then applied to the faulty parameters estimation of the elevator. Simulation results show that the estimations are accurate even when the system is subject to both unknown disturbances and measurement noises.

CHAPTER 5

UNITARY SYSTEM

In this chapter, a unitary system is defined as a multi-input multi-output (MIMO) linear time-invariant (LTI) system with a special property that all singular values of its transfer matrix are equal to each other. This chapter shows that, for an open-loop system satisfying certain requirement, a closed-loop unitary system can be constructed in a weighted observer form. The technique of Unitary System will be used in the next chapter to solve the H_∞ / H_- optimization problem.

5.1 Introduction

The singular values of a transfer matrix [81] are non-negative functions of frequency that determine the gains of the matrix. Important properties such as H_2 norm [82], H_∞ norm [83], and H_- index [42] are defined based on these singular values. In the theories of robust control, robust estimation, and model-based fault detection, one active research topic is about how to construct a closed-loop system with those properties being optimized.

As those properties present features of a system from different aspects, the singular values give a more detailed and accurate description of the system. However, the studies on the singular values and more importantly the studies on how to construct a closed-loop system with pre-defined singular values are still rare. The reason partially lies in the complexity of the singular values of a transfer matrix. In [84], it is shown that the singular values of a transfer matrix - more accurately, the square of the singular

values - are roots of a polynomial, whose coefficients are polynomials of complex variable s (usually taken as $s = j\omega$ with ω as frequency) and its conjugate. The authors thus concluded that these singular values, as functions of s, are locally analytical. In [85], the authors further proved that the "unordered unsigned" singular values, which belong to a set of real functions, are globally analytical. The analytical forms of these singular values (as functions of s), however, are not available for a generic transfer matrix.

Even though, the analytical forms of singular values are available for some specific systems such as the closed-loop unitary system discussed in this chapter. A unitary system is defined as a system whose singular values of the transfer matrix are equal to each other as functions of frequency.

The advantage of a unitary system is that the magnitude of its output depends only on the magnitude and frequency rather than the direction of the input. In a fault detection observer, such a property means that, for different faults with the same magnitude, the magnitude of the residuals is always the same independent of the type of faults. As introduced in Section 2.1, residuals are defined as the functions of faults. The deviation of residuals from zero, when exceeds some given thresholds, is taken as a sign of occurring faults. The selection of these thresholds depends on the size of faults as well as the transfer functions from faults to residuals. As these transfer functions are different, there is a threshold for each fault. In the fault isolation case with multiple residuals, multiple thresholds can be assigned. In the case of single observer for multiple faults detection, the threshold is usually chosen using the minimum gain of the transfer matrix from faults to the residual or the $H_{\_}$ index. As this is a conservative solution, false alarms

will occur. For the observer in the form of a unitary system, however, it is easy to select this threshold since the gains from different faults to the residuals are all the same.

5.2 Preliminary of Unitary System

Some preliminary information related to Unitary System [86] will be presented. In this section, for simplicity, only a square system, whose number of inputs and outputs are equal, will be discussed.

5.2.1 Singular value decomposition (SVD) of a transfer matrix

The SVD [82] of a constant complex matrix, $G \in C^{m \times m}$, has the form of:

$$G = U\Sigma V^{\sim}, \tag{5.1}$$

where $\Sigma = diag(\sigma_1, \sigma_2, \ldots \sigma_m)$ is a diagonal matrix consisting of m non-negative real singular values (σ_i); U and V are unitary complex matrices such that $UU^{\sim} = V^{\sim}V = I$ (the sign of "$\sim$" denotes the transpose of the conjugate).

As a matrix presents the linear transformation from one vector field to another, its singular values define the gains of transformation. If two vectors x and y satisfy:

$$y = Gx,$$

then the norms of the two vectors always satisfy:

$$\underline{\sigma}\|x\| \le \|y\| \le \bar{\sigma}\|x\|$$

where $\underline{\sigma}$ and $\bar{\sigma}$ are the smallest and the largest singular value respectively.

A multi-input multi-output (MIMO) linear time-invariant (LTI) system can be described by a transfer matrix. The elements of a transfer matrix are complex-valued transfer functions. The SVD of a transfer matrix $G(s) \in C^{m \times m}$ [81] is expressed in the form of:

$$G(s) = U(s)\Sigma(s)V^{\sim}(s) \tag{5.2}$$

with:

$$\Sigma(s) = diag[\sigma_1(s), \sigma_2(s), \ldots \sigma_m(s)]$$

$$U^{\sim}(s) = U^T(\bar{s})$$

$$V^{\sim}(s) = V^T(\bar{s})$$

$$U(s)U^{\sim}(s) = U^{\sim}(s)U(s) = V^{\sim}(s)V(s) = V(s)V^{\sim}(s) = I_m$$

where, $\bar{s}$ is the conjugate of s.

The only difference between equations (5.1) and (5.2) is that the SVD in (5.2) depends on the complex variable s which is usually taken as $s = j\omega$ where ω is frequency. Therefore, U, Σ and V are constant matrices; $U(s)$, $\Sigma(s)$ and $V(s)$ are matrices of functions of s (or equivalently, functions of ω).

The SVD of a transfer matrix always exists - at least in a numerical form, which is available by varying the frequency in $s = j\omega$ and taking SVD for the constant complex matrix of $G(j\omega)$. The analytical form of the SVD, however, is available only for the

transfer matrix in some special forms, such as the unitary system defined in the next section.

5.2.2 Definition of Unitary System

The singular values of a transfer matrix, which are non-negative real functions of frequency, define the magnitude frequency response of an MIMO system. Of all singular values, two of the most importance are the largest one $\bar{\sigma}(s)$ and the smallest one $\underline{\sigma}(s)$ which give the maximum and minimum possible gains of a system: if the system has an input $u(s)$ with a magnitude $\|u(s)\|$, then the magnitude of the output always satisfies:

$$\underline{\sigma}(s)\|u(s)\| \le \|y(s)\| \le \bar{\sigma}(s)\|u(s)\|. \tag{5.3}$$

where $\|\bullet\|$ denotes the norm of a vector.

Apparently the smaller the difference between these two singular values is, the less the variation of $\|y(s)\|$ is. In the case $\underline{\sigma}(s) = \bar{\sigma}(s)$, where these two and consequently all singular values are equal, $\|y(s)\|$ satisfies $\|y(s)\| = \bar{\sigma}(s)\|u(s)\| = \underline{\sigma}(s)\|u(s)\|$. Thus $\|y(s)\|$ depends only on the frequency and the magnitude of $u(s)$. In this section, a system with such a property is defined as a unitary system.

Definition: A stable linear multi-input multi-output system is defined as unitary if its transfer function matrix $G(s) \in C^{m\times m}$ satisfies:

$$\sigma_1(s) = \sigma_2(s) = \ldots = \sigma_m(s) \ , \tag{5.4}$$

where $\sigma_i(s)$ is the *ith* singular value of $G(s)$ so that the singular value decomposition of $G(s)$ has the form of:

$$G(s) = U(s)\begin{bmatrix} \sigma_1(s) & 0 & \dots & 0 \\ 0 & \sigma_2(s) & \dots & 0 \\ \vdots & \vdots & \ddots & \vdots \\ 0 & 0 & \dots & \sigma_m(s) \end{bmatrix} V^{\sim}(s) \tag{5.5}$$

with

$$U(s)U^{\sim}(s) = U^{\sim}(s)U(s) = V^{\sim}(s)V(s) = V(s)V^{\sim}(s) = I_m .$$

The advantage of a unitary system is that the magnitude of its output depends only on the magnitude and frequency rather than the direction (or component) of the input.

Property 1 of Unitary System: For a unitary system $G(s)$ shown in the above definition, $\sigma_i^2(s)$ is a rational function of s and:

$$\sigma_i^2(s) = \left(k^2 \frac{\prod_{j=1}^{n_z} (s - z_j)(\bar{s} - z_j)}{\prod_{l=1}^{n_p} (s - p_l)(\bar{s} - p_l)} \right)^{\frac{1}{m}}, \tag{5.6}$$

where z_j and p_l are the *jth* zero (transmission zero as defined in [87]) and the *lth* pole respectively; n_z and n_p are the numbers of zeros and poles; k denotes the constant gain of $\det(G(s))$.

Proof:

For a unitary system, the SVD of $G(s)$ is in the form of:

$$G(s) = U(s)\sigma_i(s)IV^{\sim}(s) = \sigma_i(s)U(s)V^{\sim}(s).$$

It thus can be derived that:

$$G(s)G^{\sim}(s) = \sigma_i(s)U(s)V^{\sim}(s)V(s)U^{\sim}(s)\sigma_i(s) = \sigma_i^2(s)I.$$

Since the diagonal elements of $G(s)G^{\sim}(s)$ are rational functions, $\sigma_i^2(s)$ is a rational function.

A useful property [81] of the singular values of $G(s)$ is:

$$\prod_{i=1}^{m}\sigma_i(s) = \left|\det\left(G(s)\right)\right| = \left|k\frac{\prod_{j=1}^{n_z}(s-z_j)}{\prod_{l=1}^{n_p}(s-p_l)}\right| \tag{5.7}$$

or

$$\prod_{i=1}^{m}\sigma_i^2(s) = k^2\frac{\prod_{j=1}^{n_z}(s-z_j)(\bar{s}-z_j)}{\prod_{l=1}^{n_p}(s-p_l)(\bar{s}-p_l)} \tag{5.8}$$

where $\det\left(G(s)\right)$ is the determinant of $G(s)$.

It therefore can be concluded that:

$$\sigma_i^{\,2}(s)=\left(k^2\frac{\prod_{j=1}^{n_z}(s-z_j)(\bar{s}-z_j)}{\prod_{l=1}^{n_p}(s-p_l)(\bar{s}-p_l)}\right)^{\frac{1}{m}}.$$

Q. E. D.

Property 2 of Unitary System: If a transfer matrix $G(s)\in C^{m\times m}$ is unitary with singular values as $\sigma(s)$, then all non-zero singular vales of $G_1(s)$ and $G_2(s)$ are equal to $\sigma(s)$, where $G_1(s)\in C^{m\times r}$ and $G_2(s)\in C^{m\times(m-r)}$ is a part of $G(s)$ in the form of:

$$G(s)=\left[G_1(s)\quad G_2(s)\right].$$

Proof:

Since $G(s)$ is unitary with singular values as $\sigma(s)$, then, with $U^*(s)=U(s)V^{\sim}(s)$, one has:

$$G(s)=U(s)\sigma(s)IV^{\sim}(s)=\sigma(s)U(s)V^{\sim}(s)=\sigma(s)U^*(s).$$

It thus can be obtained that:

$$G(s)=\left[G_1(s)\quad G_2(s)\right]=\sigma\left[U^*{}_1(s)\quad U^*{}_2(s)\right]$$

where, $G_1(s)=\sigma U^*{}_1(s)$; $G_2(s)=\sigma U^*{}_2(s)$; $U^*{}_1(s)\in C^{m\times r}$; $U^*{}_2(s)\in C^{m\times(m-r)}$; and $\left[U^*{}_1(s)\quad U^*{}_2(s)\right]=U^*(s)$.

The SVD of $U^*_1(s)$ and $U^*_2(s)$ has the form of:

$$U^*_1(s) = U_1(s)\begin{bmatrix} I_r \\ 0_{m\times(m-r)} \end{bmatrix} V_1^{\sim}(s)$$

$$U^*_2(s) = U_2(s)\begin{bmatrix} I_{(m-r)} \\ 0_{m\times r} \end{bmatrix} V_2^{\sim}(s),$$

where $U_1(s) \in C^{m\times m}$, $U_2(s) \in C^{m\times m}$, $V_1^{\sim}(s) \in C^{r\times r}$ and $V_2^{\sim}(s) \in C^{(m-r)\times(m-r)}$ are unitary matrices of proper dimensions.

It thus can be derived that:

$$G_1(s) = U_1(s)\begin{bmatrix} \sigma(s)I_r \\ 0_{m\times(m-r)} \end{bmatrix} V_1^{\sim}(s)$$

$$G_2(s) = U_2(s)\begin{bmatrix} \sigma(s)I_{(m-r)} \\ 0_{m\times r} \end{bmatrix} V_2^{\sim}(s).$$

Therefore, all non-zero singular vales of $G_1(s)$ and $G_2(s)$ are equal to $\sigma(s)$.

Q. E. D.

5.2.3 A closed-loop unitary system in a weighted observer form

For an open-loop system $G(s) \in C^{m\times m}$ with a minimal realization as:

$$G(s) = C(sI - A)^{-1} B \tag{5.9}$$

where $A \in R^{n\times n}$, $C \in R^{m\times n}$ and $B \in R^{n\times m}$, its state space presentation has the form of:

$$\dot{x} = Ax + Bu$$

$$y = Cx \tag{5.10}$$

where x are states, y are outputs, and u are generic unknown inputs. Only unknown inputs are considered in the observer design since known inputs can be cancelled from the dynamics of the observer. In the transfer matrix form, $y(s) = G(s)u(s)$. An observer for System (5.10) can be built as:

$$\dot{\hat{x}} = A\hat{x} - L(y - \hat{y})$$

$$\hat{y} = C\hat{x}\,. \tag{5.11}$$

The estimation errors are:

$$\tilde{x} = x - \hat{x}$$

$$\tilde{y} = y - \hat{y}$$

where

$$\dot{\tilde{x}} = (A + LC)\tilde{x} + Bu$$

$$\tilde{y} = C\tilde{x}\,. \tag{5.12}$$

The weighted estimation errors of the outputs are taken as $r = W\tilde{y}$ with W as a constant weight matrix so that $r(s) = G_U(s)u(s)$, where $G_U(s)$ is a closed-loop transfer matrix in a weighted observer form as:

$$G_U(s) = WC(sI - A - LC)^{-1}B. \tag{5.13}$$

The problem of constructing a closed-loop unitary system is to select L and W so that $G_U(s)$ is unitary.

It is not always possible to convert $G(s)$ to a unitary $G_U(s)$. However for System (5.9) or (5.10), the solution, which is given in next section, exists if the following conditions are satisfied:

1. $rank(CB) = m$ or equivalently CB is non-singular. This is a measurement requirement so that, if satisfied, the states in (5.10) can be classified into two groups through linear transformation: one group of measured states whose dynamics contains u explicitly and one group of unmeasured states whose dynamics does not contain u;

2. $G(s)$ does not have zeros on the imaginary axis. This is required for the purpose of fault detection. If $G(s)$ contains any zero on the imaginary axis, for example zeros at $\pm j\omega_o$, then the signal u of frequency ω_o, for example $u = \sin(\omega_o t)$, cannot be detected from y [32].

5.3 Constructing a Closed-Loop Unitary System

This section will present how to construct a closed-loop unitary system in the form of (5.13). For a square transfer matrix satisfying certain conditions, an exact solution is given first in Section 5.3.1 followed by an approximate solution for more general cases in Section 5.3.2. For a non-square open-loop system, as will be shown in Section 5.3.3, a closed-loop unitary system can be constructed by transforming the non-square transfer matrix into a square transfer matrix.

5.3.1 An exact solution

An exact solution is given in this section for System (5.10) satisfying the following two conditions:

1. $rank(CB) = m$;

2. $G(s)$ does not have zeros on the imaginary axis.

The open-loop system is transformed to a special form $G_r(s)$ by applying a first feedback (Lemma 5.1). Then it will be shown that all possible closed-loop systems in the form of (5.13) can be built from $G_r(s)$ with a second feedback (Lemma 5.2). In Lemma 5.3, it is shown that there exists a companion system $G_2(s) = G_r(s) + CB$ for $G_r(s)$ such that if $G_{2c}(s)$ - the closed-loop system of $G_2(s)$ with any feedback - is unitary, then $G_{rc}(s)$ - the closed-loop system of $G_r(s)$ with the same feedback - is also unitary. Lemma 5.4 and 5.5 demonstrate that there exists a feedback gain such that the singular

values of $G_{2c}(s)$ are equal to those of CB. Thus if the singular values of CB are equal to each other, which can always be satisfied for the non-singular CB through a weight matrix $W = (CB)^{-1}$, then $G_{2c}(s)$ is unitary. The method of constructing a closed-loop unitary system is summarized in Theorem 5.1 which follows the route of $G(s) \to G_r(s) \to G_2(s) \to G_{2c}(s) \to G_{rc}(s) \to G_U(s)$ with $G_U(s)$ as the closed-loop unitary system.

Lemma 5.1: A transfer matrix $G(s) = C(sI - A)^{-1}B$ with CB non-singular can be transformed to:

$$G_r(s) = C(sI - A - L_1C)^{-1}B = CB\frac{1}{s+k} \tag{5.14}$$

with a feedback L_1, where k is a selectable parameter.

Proof:

Since CB is non-singular, there always exists an invertible matrix T in the form of:

$$T = \begin{bmatrix} (CB)^{-1}C \\ B^{\perp} \end{bmatrix} \tag{5.15}$$

so that $C = [CB \quad 0]T$ and $TB = [I \quad 0]^T$, where $B^{\perp}$ is the transpose of the null space basis of B^T so that $B^{\perp}B = 0_{(n-m)\times m}$. With T, the original $G(s) = C(sI - A)^{-1}B$ can be transformed to:

$$G(s) = CT^{-1}(sI - \tilde{A})^{-1}TB = \begin{bmatrix} CB & 0 \end{bmatrix}(sI - \tilde{A})^{-1}\begin{bmatrix} I \\ 0 \end{bmatrix}, \tag{5.16}$$

where

$$\tilde{A} = TAT^{-1} = \begin{bmatrix} \tilde{A}_{11} & \tilde{A}_{12} \\ \tilde{A}_{21} & \tilde{A}_{22} \end{bmatrix}. \tag{5.17}$$

For any k, with:

$$\tilde{L}_1 = \begin{bmatrix} -\left(kI_m + \tilde{A}_{11}\right)(CB)^{-1} \\ -\tilde{A}_{21}(CB)^{-1} \end{bmatrix} \tag{5.18}$$

the closed-loop system has the form of:

$$\begin{aligned} G_r(s) &= CT^{-1}(sI - \tilde{A} - \tilde{L}_1 CT^{-1})^{-1}TB \\ &= CT^{-1}\left(sI - \begin{bmatrix} \tilde{A}_{11} & \tilde{A}_{12} \\ \tilde{A}_{21} & \tilde{A}_{22} \end{bmatrix} - \begin{bmatrix} -\left(kI_m + \tilde{A}_{11}\right) & 0 \\ -\tilde{A}_{21} & 0 \end{bmatrix} \right)^{-1} TB \\ &= CT^{-1}\begin{bmatrix} sI + kI_m & -\tilde{A}_{12} \\ 0 & sI - \tilde{A}_{22} \end{bmatrix}^{-1} TB \\ &= \begin{bmatrix} CB & 0 \end{bmatrix}\begin{bmatrix} \left(sI + kI_m\right)^{-1} & \Delta \\ 0 & \left(sI - \tilde{A}_{22}\right)^{-1} \end{bmatrix}\begin{bmatrix} I \\ 0 \end{bmatrix} \\ &= CB(s+k)^{-1}I_m \\ &= CB(s+k)^{-1} \end{aligned} \tag{5.19}$$

where Δ is a block matrix calculated from the inverse of the upper triangle block matrix.

Therefore, one has:

$$G_r(s) = C(sI - T^{-1}\tilde{A}T - T^{-1}\tilde{L}_1 C)^{-1}B = C(sI - A - T^{-1}\tilde{L}_1 C)^{-1}B = CB(s+k)^{-1}. \tag{5.20}$$

The transfer matrix $G(s)$ is transformed to the closed-loop system in (5.14) if the feedback gain is chosen as:

$$L_1 = T^{-1}\tilde{L}_1 . \tag{5.21}$$

Q. E. D.

Remark 5.1: For matrix $B^T \in R^{m\times n}$ $(m < n)$, its null space $N(B^T)$ contains all vectors z that satisfy $B^T z = 0$ so that $N(B^T) = \{z \in R^n : \ B^T z = 0\}$. $B^{\perp} \in R^{(n-m)\times n}$ is the transpose of the basis of $N(B^T)$ which means the range of $\left(B^{\perp}\right)^T$ is $N(B^T)$ so that $N(B^T) = \left\{\left(B^{\perp}\right)^T z_o : \ z_o \in R^{n-m}\right\}$. Thus for all $z_o \in R^{n-m}$, one has $B^T\left(B^{\perp}\right)^T z_o = 0$, which means $B^T\left(B^{\perp}\right)^T = 0_{m\times(n-m)}$, or $B^{\perp}B = 0_{(n-m)\times m}$.

With Lemma 1, the original system in (5.10) with n states is reduced to a closed-loop system in (5.14) whose minimal realization has only m states. Therefore, $G_r(s)$ has cancelled poles and zeros. From (5.14), it can be seen that the singular values of $G_r(s)$ is $|s+k|^{-1}\Sigma_{CB}$ where Σ_{CB} are the singular values of CB. This implies that, if all singular values of CB are equal, the singular values of $G_r(s)$ are also equal to each other. However as the hidden poles of $G_r(s)$ could not be determined, its stability cannot be guaranteed.

In the next step, it will be shown that a closed-loop system in the form of (5.13) can be built based on $G_r(s)$. A closed-loop unitary system thus can also be built based on $G_r(s)$, if it exists.

Lemma 5.2: A closed-loop system in the form of $G_c(s) = C(sI - A - LC)^{-1}B$ can always be expressed as:

$$G_c = \left[I - C(sI - A - L_1C)^{-1}L_2 \right]^{-1} CB\frac{1}{s+k} \tag{5.22}$$

with $L = L_1 + L_2$, where L_1 is selected as in Lemma 5.1.

Proof:

The closed-loop transfer matrix can be expressed as a serial connection of two systems as:

$$G_c(s) = C(sI - A - LC)^{-1}B = \left[I - C(sI - A)^{-1}L \right]^{-1} C(sI - A)^{-1}B, \tag{5.23}$$

which also means, with $L = L_1 + L_2$,

$$\begin{aligned} G_c(s) &= C(sI - A - L_1C - L_2C)^{-1}B \\ &= \left[I - C(sI - A - L_1C)^{-1}L_2 \right]^{-1} C(sI - A - L_1C)^{-1}B \end{aligned}. \tag{5.24}$$

By selecting L_1 as shown in Lemma 5.1, the closed-loop transfer matrix it is obtained as:

$$G_c(s) = \left[I - C(sI - A - L_1C)^{-1}L_2 \right]^{-1} G_r(s) = \left[I - C(sI - A - L_1C)^{-1}L_2 \right]^{-1} CB\frac{1}{s+k}. \tag{5.25}$$

Q. E. D.

From Lemma 5.2 it can be concluded that if there exists a closed-loop unitary system $G_U(s)$ for $G(s)$, it can be constructed from $G_r(s)$ in the form of $G_U(s) = WG_c(s)$.

Lemma 5.3: If the singular values of $G_{2c}(s)$ are $\Sigma(s)$, then the singular values of $G_{rc}(s)$ are:

$$\Sigma_{rc}(s) = |s+k+1|^{-1}\Sigma(s), \tag{5.26}$$

where:

$$G_{rc}(s) = C(sI - A - LC)^{-1}B \tag{5.27}$$

$$G_{2c}(s) = C(sI - A - LC)^{-1}(B + LCB) + CB \tag{5.28}$$

are, respectively, the closed-loop systems of:

$$G_r(s) = C(sI - A)^{-1}B = CB\frac{1}{s+k} \tag{5.29}$$

$$G_2(s) = G_r(s) + CB = C(sI - A)^{-1}B + CB. \tag{5.30}$$

Proof:

The closed-loop systems in (5.27) and (5.28) can be presented in the following forms:

$$G_{rc}(s) = \left[I - C(sI - A)^{-1}L\right]^{-1}C(sI - A)^{-1}B \tag{5.31}$$

$$G_{2c}(s) = \left[I - C(sI - A)^{-1} L \right]^{-1} \left[C(sI - A)^{-1} B + CB \right] \ . \tag{5.32}$$

Since the SVD of $G_{2c}(s)$ is:

$$\begin{aligned} G_{2c}(s) &= U(s)\Sigma(s)V^{\sim}(s) = \left[I - C(sI - A)^{-1} L \right]^{-1} CB\left(\frac{1}{s+k} + 1 \right) \\ &= \left[I - C(sI - A)^{-1} L \right]^{-1} CB\left(\frac{s+k+1}{s+k} \right) \end{aligned}, \tag{5.33}$$

it is obvious that:

$$G_{rc}(s) = \left[I - C(sI - A)^{-1} L \right]^{-1} CB\frac{1}{s+k} = G_{2c}(s)\frac{1}{s+k+1} = U(s)\frac{\Sigma(s)}{s+k+1}V^{\sim}(s). \tag{5.34}$$

Thus, the singular values of $G_{rc}(s)$ are $\Sigma_{rc}(s) = |s+k+1|^{-1}\Sigma(s)$.

Q. E. D.

From Lemma 5.3, it can be concluded that, if $G_{2c}(s)$ is unitary, $G_{rc}(s)$ is also unitary given $k+1>0$.

Lemma 5.4: A system $G(s) \in C^{m\times m}$, whose minimal realization is:

$$G(s) = C\left(sI - A\right)^{-1} B + D, \tag{5.35}$$

satisfies $G(s)G(-s)^T = G(s)G(s)^{\sim} = DD^T$ if D is invertible and there exists a positive definite Y such that the following equations hold:

$$AY + YA^T + BB^T = 0 \tag{5.36}$$

$$YC^T = -BD^T . \tag{5.37}$$

Proof:

From Equation (5.36), it is derived that $(sI - A)Y + Y(-sI - A)^T - BB^T = 0$, which means, by multiplying $C(sI - A)^{-1}$ to the left and $(-sI - A)^{-T} C^T$ to right:

$$C(sI - A)^{-1} YC^T + CY(-sI - A)^{-T} C^T - C(sI - A)^{-1} BB^T (-sI - A)^{-T} C^T = 0 . \tag{5.38}$$

Equation (5.38) is the same as:

$$\begin{aligned} &C(sI - A)^{-1} YC^T + CY(-sI - A)^{-T} C^T \\ &-\left[C(sI - A)^{-1} B + D\right]\left[C(-sI - A)^{-1} B + D\right]^T \\ &+DD^T + C(sI - A)^{-1} BD^T + DB^T (-sI - A)^{-1} C^T = 0 \end{aligned} \tag{5.39}$$

Thus if Equation (5.37) is satisfied, then:

$$-\left[C(sI - A)^{-1} B + D\right]\left[C(-sI - A)^{-1} B + D\right]^T + DD^T = 0 , \tag{5.40}$$

which means $G(s)G(-s)^T = DD^T$.

Q. E. D.

Lemma 5.5: The closed-loop system:

$$G_c(s) = C(sI - A - LC)^{-1}(B + LD) + D \tag{5.41}$$

satisfies $G_c(s)G_c(-s)^T = DD^T$ if the feedback gain L is chosen as:

$$L = -\left(YC^T + BD^T\right)\left(DD^T\right)^{-1}, \tag{5.42}$$

where Y is the solution to the following Algebraic Riccati equation:

$$\left(A - BD^{-1}C\right)Y + Y\left(A - BD^{-1}C\right)^T - YC^T D^{-T} D^{-1} CY = 0 \tag{5.43}$$

Proof:

Following Lemma 5.4, the sufficient condition for $G_c(s)G_c(-s)^T = DD^T$ is that Y and L are solutions to:

$$YC^T = -\left(B + LD\right)D^T \tag{5.44}$$

$$\left(A + LC\right)Y + Y\left(A + LC\right)^T + \left(B + LD\right)\left(B + LD\right)^T = 0, \tag{5.45}$$

which means $\left(B + LD\right) = -YC^T D^{-T}$ and:

$$AY + YA^T - LD\left(B + LD\right)^T - \left(B + LD\right)D^T L^T + \left(B + LD\right)\left(B + LD\right)^T = 0 \quad . \tag{5.46}$$

Since Equation (5.46) is the same as $AY + YA^T + BB^T - LDD^T L^T = 0$ and:

$$AY + YA^T - \left(B + LD\right)\left(B + LD\right)^T + B\left(B + LD\right)^T + \left(B + LD\right)B^T = 0, \tag{5.47}$$

it is derived that, with Equation (5.44), Y is the solution of:

$$AY + YA^T - YC^T D^{-T} D^{-1} CY - BD^{-1} CY - YC^T D^{-T} B^T = 0 \tag{5.48}$$

which is the same as Equation (5.43).

From Equation (5.44), L is designed as:

$$L = -\left(YC^T + BD^T\right)\left(DD^T\right)^{-1}.$$

Therefore, if equations (5.42) and (5.43) are satisfied, one has:

$$G_c(s)G_c(-s)^T = DD^T.$$

The above equation also means that the singular values of $G_c(s)$ are constants and equal to the singular values of D. Since Y is the positive-definite solution to the Algebraic Riccati equation (5.43), it is a positive definite matrix. With Equation (5.45), it can be concluded that $G_c(s)$ is stable. Therefore, if the singular values of D are all the same, $G_c(s)$ is a unitary system.

Theorem 5.1: For a linear multi-input multi-output system $G(s) \in C^{m\times m}$ with a minimal realization of:

$$G(s) = C\left(sI - A\right)^{-1} B, \tag{5.49}$$

if CB is non-singular and $G(s)$ does not have zeros on imaginary axis, then a unitary system can be constructed so that the singular values of the closed-loop system:

$$G_{ll}(s) = (CB)^{-1}C\left(sI - A - LC\right)^{-1} B \tag{5.50}$$

satisfy:

$$\sigma_1(s) = \sigma_2(s) = \ldots = \sigma_m(s) = |s + k + 1|^{-1}. \quad (5.51)$$

Moreover, the SVD of $G_U(s)$ has the form of:

$$G_U(s) = |s + k + 1|^{-1} U(s) \quad (5.52)$$

where, k is a selectable parameter and $k+1>0$; $U(s)$ is a unitary matrix as $U(s)U(s)^{\sim} = I$.

The feedback gain L in Equation (5.50) is calculated as:

$$L = L_1 + L_2, \quad (5.53)$$

where L_1 transforms the system $G(s)$ (following Lemma 5.1) to:

$$G_r(s) = C(sI - A - L_1C)^{-1} B = \frac{1}{s+k} CB; \quad (5.54)$$

and L_2 transforms (following Lemma 5.5):

$$G_2(s) = G_r(s) + CB \quad (5.55)$$

to:

$$G_{2c}(s) = C(sI - A - L_1C - L_2C)^{-1}(B + L_2CB) + CB \quad (5.56)$$

such that:

$$G_{2c}(s)G_{2c}{}^{T}(-s) = (CB)(CB)^{T}. \quad (5.57)$$

Proof:

It has been proven that System (5.49) can be transformed to $G_r(s)$ in Equation (5.54) with the feedback gain L_1 following Lemma 5.1. For $G_2(s)$, L_2 can also be calculated according to Lemma 5.5 so that Equation (5.57) is satisfied, where:

$$L_2 = -\left[YC^T + B(CB)^T\right]\left[(CB)(CB)^T\right]^{-1} \tag{5.58}$$

$$\left[A + L_1C - B(CB)^{-1}C\right]Y + Y\left[A + L_1C - B(CB)^{-1}C\right]^T - YC^T(CB)^{-T}(CB)^{-1}CY = 0. \tag{5.59}$$

By multiplying $(CB)^{-1}$ and $(CB)^{-T}$ to the left and right side of Equation (5.57) respectively, the following equation is obtained:

$$\left[(CB)^{-1}G_{2c}(s)\right]\left[(CB)^{-1}G_{2c}(-s)\right]^T = I,$$

which means $\left[(CB)^{-1}G_{2c}(s)\right]$ is a unitary system with singular values as *1*. From Lemma 5.3, $G_{rc}(s)$ can be built with the same feedback L_2 such that:

$$G_{rc}(s) = C(sI - A - L_1C - L_2C)^{-1}B = C(sI - A - LC)^{-1}B. \tag{5.60}$$

As $G_{rc}(s) = G_{2c}(s)/(s+k+1)$ from Equation (5.34), one has:

$$G_U(s) = (CB)^{-1}G_{rc}(s) = (CB)^{-1}G_{2c}(s)\frac{1}{s+k+1}. \tag{5.61}$$

Since the singular values of $\left[(CB)^{-1}G_{2c}(s)\right]$ are *1*, $G_U(s)$ is a unitary system with singular values of $|s+k+1|^{-1}$. The SVD of $G_U(s)$ therefore has the form of:

$$G_U(s) = U(s)|s+k+1|^{-1}V^{\sim}(s) = |s+k+1|^{-1}U(s)V^{\sim}(s) = |s+k+1|^{-1}U'(s) \qquad (5.62)$$

where $U'(s) = U(s)V^{\sim}(s)$ is also a unitary matrix.

Q. E. D.

Remark 5.2: The Algebraic Riccati equation (5.59) has a solution $Y > 0$ if $\left(A + L_1C - B(CB)^{-1}C,\ \ (CB)^{-1}C\right)$ is an observable pair and the following Hamilton matrix H does not have eigenvalues on the imaginary axis [50]:

$$H = \begin{bmatrix} A + L_1C - B(CB)^{-1}C & -C^T(CB)^{-T}(CB)^{-1}C \\ 0 & -\left(A + L_1C - B(CB)^{-1}C\right)^T \end{bmatrix}.$$

The observability requirement can be satisfied since Equation (5.49) is a minimal realization which is both observable and controllable. The eigenvalues requirement of H in the above form can be satisfied if the open-loop $G(s)$ does not have zeros on the imaginary axis. This is a reasonable assumption in faults detection studies. If $G(s)$ has a zero at $j\omega_o$, the lower bound of its response to a fault signal with frequency ω_o is zero, which means the fault cannot be detected.

Remark 5.3: $|s+k+1|^{-1}$ is the magnitude of the transfer function $1/(s+k+1)$. The singular values of $G_U(s)$ therefore present a first order magnitude frequency

response characteristic. $-(k+1)$ is the pole of the transfer function $1/(s+k+1)$. The difference between $G_{rc}(s)$ and $G_U(s)$ is an artificial weight of $(CB)^{-1}$. The singular values of $G_{rc}(s)$ are $|s+k+1|^{-1}\Sigma_{CB}$ which, although not necessarily equal to each other, are still the magnitudes of first order transfer functions. These transfer functions have the same pole $-(k+1)$ but with different gains.

5.3.2 An approximate solution

The non-singularity requirement of CB cannot always be satisfied. In such a case, an approximate solution is given in this section.

Lemma 5.6: For matrices $A, B \in C^{m\times m}$, their singular values satisfy the following [82]:

$$\bar{\sigma}(A \pm B) \le \bar{\sigma}(A) + \bar{\sigma}(B) \tag{5.63}$$

$$\underline{\sigma}(A) + \bar{\sigma}(B) \ge \underline{\sigma}(A \pm B) \ge \underline{\sigma}(A) - \bar{\sigma}(B) \tag{5.64}$$

$$\bar{\sigma}(AB) \ge \bar{\sigma}(A)\underline{\sigma}(B) \quad . \tag{5.65}$$

Lemma 5.7: If $A, B, C \in C^{m\times m}$, $U \in R^{m\times m}$ and $\sigma \in R^1$ satisfy the following 3 conditions:

1. $UU^T = I$;

2. $C = A(B + \sigma U)$;

3. All singular values of C are equal to σ as $\sigma_C = \sigma$,

then the following inequalities hold:

$$\bar{\sigma}(AB) - \sigma \le \sigma^2 / \left[\underline{\sigma}(B) - \sigma\right] \tag{5.66}$$

$$\bar{\sigma}(AB) - \underline{\sigma}(AB) \le 2\sigma^2 / \left[\underline{\sigma}(B) - \sigma\right] \tag{5.67}$$

where $\bar{\sigma}$ and $\underline{\sigma}$ denote the largest and smallest singular values.

Proof:

With $AB = C - \sigma AU$ and $\sigma_C = \sigma$, it is obvious from inequalities (5.64) and (5.65) that:

$$\bar{\sigma}(AB) \le \sigma + \bar{\sigma}(\sigma AU) = \sigma + \sigma\bar{\sigma}(A) \tag{5.68}$$

$$\underline{\sigma}(AB) \ge \sigma - \bar{\sigma}(\sigma AU) = \sigma - \sigma\bar{\sigma}(A) \tag{5.69}$$

which means $\bar{\sigma}(AB) - \sigma \le \sigma\bar{\sigma}(A)$ and $\bar{\sigma}(AB) - \underline{\sigma}(AB) \le 2\sigma\bar{\sigma}(A)$.

From inequality (5.66) and conditions 2 and 3, one has $\sigma \ge \bar{\sigma}(A)\underline{\sigma}(B + \sigma U)$ and thus the inequality $\bar{\sigma}(A) \le \sigma / \underline{\sigma}(B + \sigma U)$ holds. From inequality (5.65), we have $\underline{\sigma}(B + \sigma U) \ge \underline{\sigma}(B) - \sigma$, which means:

$$\bar{\sigma}(A) \le \sigma / \underline{\sigma}(B + \sigma U) \le \sigma / \left[\underline{\sigma}(B) - \sigma\right]. \tag{5.70}$$

It is thus derived that:

$$\bar{\sigma}(AB) - \sigma \le \sigma^2 / \left[\underline{\sigma}(B) - \sigma\right] \tag{5.71}$$

$$\bar{\sigma}(AB) - \underline{\sigma}(AB) \le 2\sigma^2 / \left[\underline{\sigma}(B) - \sigma\right] \quad . \tag{5.72}$$

Q. E. D.

Theorem 5.2: For a linear MIMO system $G(s) \in C^{m \times m}$ with a minimum realization of:

$$G(s) = C(sI - A)^{-1} B \tag{5.73}$$

and its companion system:

$$G_2(s) = G(s) + \sigma U = C(sI - A)^{-1} B + \sigma U \tag{5.74}$$

where U is any real unitary matrix, a feedback gain will transform the two systems in (5.73) and (5.74) to the following two closed-loop systems:

$$G_c(s) = C(sI - A - LC)^{-1} B \tag{5.75}$$

$$G_{2c}(s) = C(sI - A - LC)^{-1}(B + \sigma LU) + \sigma U \quad . \tag{5.76}$$

If the singular values of $G_{2c}(s)$ are all equal and satisfy:

$$\sigma\left[G_{2c}(s)\right] = \sigma \tag{5.77}$$

then the singular values of $G_c(s)$ satisfy the following inequalities:

$$\bar{\sigma}[G_c(s)] - \sigma \le \frac{\sigma}{\underline{\sigma}[G(s)]/\sigma - 1} \tag{5.78}$$

$$\bar{\sigma}[G_c(s)] - \underline{\sigma}[G_c(s)] \le \frac{2\sigma}{\underline{\sigma}[G(s)]/\sigma - 1}. \tag{5.79}$$

Proof:

The closed-loop transfer matrices in (5.76) and (5.77) are the same as:

$$G_c(s) = \left[I - C(sI - A)^{-1}L\right]^{-1} C(sI - A)^{-1}B \tag{5.80}$$

$$G_{2c}(s) = \left[I - C(sI - A)^{-1}L\right]^{-1}\left[C(sI - A)^{-1}B + \sigma U\right], \tag{5.81}$$

which also means that, with $G_L(s) = \left[I - C(sI - A)^{-1}L\right]^{-1}$,

$$G_c(s) = G_L(s)G(s) \tag{5.82}$$

$$G_{2c}(s) = G_L(s)\left[G(s) + \sigma U\right]. \tag{5.83}$$

If the singular values of $G_{2c}(s)$ are equal to σ, all 3 conditions of Lemma 5.7 are satisfied with $A = G_L(s)$, $B = G(s)$, and $C = G_{2c}(s)$. Thus the following inequalities hold:

$$\bar{\sigma}[G_c(s)] - \sigma \le \frac{\sigma}{\underline{\sigma}[G(s)]/\sigma - 1} \tag{5.84}$$

$$\bar{\sigma}\left[G_L(s)G(s)\right]-\underline{\sigma}\left[G_L(s)G(s)\right]\le\frac{\sigma^2}{\underline{\sigma}\left[G(s)\right]-\sigma}=\frac{\sigma}{\underline{\sigma}\left[G(s)\right]/\sigma-1} \quad . \tag{5.85}$$

Q. E. D.

According to Lemma 5.5, a feedback gain L can be calculated so that the singular values of $G_{2c}(s)$ are equal to those of σU. Since U is a selectable unitary real matrix, $G_{2c}(s)$ satisfies inequality (5.77). With the same L, $G_c(s)$ will satisfy inequalities (5.78) and (5.79).

As σ and U can be chosen as any values, an approximate unitary system can be built by selecting $\sigma << \underline{\sigma}\left[G(s)\right]$ for all $s = j\omega$ in the frequency range of interest, which means $\sigma << H_{\_}\left[G(s)\right]$. The inaccuracy of the approximation can be calculated with inequalities (5.78) and (5.79).

5.3.3 Solutions to a non-square system

Thus far, discussions only concerned a square transfer matrix with the same number of input and output. In this section, a non-square system in the following form is considered:

$$G(s) = C(sI - A)^{-1}B \tag{5.86}$$

where, $A \in R^{n\times n}$, $C \in R^{m\times n}$ and $B \in R^{n\times r}$ with the assumptions of:

1. $m > r$;

2. $rank(CB) = r$ so that CB has full column rank.

There are two ways of transforming (5.86) into a unitary system.

1. Reduce the dimension of C:

For such a system, a corresponding square system can be constructed as:

$$G_a(s) = W_1 C(sI - A)^{-1} B \tag{5.87}$$

where, $W_1 \in R^{r \times m}$ is a real constant matrix so that $rank(W_1 CB) = r$. If $G_a(s)$ does not have zeros on the imaginary axis, it satisfies all conditions required in Section 5.3.1. A closed-loop unitary system thus can be constructed for $G_a(s)$ in the form of:

$$G_u(s) = \left(W_1 CB\right)^{-1} W_1 C(sI - A - LC)^{-1} B. \tag{5.88}$$

2. Increase the dimension of B:

Another method is to construct a square transfer matrix in the following form:

$$G_b(s) = C(sI - A)^{-1} \begin{bmatrix} B & B_o \end{bmatrix} \tag{5.89}$$

where B_o is selected so that $rank\left(C\begin{bmatrix} B & B_o \end{bmatrix}\right) = m$. If $G_b(s)$ does not have zeros on the imaginary axis, it satisfies all conditions required in Section 5.3.1. A closed-loop unitary system thus can be constructed for $G_b(s)$ in the form of:

$$G_u(s) = \left(C\begin{bmatrix} B & B_o \end{bmatrix}\right)^{-1} C(sI - A - LC)^{-1} \begin{bmatrix} B & B_o \end{bmatrix}. \tag{5.90}$$

Moreover, according to Property 2 of Unitary System, all non-zero singular values of

$$G_{u1}(s) = \left(C\begin{bmatrix} B & B_o \end{bmatrix}\right)^{-1} C(sI - A - LC)^{-1} B$$

are equal.

5.4 Examples

In this section, two examples are given to illustrate the procedures of constructing a closed-loop unitary system.

Example 1: In this example, a closed-loop unitary system in the form of:

$$G_U(s) = (CB)^{-1} C(sI - A - LC)^{-1} B$$

is constructed for an open-loop system:

$$G(s) = C(sI - A)^{-1} B,$$

which is adopted from [37] with:

$$A = \begin{bmatrix} -0.0139 & 0 & 0.0139 \\ 0 & -0.027 & 0.0139 \\ 0.0139 & 0.0139 & -0.0278 \end{bmatrix},\ B = \begin{bmatrix} 0.007 & 0 \\ 0 & 0.0131 \\ 0 & 0 \end{bmatrix},\ C = \begin{bmatrix} 143.7908 & 0 & 0 \\ 0 & 76.2566 & 0 \end{bmatrix}.$$

The first step is to find L_1 that transforms the original system into $G_r(s)$ form. With:

$$T = \begin{bmatrix} (CB)^{-1} C \\ B^{\perp} \end{bmatrix} = \begin{bmatrix} 143.7908 & 0 & 0 \\ 0 & 76.2566 & 0 \\ 0 & 0 & 1 \end{bmatrix}, \text{ and } \tilde{A} = TAT^{-1} = \begin{bmatrix} \tilde{A}_{11} & \tilde{A}_{12} \\ \tilde{A}_{21} & \tilde{A}_{22} \end{bmatrix},$$

the feedback gain L_1 is calculated as $L_1 = T^{-1}\tilde{L}_1$, where, with k selected as $k=10$:

$$\tilde{L}_1 = \begin{bmatrix} -\left(kI_2 + \tilde{A}_{11}\right)(CB)^{-1} \\ -\tilde{A}_{21}(CB)^{-1} \end{bmatrix}.$$

The closed-loop system then has the form of:

$$G_{rc}(s) = C(sI - A - L_1C)^{-1}B = CB/(s+11) = I_2/(s+11)$$

as $CB=I_2$ in this example. The companion system is constructed as:

$$G_2(s) = G_{rc}(s) + CB$$

and the Algebraic Riccati equation:

$$\left[A + L_1C - B(CB)^{-1}C\right]Y + Y\left[A + L_1C - B(CB)^{-1}C\right]^T - YC^T(CB)^{-T}(CB)^{-1}CY = 0$$

is solved for Y. The feedback gain L_2 is calculated as:

$$L_2 = -\left[YC^T + B(CB)^T\right]\left[(CB)(CB)^T\right]^{-1}.$$

Therefore, the feedback gain L transforms the original system to a closed-loop unitary system in the form of:

$$G_{U}(s) = C(sI - A - LC)^{-1}B$$

with singular values of $|s+11|^{-1}$, where:

$$L = L_1 + L_2 = \begin{bmatrix} -0.0764 & 0 \\ 0 & -0.1439 \\ -0.0001 & -0.0002 \end{bmatrix}.$$

The singular values plots of the open-loop $G(s)$ and the closed-loop $G_U(s)$ are shown in Figures 5.1 and 5.2.

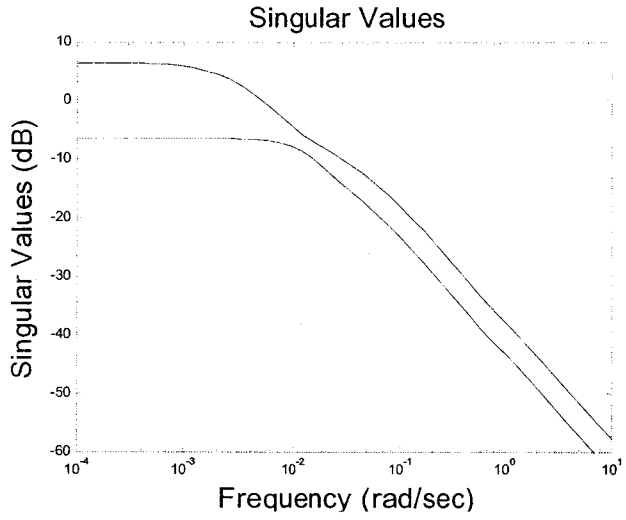

Figure 5.1 Example 1: singular values of the open-loop system

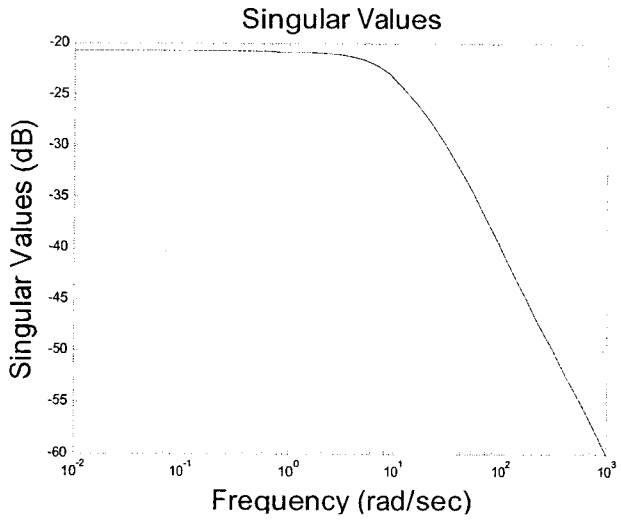

Figure 5.2 Example 1: singular values of the closed-loop system

Remark 5.4: Since $|s+k+1|^{-1}$ is the magnitude frequency response of the transfer function $1/(s+k+1)$, the singular values plot of the closed-loop system is the same as the bode magnitude plot of $1/(s+k+1)$. From Figure 5.1, it can be seen that all singular values of the close-loop system are equal to the magnitude of $1/(s+11)$ which is $(\omega^2+11^2)^{-1/2}$ as a function of frequency.

Example 2: In this example, a closed-loop unitary system:

$$G_U(s) = (CB)^{-1}C(sI-A-LC)^{-1}B$$

is constructed for an open-loop system:

$$G(s) = C(sI-A)^{-1}B,$$

which is randomly generated as:

$$A=\begin{bmatrix} 0.5046 & 0.0070 & 0.2952 & 1.2408 \\ 1.6265 & 0.4572 & 0.5554 & 1.8668 \\ 0.1535 & 0.0027 & 0.3623 & 1.9462 \\ 0.8160 & 0.3919 & 0.2873 & 0.4583 \end{bmatrix},\ B=\begin{bmatrix} 0.5529 & 0.6416 & 0.6332 \\ 0.7702 & 0.2557 & 1.4140 \\ 0.3895 & 0.0384 & 1.1211 \\ 0.1005 & 1.4039 & 0.0108 \end{bmatrix}$$

$$C=\begin{bmatrix} 0.7756 & 0.2396 & 0.4075 & 0.4421 \\ 0.7088 & 0.8486 & 0.9788 & 0.3494 \\ 0.6068 & 0.2505 & 0.9409 & 0.6687 \end{bmatrix}.$$

The first step is to find L_1 that transforms the original system into $G_r(s)$ form. With:

$$T=\begin{bmatrix} (CB)^{-1}C \\ B^{\perp} \end{bmatrix}=\begin{bmatrix} 0.7756 & 0.2396 & 0.4075 & 0.4421 \\ 0.7088 & 0.8486 & 0.9788 & 0.3494 \\ 0.6068 & 0.2505 & 0.9409 & 0.6687 \\ -0.4484 & 0.4916 & -0.3680 & 0.1255 \end{bmatrix},\ \text{and}\ \tilde{A}=TAT^{-1}=\begin{bmatrix} \tilde{A}_{11} & \tilde{A}_{12} \\ \tilde{A}_{21} & \tilde{A}_{22} \end{bmatrix},$$

the feedback gain L_1 is calculated as $L_1=T^{-1}\tilde{L}_1$, where, with k selected as $k=10$:

$$\tilde{L}_1=\begin{bmatrix} -\left(kI_2+\tilde{A}_{11}\right)(CB)^{-1} \\ -\tilde{A}_{21}(CB)^{-1} \end{bmatrix}.$$

The closed-loop system then has the form of:

$$G_{rc}(s)=C(sI-A-L_1C)^{-1}B=CB/(s+11).$$

The companion system is constructed as:

$$G_2(s)=G_{rc}(s)+CB$$

and the Algebraic Riccati equation:

$$\left[A+L_1C-B(CB)^{-1}C\right]Y+Y\left[A+L_1C-B(CB)^{-1}C\right]^T-YC^T(CB)^{-T}(CB)^{-1}CY=0$$

is solved for Y. The feedback gain L_2 is calculated as:

$$L_2=-\left[YC^T+B(CB)^T\right]\left[(CB)(CB)^T\right]^{-1}.$$

Therefore, the feedback gain L transforms the original system to a closed-loop unitary system in the form of:

$$G_U(s)=(CB)^{-1}C(sI-A-LC)^{-1}B$$

with singular values of $|s+1|^{-1}$, where:

$$L=L_1+L_2=\begin{bmatrix} -19.9902 & -0.3428 & 10.6200 \\ -5.0800 & -8.5893 & 6.8353 \\ 16.8744 & -4.1290 & -12.9409 \\ -8.6851 & 14.2991 & -16.4507 \end{bmatrix}.$$

The singular values plots of the open-loop $G(s)$ and the closed-loop $G_U(s)$ are shown in Figures 5.3 and 5.4.

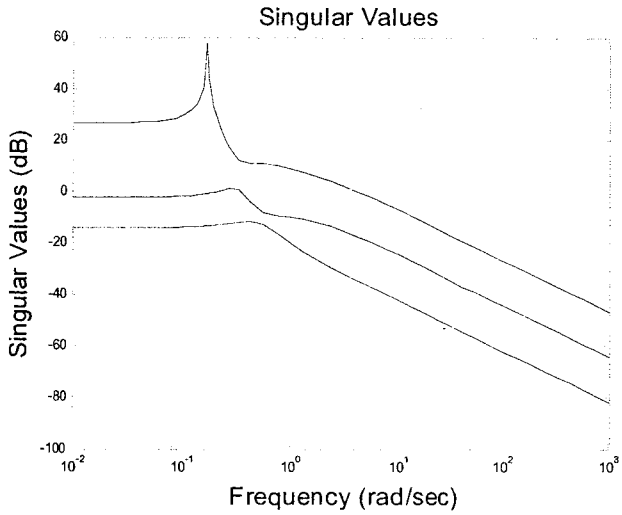

Figure 5.3 Example 2: singular values of the open-loop system

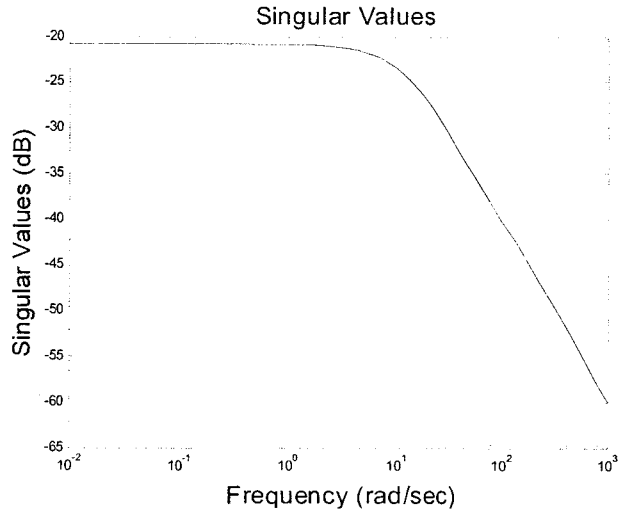

Figure 5.4 Example 2: singular values of the closed-loop system

Remark 5.5: In [85], it was shown that the "unordered unsigned" singular values, which belong to a set of real functions, are globally analytical. The analytical forms of

these functions are not available for a generic transfer matrix, which can be seen in the open-loop singular values plot. For a closed-loop unitary system, however, these functions are available in the form of $|s+k+1|^{-1}$, where k is a selectable parameter. Important properties of a transfer matrix, such as the H_2 and H_∞ norms thus can be determined from $|s+k+1|^{-1}$.

5.5 Summary

In this chapter, a unitary system is defined as a multi-input multi-output linear time-invariant system whose singular values of transfer matrix are equal. An open-loop system can be transformed to a closed-loop unitary system when certain requirements are met. For a strictly-proper open-loop system, the singular values of the corresponding closed-loop unitary system are $|s+k+1|^{-1}$, which is the magnitude frequency response of the transfer function $1/(s+k+1)$. With the method presented in this chapter, the singular values of the closed-loop unitary system thus can be assigned as a function of s in the form of $|s+k+1|^{-1}$ or equivalently, as a function of frequency in the form of $[\omega^2+(k+1)^2]^{-1/2}$. Singular-value-related properties of an MIMO system are therefore defined by the function $|s+k+1|^{-1}$.

CHAPTER 6

H_∞/H_- ADAPTIVE OBSERVER BASED ON UNITARY SYSTEM

Chapter 4 introduced the disturbance decoupled fault estimation with Adaptive Unknown Input Observer (AUIO). However, the measurement redundancy requirements on AUIO cannot be always met. A less restricted approach is to construct an optimized observer so that the response to faults is maximized whereas the response to disturbances is minimized. This approach is defined as H_∞/H_- optimization in the studies of fault detection. In this chapter, the H_∞/H_- optimization problem is solved for strictly-proper multi-input multi-output linear time-invariant systems with an approach of Unitary System.

6.1 H_∞/H_- Optimization

For a transfer matrix, H_∞ is the supremum of the largest singular value $\bar{\sigma}(s)$ in the considered frequency range of s and H_- is the infimum of the smallest singular value $\underline{\sigma}(s)$. Mathematically, H_∞ [50] and H_- [43] are defined as, for a transfer matrix $G(s)$ in a given frequency range $[0 \quad \Omega]$:

$$H_\infty[G(s)] = \sup_{\omega\in[0\ \ \Omega]} \bar{\sigma}[G(s)]_{s=j\omega} \tag{6.1}$$

$$H_-[G(s)] = \inf_{\omega\in[0\ \ \Omega]} \underline{\sigma}[G(s)]_{s=j\omega}. \tag{6.2}$$

The H_x/H_- optimization is a combined optimization which, in the area of fault detection, seeks the balance between robustness and sensitivity. Consider a system with two unknown inputs d and f in the following form:

$$\dot{x} = Ax + Ed + Ff$$

$$y = Cx\,, \tag{6.3}$$

where d and f are disturbances and faults respectively, $A \in R^{n\times n}$, $E \in R^{n\times p}$, $F \in R^{n\times m}$, $C \in R^{m\times n}$. An observer for the purpose of fault detection can be designed as:

$$\dot{\hat{x}} = A\hat{x} - L\left(y - \hat{y}\right)$$

$$\hat{y} = C\hat{x} \qquad . \tag{6.4}$$

The estimation errors $\tilde{x} = x - \hat{x}$ and $\tilde{y} = y - \hat{y}$ thus have the form of:

$$\dot{\tilde{x}} = \left(A + LC\right)\tilde{x} + Ed + Ff$$

$$\tilde{y} = C\tilde{x} \qquad . \tag{6.5}$$

The residuals are defined as the weighted estimation errors:

$$r = W\tilde{y} \tag{6.6}$$

where $W \in R^{m\times m}$ is a weight matrix. In the transfer matrix form, it is represented as:

$$r(s) = G_{rd}(s)d(s) + G_{rf}(s)f(s) \tag{6.7}$$

where:

$$G_{rd}(s) = WG_{dc}(s)$$

$$G_{rf}(s) = WG_{fc}(s) \tag{6.8}$$

with:

$$G_{dc}(s) = C\left(sI - A - LC\right)^{-1} E$$

$$G_{fc}(s) = C\left(sI - A - LC\right)^{-1} F \tag{6.9}$$

as the closed-loop transfer matrices from the disturbances and faults to the estimation error $\tilde{y}$.

The structure of a fault detection observer is shown in Figure 6.1. The objective of fault detection is that, by observing the residuals, the occurring faults f can be detected even with the interference of disturbances d. From Equation (6.7), it can be seen that the residuals have two contributors as disturbances and faults, which means r will stay at zero in the steady state for a disturbance-free and fault-free system. For such a system, any occurring fault can be detected since r will deviate from zero accordingly. In a practical system, however, disturbances cannot be totally avoided. The H_∞/H_- optimization is to minimize the influence of disturbances on the residuals (or keep the

influence under certain level) and meanwhile maximize that of faults so that the fault detection observer has both the robustness to disturbances and the sensitivity to faults.

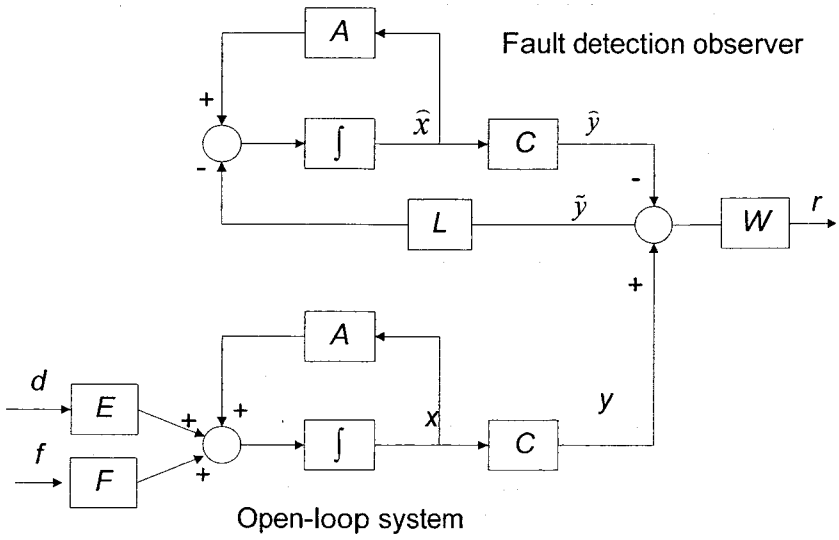

Figure 6.1 Fault detection observer

The measurement of the robustness to disturbance is taken as $H_{\infty}[G_{rd}(s)]$ since one has:

$$\|G_{rd}(s)d(s)\| \le H_{\infty}[G_{rd}(s)]\|d(s)\|. \tag{6.10}$$

Similarly, the measurement of the sensitivity to faults $f(s)$ is taken as $H_{-}[G_{rf}(s)]$ since one has:

$$\|G_{rf}(s)f(s)\| \ge H_{-}[G_{rf}(s)]\|f(s)\|. \tag{6.11}$$

To increase the robustness to disturbances, it is desirable to reduce $H_\infty[G_{rd}(s)]$. To increase the sensitivity to faults, it is required to increase $H_-[G_{rf}(s)]$. To obtain the best balanced robustness and sensitivity, the H_∞/H_- optimization is formulated to:

$$\min_{W,L} \frac{H_\infty[G_{rd}(s)]}{H_-[G_{rf}(s)]} \tag{6.12}$$

with the selection of constant matrices $W \in R^{m\times m}$ and $L \in R^{n\times m}$.

As $G_{rf}(s)$ is strictly-proper, its H_- is always zero over the whole frequency range, which means, for System (6.3), the optimization cannot be solved without considering the frequency range. In this chapter, the frequency range is set as $\omega \in [0 \quad \Omega]$ with Ω as any selected upper bound.

6.2 A Unitary System Solution to the H_∞/H_- Optimization

The following shows the procedure to solve the H_∞/H_- optimization problem discussed in Section 6.1:

$$\min_{W,L} \frac{H_\infty[G_{rd}(s)]}{H_-[G_{rf}(s)]}, \qquad s = j\omega,\ \omega \in [0 \quad \Omega]. \tag{6.13}$$

The closed-loop transfer functions can be expressed in the following forms:

$$G_{rd}(s) = WG_L(s)G_d(s) = W\left[I - C(sI - A)^{-1}L\right]^{-1} C(sI - A)^{-1}E \tag{6.14}$$

$$G_{rf}(s) = WG_L(s)G_f(s) = W\left[I - C(sI - A)^{-1}L\right]^{-1} C(sI - A)^{-1}F \tag{6.15}$$

where,

$$G_L(s) = \left[I - C(sI - A)^{-1}L\right]^{-1}, \tag{6.16}$$

$$G_d(s) = C(sI - A)^{-1}E, \tag{6.17}$$

$$G_f(s) = C(sI - A)^{-1}F. \tag{6.18}$$

The H_∞/H_- optimization problem is thus equivalent to the problem of:

$$\min_{W,L}\left\{\frac{H_\infty[WG_L(s)G_d(s)]}{H_-[WG_L(s)G_f(s)]}\right\} \tag{6.19}$$

by selecting W and L, where $s = j\omega$ and $\omega \in [0 \quad \Omega]$. In [32], the solution to the general problem of:

$$\min\left\{\frac{H_\infty[G(s)G_d(s)]}{H_-[G(s)G_f(s)]}\right\} \tag{6.20}$$

is given as:

$$G(s) = \sigma_o N(s)G_f^{-1}(s). \tag{6.21}$$

where σ_o is any constant value and $N(s)N^{\sim}(s) = I$, where $N^{\sim}(s) = N^T(\bar{s})$ is the conjugate transpose of $N(s)$. The minimal value is:

$$\min\left\{\frac{H_\infty[G(s)G_d(s)]}{H_-[G(s)G_f(s)]}\right\} = H_\infty\left[G_f^{-1}(s)G_d(s)\right]. \tag{6.22}$$

Although $G_f^{-1}(s)$ cannot be obtained practically for a strictly-proper $G_f(s)$, Equation (6.22) still gives the theoretical minimum to the optimization problem of (6.19), where $G(s)$ in (6.20) and (6.21) can be replaced with $WG_L(s)$.

Theorem 6.1: For System (6.3) with non-singular CF, if $G_f(s) = C(sI - A)^{-1}F$ does not have zeros on the imaginary axis, then there exists a feedback gain L and a weight matrix $W = (CF)^{-1}$ so that:

$$G_{rf}(s) = WC(sI - A - LC)^{-1}F$$

is unitary with singular values $|s + k + 1|^{-1}$; the obtained L and W also solve the H_∞/H_- optimization problem (6.13) so that the following inequalities hold:

$$\frac{H_\infty[G_{rd}(s)]}{H_-[G_{rf}(s)]} \le \frac{\sqrt{\Omega^2 + (k+1)^2}}{|k+1|} H_\infty\left[G_f^{-1}(s)G_d(s)\right] \tag{6.23}$$

$$\frac{H_\infty[G_{rd}(s)]}{H_-[G_{rf}(s)]} \ge H_\infty\left[G_f^{-1}(s)G_d(s)\right] \tag{6.24}$$

where $H_\infty\left[G_f^{-1}(s)G_d(s)\right]$ is the theoretical optimum.

Proof:

By taking $W = (CF)^{-1}$, the following is obtained:

$$\frac{H_\infty[G_{rd}(s)]}{H_-[G_{rf}(s)]} = \frac{H_\infty[(CF)^{-1}C(sI-A-LC)^{-1}E]}{H_-[(CF)^{-1}C(sI-A-LC)^{-1}F]} \quad . \tag{6.25}$$

According to Theorem 5.1 in Chapter 5, there exists an L that transforms $C(sI-A)^{-1}F$ to a closed-loop unitary system in the form of:

$$G_{rf}(s) = (CF)^{-1}C(sI-A-LC)^{-1}F .$$

Also from Theorem 5.1, the closed-loop system satisfies:

$$G_{rf}(s) = |s+k+1|^{-1}U(s) .$$

With closed-loop transfer matrix (6.15), it is then derived that:

$$WG_L(s) = |s+k+1|^{-1}U(s)G_f^{-1}(s) .$$

Thus from closed-loop transfer matrix (6.14), the following equation is obtained:

$$\frac{H_\infty[G_{rd}(s)]}{H_-[G_{rf}(s)]} = \frac{H_\infty[|s+k+1|^{-1}U(s)G_f^{-1}(s)G_d(s)]}{H_-[|s+k+1|^{-1}U(s)]} . \tag{6.26}$$

For $s = j\omega$ and $\omega \in [0 \quad \Omega]$, it is derived that:

$$\begin{aligned} H_\infty[G_{rd}(s)] &= H_\infty[|s+k+1|^{-1}U(s)G_f^{-1}(s)G_d(s)] \\ &= \sup_\omega \{|j\omega+k+1|^{-1}\bar{\sigma}[G_f^{-1}(j\omega)G_d(j\omega)]\} \end{aligned} \tag{6.27}$$

which means the following inequalities hold:

$$H_\infty\left[G_{rd}(s)\right] \le \max_\omega \left|j\omega+k+1\right|^{-1} H_\infty\left[G_f^{-1}(j\omega)G_d(j\omega)\right] = \left|k+1\right|^{-1} H_\infty\left[G_f^{-1}(j\omega)G_d(j\omega)\right] \tag{6.28}$$

$$H_\infty\left[G_{rd}(s)\right] \ge \min_\omega \left|j\omega+k+1\right|^{-1} H_\infty\left[G_f^{-1}(j\omega)G_d(j\omega)\right] = \frac{1}{\sqrt{\Omega^2+(k+1)^2}} H_\infty\left[G_f^{-1}(j\omega)G_d(j\omega)\right]. \tag{6.29}$$

On the other hand, $H_-\left[G_{rf}(s)\right]$ is calculated as:

$$\begin{aligned} H_-\left[G_{rf}(s)\right] &= H_-\left[\left|s+k+1\right|^{-1}U(s)\right] = \inf_\omega \underline{\sigma}\left[\left|j\omega+k+1\right|^{-1}U(j\omega)\right] \\ &= \min_\omega \left|j\omega+k+1\right|^{-1} = 1/\sqrt{\Omega^2+(k+1)^2} \end{aligned} \tag{6.30}$$

Thus the following inequality holds:

$$\sqrt{\Omega^2/(k+1)^2+1}\,H_\infty\left[G_f^{-1}(s)G_d(s)\right] \ge \frac{H_\infty\left[G_{rd}(s)\right]}{H_-\left[G_{rf}(s)\right]} \ge H_\infty\left[G_f^{-1}(s)G_d(s)\right]. \tag{6.31}$$

Q. E. D.

Remark 6.1: The above have shown that the theoretical minimum of the H_∞/H_- optimization is $H_\infty\left[G_f^{-1}(s)G_d(s)\right]$. For a strictly-proper $G_f(s)$, its inverse $G_f^{-1}(s)$ is an improper transfer matrix, which cannot be constructed practically. Therefore, the theoretical minimum of the H_∞/H_- optimization is not realizable if $G_f(s)$ is strictly-proper. However by transforming $G_{rf}(s)$ into a closed-loop unitary system, the H_∞/H_- of the observer can approximate closely to the theoretical optimum by selecting a large

$|k+1|$. The result in Theorem 6.1 is at most $\sqrt{\Omega^2/(k+1)^2+1}-1$ times larger than the theoretical optimum. The difference can be further reduced by increasing $|k+1|$.

The absolute value of $H_-\left[G_{rf}(s)\right]$ can be increased with a smaller $|k+1|$ as shown in Equation (6.30). However, the value of H_∞/H_- might be also increased since its upper bound has increased according to inequality (6.31).

6.3 H_∞/H_- Adaptive Observer

The procedure from Section 6.2 with respect to the H_∞/H_- optimization is adopted here to construct the H_∞/H_- Adaptive Observer.

Theorem 6.2: For a system in the form of:

$$\dot{x} = Ax + F\phi\theta + Ed \tag{6.32}$$

an H_∞/H_- adaptive observer can be constructed in the following form:

$$\dot{\hat{x}} = A\hat{x} - Ly + F\phi\hat{\theta} + \Gamma\dot{\hat{\theta}}$$

$$\dot{\hat{\theta}} = \Sigma^{-1}\Gamma^T C^T W^T W(y - C\hat{x})$$

$$\dot{\Gamma} = (A+LC)\Gamma + F\phi \tag{6.33}$$

where the feedback gain L and the weight W are calculated in the same way as the H_∞/H_- optimization in Section 6.2. All the estimations of the observer converge to their real values if the disturbance d is zero. If the disturbance is not zero, the estimation error of

θ is optimized for disturbance rejection. The convergence requirements are similar to those of the adaptive unknown input observer, which are listed below as:

1. $\int_{t_o}^{t_o+T_o} \underline{\sigma}\left(-\Sigma^{-1}\Gamma^T C^T C\Gamma\right) dt \geq \alpha > 0$ for a constant T_o, where α is any positive constant;

2. $\left\|\Sigma^{-1}\Gamma^T C^T C\right\| \leq \beta$, where β is any positive constant.

Proof:

From (6.32) and (6.33), it can be obtained that:

$$\left(\dot{\tilde{x}} - \Gamma\dot{\tilde{\theta}}\right) = (A+LC)\tilde{x} + F\phi\tilde{\theta} - \Gamma\dot{\hat{\theta}} + Ed - \dot{\Gamma}\tilde{\theta} - \Gamma\dot{\tilde{\theta}} \tag{6.34}$$

where

$\tilde{x} = x - \hat{x}$

$\tilde{\theta} = \theta - \hat{\theta}$.

With (6.34), it is derived that:

$$\left(\dot{\tilde{x}} - \Gamma\dot{\tilde{\theta}}\right) = (A+LC)\left(\tilde{x} - \Gamma\tilde{\theta}\right) + Ed \tag{6.35}$$

Since the following equality:

$$\dot{\hat{\theta}} = \Sigma^{-1}\Gamma^T C^T W^T W(y - C\hat{x}) \tag{6.36}$$

is equivalent to:

$$\dot{\tilde{\theta}} = -\Sigma^{-1}\Gamma^T C^T W^T WC\left(\tilde{x} - \Gamma\tilde{\theta}\right) - \Sigma^{-1}\Gamma^T C^T W^T WC\Gamma\tilde{\theta}\ , \tag{6.37}$$

the estimations thus follow:

$$\begin{bmatrix} \dot{\tilde{\theta}} \\ \dot{\left(\tilde{x} - \Gamma\tilde{\theta}\right)} \end{bmatrix} = \begin{bmatrix} -\Sigma^{-1}\Gamma^T C^T W^T WC\Gamma & -\Sigma^{-1}\Gamma^T C^T W^T WC \\ 0 & (A + LC) \end{bmatrix} \begin{bmatrix} \tilde{\theta} \\ \left(\tilde{x} - \Gamma\tilde{\theta}\right) \end{bmatrix} + \begin{bmatrix} 0 \\ E \end{bmatrix} d\ . \tag{6.38}$$

If d is zero, the convergence of the estimation can be proved since System (6.38) is the same as System (4.45) in Chapter 4. By taking the updating rate as:

$$\Sigma = \frac{1}{a}\Gamma^T C^T W^T WC\Gamma \tag{6.39}$$

with $a > 0$, the estimation error of θ has the form of:

$$\dot{\tilde{\theta}} = -a\left(\Gamma^T C^T W^T WC\Gamma\right)^{-1}\Gamma^T C^T W^T WC\left(\tilde{x} - \Gamma\tilde{\theta}\right) - a\tilde{\theta} \tag{6.40}$$

Thus the magnitude of the estimation error $\tilde{\theta}$ depends only on the magnitude of:

$$\left(\Gamma^T C^T W^T WC\Gamma\right)^{-1}\Gamma^T C^T W^T WC\left(\tilde{x} - \Gamma\tilde{\theta}\right). \tag{6.41}$$

From (6.33) and (6.38), one can derive that:

$$WC\Gamma = G_{rf}\phi$$

$$WC\left(\tilde{x} - \Gamma\tilde{\theta}\right) = G_{rd}d\ , \tag{6.42}$$

where:

$$G_{rf} = G_{rf}(s) = WC(sI - A - LC)^{-1}F$$

$$G_{rd} = G_{rd}(s) = WC(sI - A - LC)^{-1}E. \tag{6.43}$$

Therefore, (6.41) has the form of:

$$\begin{aligned}&\left(\Gamma^T C^T W^T WC\Gamma\right)^{-1}\Gamma^T C^T W^T WC\left(\tilde{x} - \Gamma\tilde{\theta}\right)\\&= \left(\phi^T {G_{rf}}^T G_{rf}\phi\right)^{-1}\phi^T {G_{rf}}^T G_{rd}d = \left(G_{rf}\phi\right)^{\dagger} G_{rd}d\end{aligned} \tag{6.44}$$

where,

$$\left(G_{rf}\phi\right)^{\dagger} = \left(\phi^T {G_{rf}}^T G_{rf}\phi\right)^{-1}\phi^T {G_{rf}}^T \tag{6.45}$$

is the pseudo-inverse of $\left(G_{rf}\phi\right)$.

Since one has:

$$\left(G_{rf}\phi\right)^{\dagger} = \left(\phi\right)^{\dagger} {G_{rf}}^{-1}, \tag{6.46}$$

for an invertible G_{rf}, (6.41) is thus equal to

$$\left(\Gamma^T C^T W^T WC\Gamma\right)^{-1}\Gamma^T C^T W^T WC\left(\tilde{x} - \Gamma\tilde{\theta}\right) = \left(\phi\right)^{\dagger} {G_{rf}}^{-1} G_{rd}d. \tag{6.47}$$

Thus the magnitude of the estimation error $\tilde{\theta}$ depends on:

$$\left\|(\phi)^{\dagger} G_{rf}^{-1} G_{rd} d\right\|. \tag{6.48}$$

Since, the following inequality holds:

$$\left\|(\phi)^{\dagger} G_{rf}^{-1} G_{rd} d\right\| \le \left\|\phi^{\dagger} G_{rf}^{-1}\right\| \left\|G_{rd} d\right\| \le \left\|\phi^{\dagger}\right\| H_{\infty}\left(G_{rf}^{-1}\right) \cdot H_{\infty}\left(G_{rd}\right) \|d\| \tag{6.49}$$

the upper bound of the estimation error is:

$$\left\|\phi^{\dagger}\right\| H_{\infty}\left(G_{rf}^{-1}\right) \cdot H_{\infty}\left(G_{rd}\right) \|d\|. \tag{6.50}$$

Therefore, (6.48) is minimized if only the following is minimized:

$$H_{\infty}\left(G_{rf}^{-1}\right) \cdot H_{\infty}\left(G_{rd}\right) = \frac{H_{\infty}\left(G_{rd}\right)}{H_{-}\left(G_{rf}\right)}, \tag{6.51}$$

which is the same as the H_{∞}/H_{-} optimization problem discussed in Section 6.2. Therefore, if L and W are selected through the H_{∞}/H_{-} optimization, the estimation error of θ is minimized.

Q. E. D.

Remark 6.2: From Equation (6.37), it can be seen that the dynamics of the estimation errors is time variant. The convergence rate of the estimation therefore depends not only on the system matrix $A+LC$ but also the signal matrix of Γ, which is a function of ϕ. To reduce the influence of Γ on the convergence rate, it is a common choice to select Σ proportional to the square magnitude of Γ such as in Equation (6.39). To avoid the singularity, Σ is practically designed as:

$$\Sigma = \frac{1}{a}\left(\gamma I + \Gamma^T C^T W^T W C \Gamma\right), \tag{6.52}$$

where γ is a small positive constant.

6.4 Simulation Results for Fault Estimation

The H_∞/H_- adaptive observer is applied to the elevator for the hydraulic parameters estimation of the left system. These parameters include the leaking faults from the chambers to the environment - C_{1L} and C_{2L} - and the leaking faults between the active and passive chambers - C_{12L}. The mathematical model of the elevator and all faults was shown in Equation (3.5) of Chapter 3. According to (3.5), the parameter θ and its estimate are defined as:

$$\theta = \begin{bmatrix} \theta_4 \\ \theta_5 \\ \theta_6 \end{bmatrix}, \hat{\theta} = \begin{bmatrix} \hat{\theta}_4 \\ \hat{\theta}_5 \\ \hat{\theta}_6 \end{bmatrix};$$

the signal matrix ϕ is defined as:

$$\phi = diag\begin{bmatrix} \phi_4 & \phi_5 & \phi_6 \end{bmatrix};$$

F is defined as:

$$F = \begin{bmatrix} F_4 & F_5 & F_6 \end{bmatrix}.$$

Since these faults interact with each other, they cannot be estimated at the same time. The simultaneous estimation will cause the estimated parameters to converge to

false values, which can be seen in Figure 6.2: the real fault is the 9 times increase of C_{12} whereas the estimations of all three parameters converge to some different values. The false estimations cannot be detected since the output estimation error $\tilde{y}$ - pressures in the two chambers - converges to zero simultaneously as the estimated parameters converge to false values.

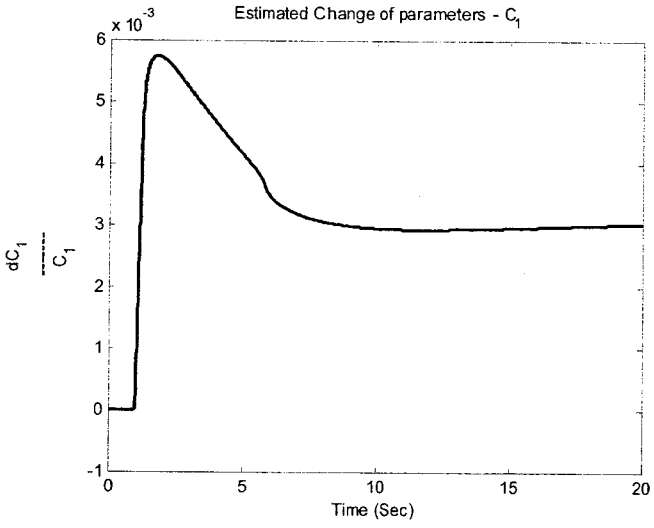

(a)

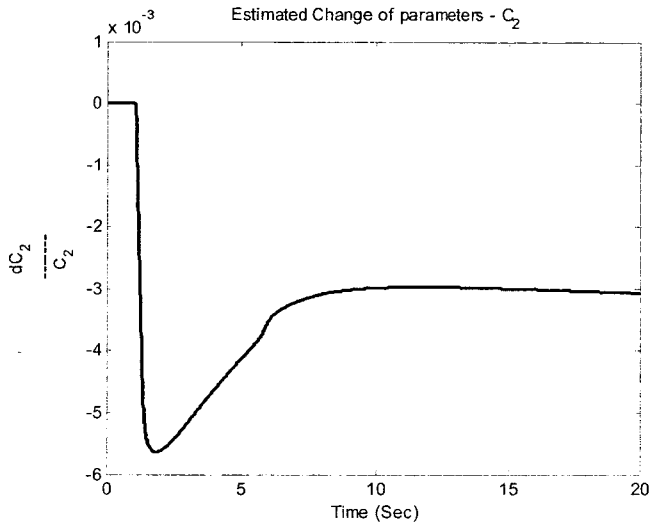
Estimated Change of parameters - C_2
x 10^{-3}
$\frac{dC_2}{C_2}$
1
0
-1
-2
-3
-4
-5
-6
0
5
10
15
20
Time (Sec)

(b)

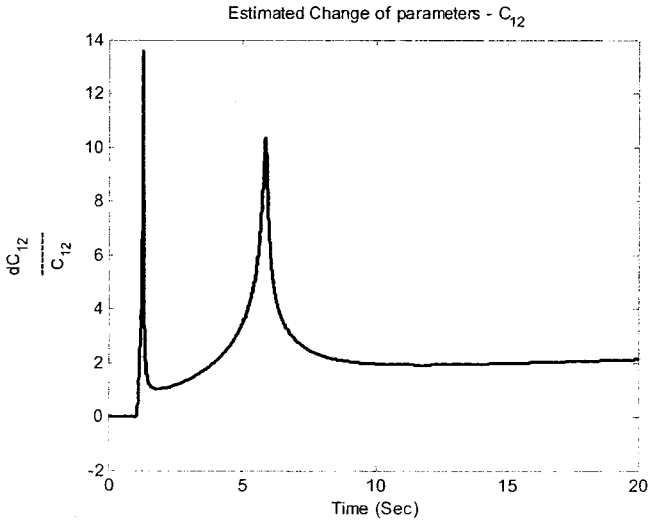
Estimated Change of parameters - C_{12}
$\frac{dC_{12}}{C_{12}}$
14
12
10
8
6
4
2
0
-2
0
5
10
15
20
Time (Sec)

(c)

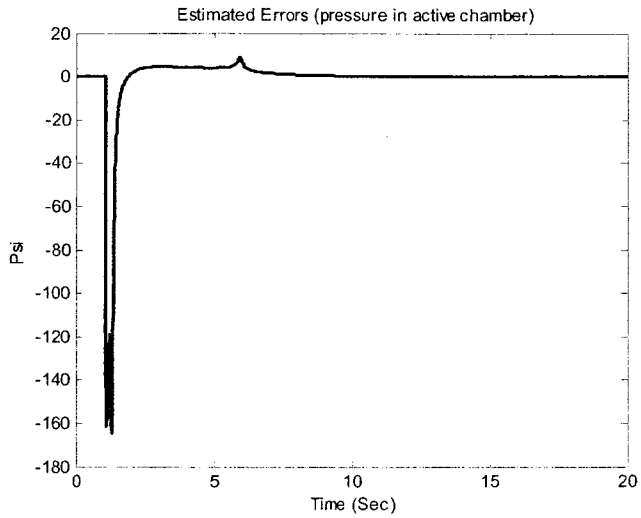

(d)

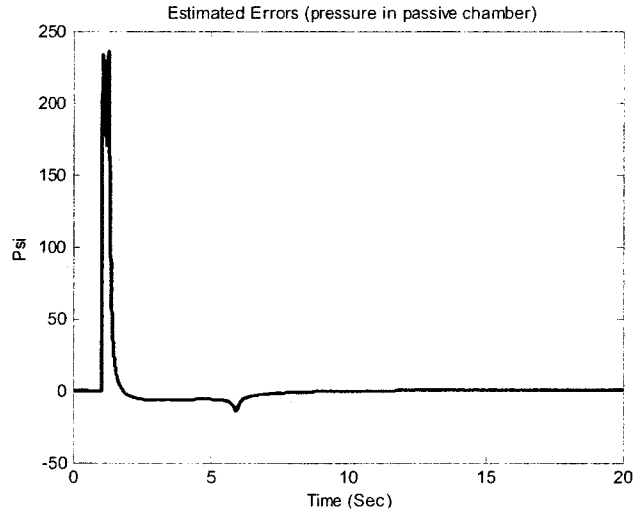

(e)

Figure 6.2 Interaction of fault estimation

The approach in this thesis is to estimate these faults separately by taking one of the faults as disturbance and evaluating the other two. In this way three adaptive observers are constructed so that each fault has two estimations: Observer 1 for C_{1L} and C_{12L}, Observer 2 for C_{2L} and C_{12L}; Observer 3 for C_{1L} and C_{2L}. A fault is identified when these two estimations converge to the same value.

Three simulations for three fault scenarios are carried out so that each simulation addresses one fault:

1. C_{1L} changes from zero to 0.003208 at 1 second;

2. C_{2L} changes from zero to 0.003208 at 1 second;

3. C_{12L} increases 9 times from 0.0003208 at 1 second.

The results of the simulations are shown in Figures 6.3 to 6.5. Each figure demonstrates the estimation results of all three observers. The real faults are shown in these figures as dashed curves.

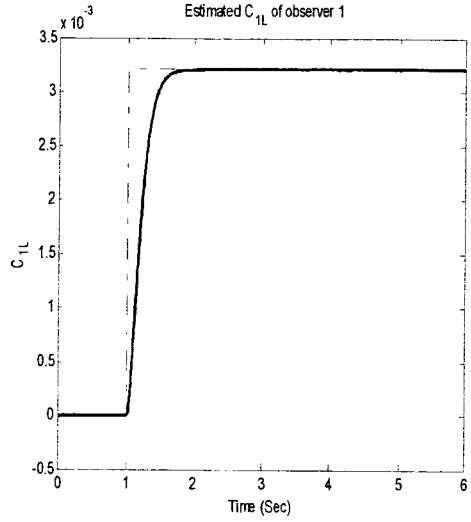
Estimated C_{1L} of observer 1
x 10^-3
C_{1L}
Time (Sec)

(a)

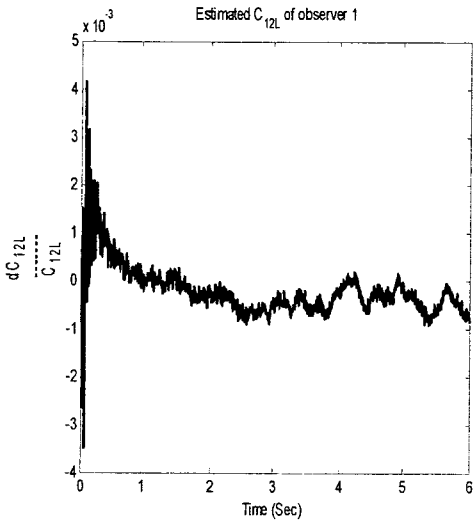
Estimated C_{12L} of observer 1
x 10^-3
dC_{12L} / C_{12L}
Time (Sec)

(b)

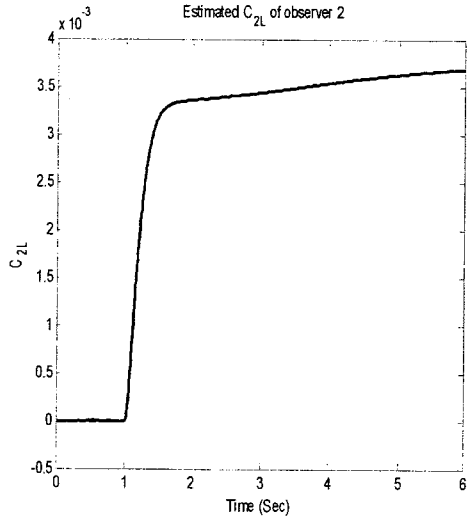
Estimated C_{2L} of observer 2
x 10^-3
C_{2L}
Time (Sec)

(c)

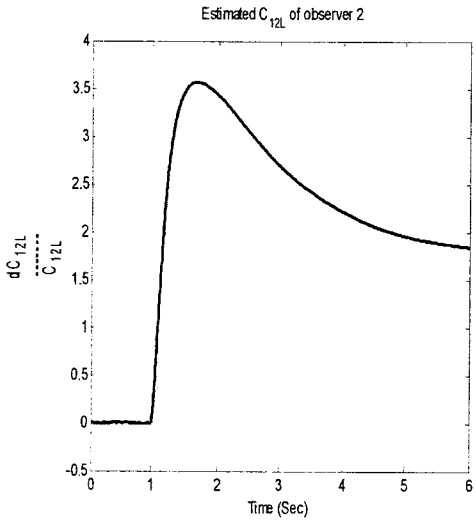
Estimated C_{12L} of observer 2
dC_{12L} / C_{12L}
Time (Sec)

(d)

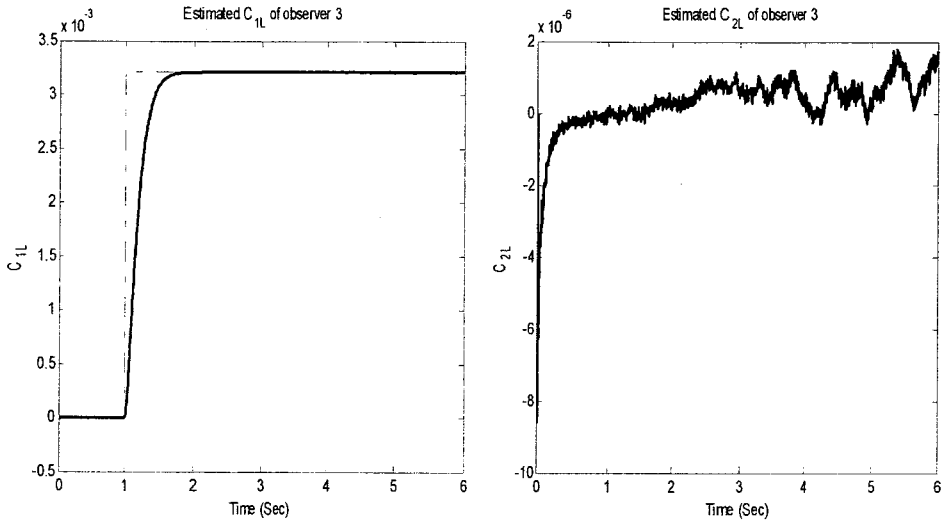

(e) (f)

Figure 6.3 Estimations of leaking in the active chamber of the left cylinder

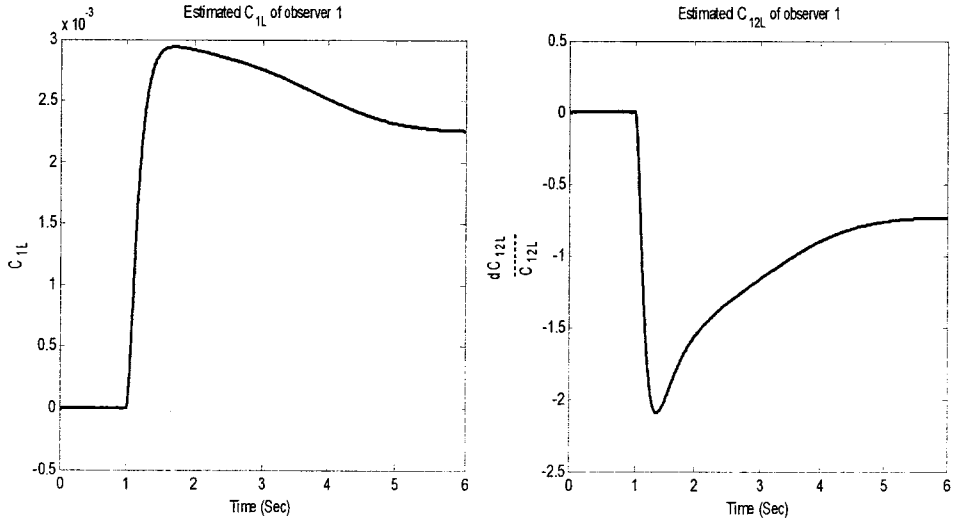

(a) (b)

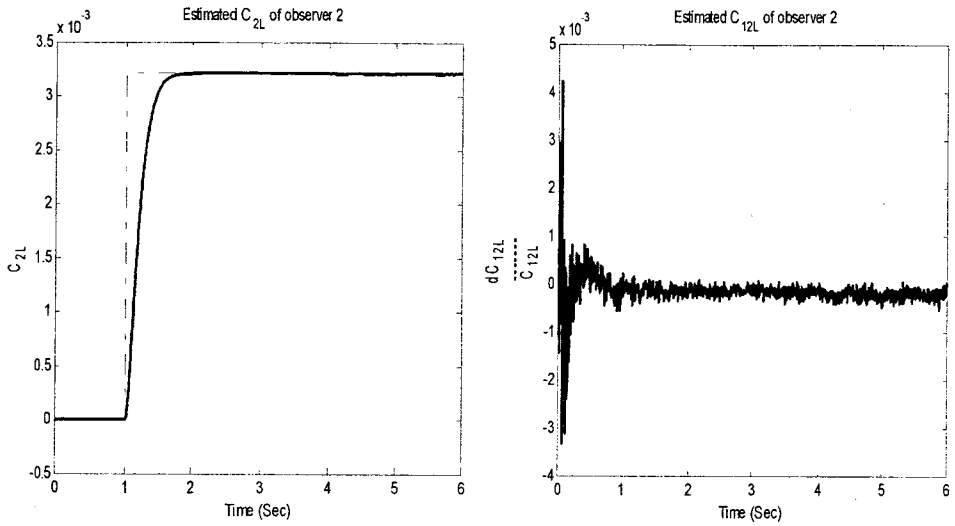

(c) (d)

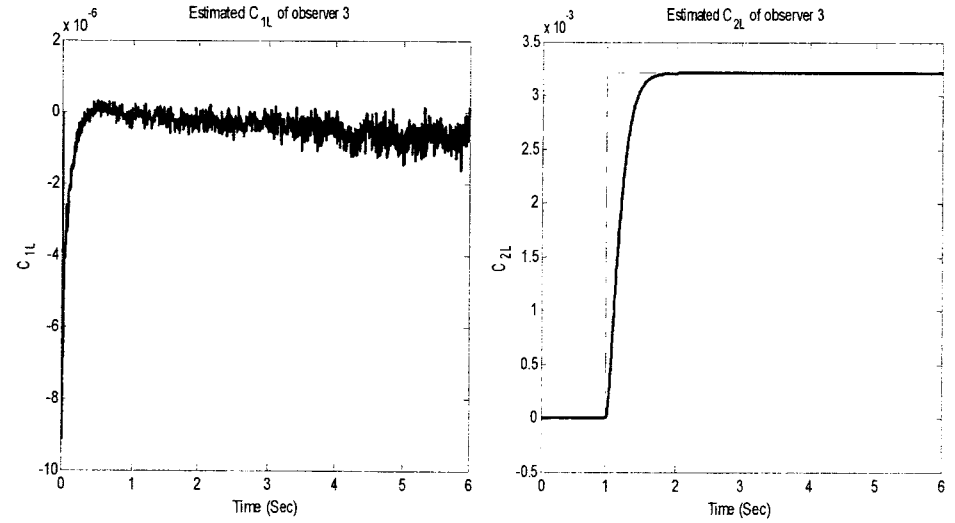

(e) (f)

Figure 6.4 Estimations of leaking in the passive chamber of the left cylinder

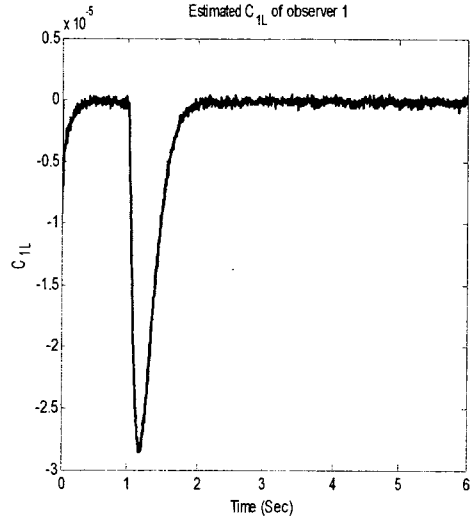
Estimated C_{1L} of observer 1
x 10^-5
C_{1L}
Time (Sec)

(a)

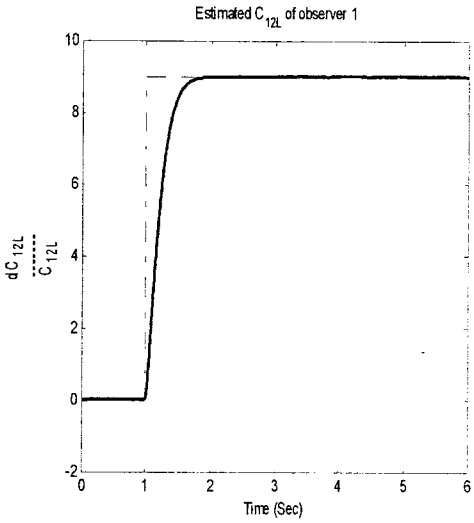
Estimated C_{12L} of observer 1
$\frac{dC_{12L}}{C_{12L}}$
Time (Sec)

(b)

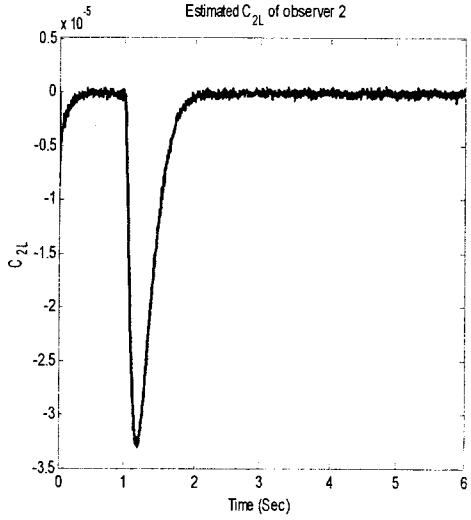
Estimated C_{2L} of observer 2
x 10^-5
C_{2L}
Time (Sec)

(c)

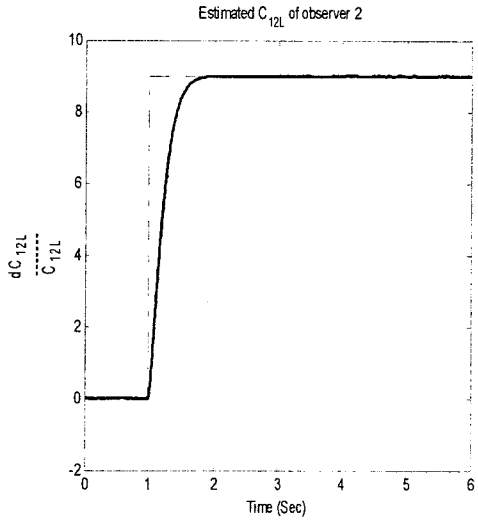
Estimated C_{12L} of observer 2
$\frac{dC_{12L}}{C_{12L}}$
Time (Sec)

(d)

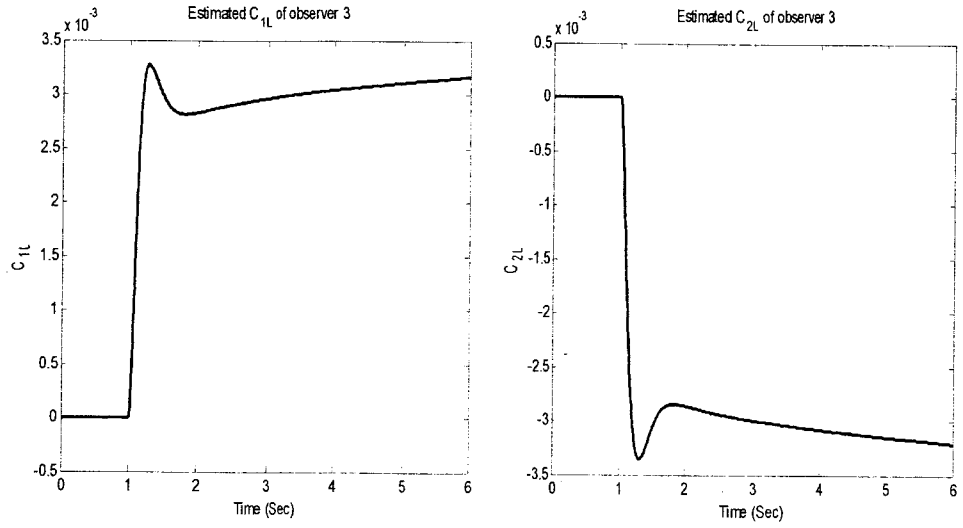

(e) (f)

Figure 6.5 Estimations of leaking between the chambers of the left cylinder

By observing the estimation results, the occurring fault can be identified when the estimations from two different observers converge to the same values:

1. In Figure 6.3, the estimations of C_{1L} in Observer 1 and 3 converge to the same value;

2. In Figure 6.4, the estimation of C_{2L} in Observer 2 and 3 converge to the same value;

3. In Figure 6.5, the estimation of C_{12L} in Observer 1 and 2 converge to the same value.

6.5 Summary

In this Chapter, a solution to the H_∞/H_- optimization of strictly-proper systems is presented by transforming one of the two involved systems into a closed-loop unitary system. For any given frequency range starting from zero, the solution can approximate as close as possible to the theoretical minimal value of the H_∞/H_- optimization by increasing the value of $|k+1|$. The optimization result is thereafter used to construct an H_∞/H_- adaptive observer for the purpose of parameter estimation for a system that is subject to disturbances. It is proved that the parameter estimation is optimized in terms of robustness against disturbances and sensitivity to faults.

CHAPTER 7

CONTROLLER AND RECONFIGURATION

In this chapter, a fuzzy PI controller is developed to deal with different situations including: the nonlinearity of the fault-free elevator; the elevator with component faults; and the elevator with actuator faults. A reconfiguration mechanism is designed based on the available fuzzy controller. By integrating with the adaptive observers for fault detection and estimation in Chapters 4, 5, and 6, a complete Active Fault Tolerant Control system is designed. The simulation results of the AFTC of the elevator are presented.

7.1 Fuzzy Tagaki-Sugeno(TS) Model of the Elevator

Fuzzy logic was first developed as an inference system of processing incomplete and ambiguous information [70,71]. In the control theory, however, the researches of fuzzy system mainly focus on its universal approximation capability [88] that makes it a great tool of modeling [89]. In this section, the fuzzy TS model of the elevator is developed.

7.1.1 Fuzzy TS model of the fault-free elevator

The fuzzy TS model was developed in [91] as a tool of approximating a nonlinear system with linear models. As nonlinearity exists in numerous forms, a generic theory about the behaviour, especially the stability, of all type of nonlinear systems is absent. Linear systems, on the other hand, have been well studied in the control theory. Therefore,

a common practice is to represent a nonlinear system with a local linear model, which is valid only around certain operating point. To enhance the modeling accuracy, multiple local models can be constructed so that a larger operating range is covered. The model of the nonlinear system thus switches discontinuously among these linear models according to different operating conditions. In the fuzzy modeling, multiple local linear models – which are also referred as rules in the term of the rule-based fuzzy logic system - are obtained in a similar way. The fuzzy TS model is constructed as a continuous blending of these local linear models.

The nonlinear model of the elevator, which is shown in (3.1), can be expressed in the following form:

$$\dot{x} = g(x) + Bu$$

$$z = C_z x \tag{7.1}$$

where, x is the vector of state variable; u is the vector of control input; z is the vector of controlled output as shown in Equation (3.3); $g(x)$ is a nonlinear function of x, which can be derived from (3.1).

From Section 3.3, a local linear model of the elevator is available in Equation (3.10). The model is linearized at v_o, where v_o is an operating point of v, which is defined as:

$$v = \begin{bmatrix} x_{3L} - x_{4L} \\ x_{5L} \\ x_{3R} - x_{4R} \\ x_{5R} \end{bmatrix}. \tag{7.2}$$

By varying v, the rules in the fuzzy TS model of the elevator are developed as:

Rule *i*:

If v is v_i, then the model of the elevator is:

$$\dot{x} = A_i x + Bu$$

$$z = C_z x, \tag{7.3}$$

where, $i = 1 \ldots n_r$ with n_r as the total number of rules – or equivalently, the total number of available local linear models; v_i is the *ith* operating point where the nonlinear model is linearized; A_i, B, and C_z are matrices of proper dimensions; v is the premise variable.

The model at a general v then has the form of:

$$\dot{x} = A(v)x + Bu$$

$$z = C_z x \tag{7.4}$$

with,

$$A(v) = \frac{\sum_{i=1}^{n_r} \alpha_i(v, \quad v_i) A_i}{\sum_{i=1}^{n_r} \alpha_i(v, \quad v_i)} \tag{7.5}$$

where, $\alpha_i(v, \quad v_i)$ is the non-negative real-valued membership of the *ith* rule, which may be taken as the weight of each rule.

A nonlinear model of the elevator in (7.1) is therefore transformed to the linear parameter-varying (LPV) fuzzy TS model (7.4). For simplicity, the membership in the fuzzy model is presented as:

$$\alpha_i = \frac{\alpha_i(v, \quad v_i)}{\sum_{i=1}^{n_r} \alpha_i(v, \quad v_i)} \tag{7.6}$$

so that:

$$A(v) = \sum_{i=1}^{n_r} \alpha_i A_i \; . \tag{7.7}$$

7.1.2 Fuzzy TS model with the consideration of faults

In this research, the faults are considered as unexpected abrupt changes of parameters. For the elevator with varying parameters θ, its dynamics is expressed as:

$$\dot{x} = g(x, \quad \theta) + B(\theta)u$$

$$z = C_z x \qquad . \tag{7.8}$$

With the premise variable as $(v, \ \theta)$, a fuzzy TS model can be constructed in a similar way as shown in Section 7.1.1. As the value of θ is not known, the premise variable is taken as $(v, \ \hat{\theta})$ instead.

1. The model of a system with component faults

For a system with component faults, only parameters in A_i change. The rules are therefore summarized as:

If $(v, \ \hat{\theta})$ is $(v_i, \ \theta_j)$, then the dynamics of the elevator is:

$$\dot{x} = A_{ij}x + Bu$$

$$z = C_z x . \tag{7.9}$$

After applying fuzzy inference, the model at $(v, \ \hat{\theta})$ is obtained as:

$$\dot{x} = A(v)x + Bu$$

$$z = C_z x \tag{7.10}$$

with,

$$A(v) = \sum_{i=1}^{n_r}\left[\alpha_i(v, \ v_i)\frac{\sum_{j=1}^{n_\theta}\beta_j(\hat{\theta}, \ \theta_j)A_{ij}}{\sum_{j=1}^{n_\theta}\beta_j(\hat{\theta}, \ \theta_j)}\right] / \sum_{i=1}^{n_r}\alpha_i(v, \ v_i). \tag{7.11}$$

In a simpler form, Equation (7.11) is rewritten as:

$$A(v) = \sum_{i=1}^{n_r} \left[\alpha_i \sum_{j=1}^{n_\theta} \beta_j A_{ij} \right] \tag{7.12}$$

where n_θ is the number of rules in θ; α_i is defined in Equation (7.7); and

$$\beta_j = \frac{\beta_j(\bar{\theta},\ \theta_j)}{\sum_{j=1}^{n_\theta} \beta_j(\bar{\theta},\ \theta_j)}. \tag{7.13}$$

2. The model for a system with actuator faults

For a system with actuator faults, only the parameters in B change. The rules are therefore summarized as:

If $(v,\ \bar{\theta})$ is $(v_i,\ \theta_j)$, then the dynamics of the elevator is:

$$\dot{x} = A_i x + B_j u$$

$$z = C_z x\,. \tag{7.14}$$

After applying fuzzy inference, the model at $(v,\ \bar{\theta})$ is:

$$\dot{x} = A(v)x + B(\bar{\theta})u$$

$$z = C_z x \tag{7.15}$$

with,

$$A(v) = \sum_{i=1}^{n_r} \alpha_i A_i \,, \tag{7.16}$$

$$B(\hat{\theta}) = \sum_{j=1}^{n_\theta} \beta_j B_j \,. \tag{7.17}$$

Remark 7.1: The membership functions of the fuzzy TS model $\alpha_i(v,\ v_i)$ and $\beta_j(\hat{\theta},\ \theta_j)$ are shown in Appendix B.

7.2 Fuzzy Controller

A fuzzy controller usually consists of multiple local controllers designed offline. For every operating point, a controller is constructed online with the fuzzy inference technique. The rules in a fuzzy controller are summarized as:

Rule *i*:

If v is v_i, then the control signal is calculated as:

$$u = u_i, \tag{7.18}$$

where u_i is a function of the states or outputs of the system to be controlled.

The rules in the fuzzy TS model of the closed-loop system therefore are summarized as:

Rule *i*:

If v is v_i, then the closed-loop dynamics of the elevator is:

$$\dot{x} = A_i x + Bu(v)$$

$$z = C_z x \,. \tag{7.19}$$

After applying fuzzy inference, the close-loop system then is expressed as:

$$\dot{x} = A(v)x + Bu(v)$$

$$z = C_z x \tag{7.20}$$

where:

$$u(v) = \sum_{i=1}^{n_r} \alpha_i u_i \,. \tag{7.21}$$

Therefore the problem for the design of a fuzzy controller is to select u_i for the linear model in every rule so that the stability and performance requirements of the closed-loop System (7.20) can be satisfied. In this research, a fuzzy output feedback controller is designed based on the state space representation of the elevator. The reasons of choosing output feedback over state feedback are:

1. Full state measurements are not available;

2. The adaptive observers are designed for the purpose of fault detection and fault estimation. When faults occur, there are false estimations of states until the estimations of faults converge, which means the performance of the system will be deteriorated if a state feedback controller is used.

The following lemma is used in the controller design.

Lemma 7.1 [92]: An LPV system in the form of:

$$\dot{x} = A(t)x \tag{7.22}$$

is stable if:

$$PA(t) + A(t)^T P \leq -2\gamma P, \tag{7.23}$$

where $P > 0$ is a positive definite matrix; $\gamma > 0$ is a positive constant. Meanwhile, the decay rate of the states satisfies:

$$\frac{d\left(x^T Px\right)}{dt} \leq -2\gamma x^T Px \ . \tag{7.24}$$

7.2.1 Controller for the fault-free system

For the fault-free model (7.4), the fuzzy rules in the output feedback controller are summarized as:

Rule *i*:

If v is v_i, then the control signal is calculated as:

$$u = K_i z = K_i C_z x \ . \tag{7.25}$$

Therefore, the control signal at a general v is:

$$u(v) = \sum_{i=1}^{n_r} \alpha_i K_i C_z x \,. \tag{7.26}$$

From Model (7.4), the closed-loop dynamics of the elevator becomes:

$$\dot{x} = A(v)x + Bu(v) = \sum_{i=1}^{n_r} \alpha_i A_i x + B\sum_{i=1}^{n_r} \alpha_i K_i C_z x$$

or

$$\dot{x} = \sum_{i=1}^{n_r} \alpha_i \left(A_i + BK_i C_z\right)x \,. \tag{7.27}$$

Theorem 7.1: If there exist a positive definite matrix P and n_r feedback gain K_i that solve the following n_r inequalities:

$$P\left(A_i + BK_i C_z\right) + \left(A_i + BK_i C_z\right)^T P \le -2\gamma P \tag{7.28}$$

where $i = 1 \ldots n_r$, then System (7.27) is stable and the decay rate of states satisfies:

$$\frac{d\left(x^T P x\right)}{dt} \le -2\gamma x^T P x \,. \tag{7.29}$$

Proof:

By multiplying $\alpha_i \ge 0$ to both sides of inequality (7.28) and then taking summation for $i = 1 \ldots n_r$, it is derived that:

$$P\sum_{i=1}^{n_r}\alpha_i\left(A_i+BK_iC_z\right)+\sum_{i=1}^{n_r}\alpha_i\left(A_i+BK_iC_z\right)^TP\le-2\gamma\sum_{i=1}^{n_r}\alpha_iP. \tag{7.30}$$

Since $\sum_{i=1}^{n_r}\alpha_i=1$, the above inequality is the same as:

$$P\sum_{i=1}^{n_r}\alpha_i\left(A_i+BK_iC_z\right)+\sum_{i=1}^{n_r}\alpha_i\left(A_i+BK_iC_z\right)^TP\le-2\gamma P. \tag{7.31}$$

From Lemma 7.1, it is concluded that System (7.27) is stable and the decay rate of states satisfies inequality (7.29).

Q. E. D.

The controller design problem is therefore to find a positive definite matrix P and n_r feedback gain K_i that solve n_r inequalities in the form of (7.28).

Remark 7.2: As inequality (7.28) is not co-convex in both P and K_i, it cannot be solved in the framework of Linear Matrix Inequality (LMI) [93]. It can be solved with a Bilinear Matrix Inequality (BMI) optimization tool such as Penopt [94]. One other option is to solve (7.28) with Iterative Linear Matrix Inequality (ILMI). A solution, which is adopted from [95], is given in Appendix A.

7.2.2 Controller for the system with component faults

The controller for the system with faults can be constructed in a similar way so that the same performance, which is the decay rate of γ in this research, can be restored for the post-fault system. This is, however, only an ideal situation since, more than often,

the performance cannot be restored because of the restricted capability of the post-fault system. In a worse case, the attempt of restoring performance may even lead to damage due to the exploring of the post-fault system limit. In this research, different performance requirements are applied to different fault situations.

For the fuzzy model (7.9), the rules of the fuzzy output controller are summarized as:

If $\left(v, \quad \hat{\theta}\right)$ is $\left(v_i, \quad \theta_j\right)$, then the control signal is calculated as:

$$u_{ij} = K_{ij} y = K_{ij} C_z x \,. \tag{7.32}$$

From Model (7.9), the dynamics of the closed-loop system becomes:

$$\dot{x} = \sum_{i=1}^{n_r}\left[\alpha_i \sum_{j=1}^{n_\theta} \beta_j A_{ij}\right] x + B \sum_{i=1}^{n_r}\left[\alpha_i \sum_{j=1}^{n_\theta} \beta_j K_{ij} C_z\right] = \sum_{i=1}^{n_r}\left[\alpha_i \sum_{j=1}^{n_\theta} \beta_j \left(A_{ij} + B K_{ij} C_z\right)\right] x \,. \tag{7.33}$$

Theorem 7.2: If there exist a positive definite matrix P and $n_r \times n_\theta$ feedback gain K_{ij} that solve the following $n_r \times n_\theta$ inequalities:

$$P\left(A_{ij} + B K_{ij} C_z\right) + \left(A_{ij} + B K_{ij} C_z\right)^T P \le -2\gamma_j P \tag{7.34}$$

where $i = 1 \ldots n_r$ and $j = 1 \ldots n_\theta$, then System (7.33) is stable and the decay rate of states satisfies:

$$\frac{d\left(x^T P x\right)}{dt} \le -2 \sum_{j=1}^{n_\theta} \beta_j \gamma_j x^T P x, \tag{7.35}$$

where, γ_j is the performance requirement (decay rate) of the system with the fault of θ_j.

Proof:

By multiplying β_j to both sides of inequality (7.33) and then taking summation for $j = 1 \ldots n_\theta$, it is derived that:

$$P\sum_{j=1}^{n_\theta}\beta_j\left(A_{ij}+BK_{ij}C_z\right)+\sum_{j=1}^{n_\theta}\beta_j\left(A_{ij}+BK_{ij}C_z\right)^T P \le -2\sum_{j=1}^{n_\theta}\beta_j\gamma_j P . \tag{7.36}$$

By multiplying α_i to both sides of the above inequality and then taking summation for $i = 1 \ldots n_r$, it is derived that:

$$\begin{aligned} &P\sum_{i=1}^{n_r}\left[\alpha_i\sum_{j=1}^{n_\theta}\beta_j\left(A_{ij}+BK_{ij}C_z\right)\right]+\sum_{i=1}^{n_r}\left[\alpha_i\sum_{j=1}^{n_\theta}\beta_j\left(A_{ij}+BK_{ij}C_z\right)^T\right]P \\ &\le -2\sum_{i=1}^{n_r}\left[\alpha_i\sum_{j=1}^{n_\theta}\beta_j\gamma_j\right]P \end{aligned}, \tag{7.37}$$

which means:

$$\begin{aligned} &P\sum_{i=1}^{n_r}\left[\alpha_i\sum_{j=1}^{n_\theta}\beta_j\left(A_{ij}+BK_{ij}C_z\right)\right]+\sum_{i=1}^{n_r}\left[\alpha_i\sum_{j=1}^{n_\theta}\beta_j\left(A_{ij}+BK_{ij}C_z\right)^T\right]P \\ &\le -2\sum_{j=1}^{n_\theta}\beta_j\gamma_j P \end{aligned} \tag{7.38}$$

since $\sum_{i=1}^{n_r}\alpha_i = 1$.

Therefore, from Lemma 7.1, the closed-loop system (7.33) is stable and its decay rate satisfies inequality (7.35). Moreover since $0 \le \beta_j \le 1$ and $\sum_{j=1}^{n_\theta} \beta_j = 1$, the decay rate of the closed-loop system satisfies:

$$\gamma_{n_\theta} \le \sum_{j=1}^{n_\theta} \beta_j \gamma_j \le \gamma_1, \tag{7.39}$$

where, $\gamma_1 = \gamma$ is the decay rate performance requirement for the fault-free system; γ_{n_θ} is the performance requirement for the system with the worst fault.

Q. E. D.

The controller design for the system with component faults is thus to find to a positive definite matrix P and $n_r \times n_\theta$ feedback gain K_{ij} that solve $n_r \times n_\theta$ inequalities in the form of (7.34).

7.2.3 Controller for the system with actuator faults

For the fuzzy model (7.14), the rules of the fuzzy output controller are summarized as:

If $\left(v, \quad \bar{\theta}\right)$ is $\left(v_i, \quad \theta_j\right)$, then the control signal is calculated as:

$$u_{ij} = K_{ij} y = K_{ij} C_z x. \tag{7.40}$$

Since the control signal at $\left(v, \quad \bar{\theta}\right)$ is:

$$u = \sum_{i=1}^{n_r}\left[\alpha_i \sum_{j=1}^{n_\theta} \beta_j K_{ij} y\right] = \sum_{i=1}^{n_r}\left[\alpha_i \sum_{j=1}^{n_\theta} \beta_j K_{ij} C_z\right] x, \tag{7.41}$$

from Model (7.14), the dynamics of the closed-loop system has the form of:

$$\dot{x} = \sum_{i=1}^{n_r} \alpha_i A_i x + \sum_{j=1}^{n_\theta} \beta_j B_j \sum_{i=1}^{n_r}\left[\alpha_i \sum_{j=1}^{n_\theta} \beta_j K_{ij} C_z\right] x, \tag{7.42}$$

which is the same as:

$$\dot{x} = \sum_{i=1}^{n_r} \alpha_i A_i x + \sum_{i=1}^{n_r}\left[\alpha_i \sum_{k=1}^{n_\theta} \beta_k B_k \sum_{j=1}^{n_\theta} \beta_j K_{ij} C_z\right] x. \tag{7.43}$$

Since $\sum_{k=1}^{n_\theta} \beta_k = 1$, System (7.43) is equivalent to:

$$\dot{x} = \sum_{i=1}^{n_r} \alpha_i \left(\sum_{k=1}^{n_\theta} \beta_k A_i\right) x + \sum_{i=1}^{n_r}\left[\alpha_i \sum_{k=1}^{n_\theta} \beta_k \left(\sum_{j=1}^{n_\theta} \beta_j B_k K_{ij} C\right)\right] x \tag{7.44}$$

and

$$\dot{x} = \sum_{i=1}^{n_r} \alpha_i \left(\sum_{k=1}^{n_\theta} \beta_k \left(\sum_{j=1}^{n_\theta} \beta_j A_i\right)\right) x + \sum_{i=1}^{n_r}\left[\alpha_i \sum_{k=1}^{n_\theta} \beta_k \left(\sum_{j=1}^{n_\theta} \beta_j B_k K_{ij} C\right)\right] x. \tag{7.45}$$

Therefore, it is derived that:

$$\dot{x} = \sum_{i=1}^{n_r}\left[\alpha_i \sum_{k=1}^{n_\theta} \beta_k \left(\sum_{j=1}^{n_\theta} \beta_j \left(A_i + B_k K_{ij} C\right)\right)\right] x. \tag{7.46}$$

Theorem 7.3: If there exist a positive definite matrix P and $n_r \times n_\theta$ feedback gain K_{ij} that solve the following $n_r \times n_\theta \times n_\theta$ inequalities:

$$P\left(A_i + B_k K_{ij} C_z\right) + \left(A_i + B_k K_{ij} C_z\right)^T P \le -2\gamma_j P, \tag{7.47}$$

where, $i = 1 \ldots n_r$, $j = 1 \ldots n_\theta$ and $k = 1 \ldots n_\theta$, then System (7.43) is stable and the decay rate of states satisfies:

$$\frac{d\left(x^T P x\right)}{dt} \le -2\sum_{j=1}^{n_\theta} \beta_j \gamma_j x^T P x, \tag{7.48}$$

where, γ_j is the performance requirement (decay rate) of the system with the fault of θ_j.

Proof:

By multiplying β_j to both sides of inequality (7.47) and then taking summation for $j = 1 \ldots n_\theta$, it is derived that:

$$P\left(\sum_{j=1}^{n_\theta} \beta_j \left(A_i + B_k K_{ij} C_z\right)\right) + \left(\sum_{j=1}^{n_\theta} \beta_j \left(A_i + B_k K_{ij} C_z\right)^T\right) P \le -\left(\sum_{j=1}^{n_\theta} 2\beta_j \gamma_j\right) P. \tag{7.49}$$

By multiplying β_k to both sides of the above inequality and then taking summation for $k = 1 \ldots n_\theta$, it is derived that:

$$P\sum_{k=1}^{n_\theta} \beta_k \left(\sum_{j=1}^{n_\theta} \beta_j \left(A_i + B_k K_{ij} C_z\right)\right) + \sum_{k=1}^{n_\theta} \beta_k \left(\sum_{j=1}^{n_\theta} \beta_j \left(A_i + B_k K_{ij} C_z\right)\right) P \le -\left(\sum_{j=1}^{n_\theta} 2\beta_j \gamma_j\right) P \tag{7.50}$$

By multiplying α_i to both sides of (7.50) and taking summation for $i = 1 \ldots n_r$, it is derived that:

$$P\sum_{i=1}^{n_r}\left[\alpha_i\sum_{k=1}^{n_\theta}\beta_k\left(\sum_{j=1}^{n_\theta}\beta_j\left(A_i + B_k K_{ij} C_z\right)\right)\right] + \sum_{i=1}^{n_r}\left[\alpha_i\sum_{k=1}^{n_\theta}\beta_k\left(\sum_{j=1}^{n_\theta}\beta_j\left(A_i + B_k K_{ij} C_z\right)^T\right)\right]P \leq -\left(\sum_{j=1}^{n_\theta} 2\beta_j\gamma_j\right)P \quad (7.51)$$

Therefore from Lemma 7.1, the closed-loop system (7.46), or equivalently (7.43), is stable and the decay rate satisfies:

$$\gamma_{n_\theta} \leq \sum_{j=1}^{n_\theta}\beta_j\gamma_j \leq \gamma_1 . \quad (7.52)$$

Q. E. D.

The controller design for the system with actuator faults is thus formulated to find to a positive definite matrix P and $n_r \times n_\theta$ feedback gain K_{ij} that solve $n_r \times n_\theta \times n_\theta$ inequalities in the form of (7.47).

7.2.4 Fuzzy PI controller

The stability of the closed-loop system and its performance of decay rate were discussed in former sections. For the purpose of following a given reference signal, the tracking accuracy such as steady-state errors needs to be considered. For low frequency reference signals, a Proportional-Integral (PI) controller will efficiently reduce the tracking errors. A fuzzy PI controller can be easily constructed with the design method

discussed in former sections. An integrator, however, needs to be added to the model in each rule. The integrator has the form of:

$$\dot{x}_a = z = C_z x, \tag{7.53}$$

so that the rules in the fuzzy model of, for example, (7.4) are now:

Rule *i*:

If v is v_i, then the dynamics of the system is:

$$\dot{x} = A_i x + Bu$$

$$\dot{x}_a = z$$

$$z = C_z x$$

$$z_a = x_a. \tag{7.54}$$

In a single state vector form, System (7.54) is the same as:

$$\dot{x}_A = A_{Ai} x_A + B_A u$$

$$y_A = C_A x_A \tag{7.55}$$

where

$$x_A = \begin{bmatrix} x \\ x_a \end{bmatrix},\ y_A = \begin{bmatrix} z \\ z_a \end{bmatrix},\ A_{Ai} = \begin{bmatrix} A_i & 0 \\ C_z & 0 \end{bmatrix},\ B_A = \begin{bmatrix} B \\ 0 \end{bmatrix}, \text{ and } C_A = \begin{bmatrix} C_z & 0 \\ 0 & I \end{bmatrix}.$$

A fuzzy PI controller therefore can be constructed with Model (7.55).

7.3 The Reconfiguration Mechanism

In this research, the reconfiguration consists of two parts: the reconfiguration of controller and the reconfiguration of reference signals.

7.3.1 Controller reconfiguration

With the fuzzy controller design method presented in Section 7.2, the controller can be reconfigured based on the operating status and the faults information of the system. The control signal can be calculated for current operating point at $\left(v, \quad \bar{\theta}\right)$ as:

$$u = \sum_{i=1}^{n_r}\left[\alpha_i \sum_{j=1}^{n_\theta} \beta_j K_{ij} z\right]. \tag{7.56}$$

To reduce the computation load, it is not necessary to recalculate the membership of $\hat{\theta}$ at every step. In fact the fuzzy inference based on the fault information - or the reconfiguration of controller - needs to be done only once for the post-fault system. After the reconfiguration, the fuzzy controller returns to the form of Equation (7.25) with a new feedback gain so that the rules of the new controller have the form of:

Rule i: If v is v_i, then the control signal is calculated as:

$$u = K_i z, \tag{7.57}$$

where,

$$K_i = \sum_{j=1}^{n_\theta} \beta_j K_{ij} \,. \tag{7.58}$$

7.3.2 Reference reconfiguration

The capacity of a system might be restricted when the faults occur. Hence the performance cannot be restored to the fault-free level. The performance degradation due to faults has been considered in the controller design. Different performance requirements of decay rate are applied to different fault situations. When a system is required to follow a given reference signal, the reference signal also needs to be reconfigured if the system might be further damaged if otherwise.

In this research, the reference signal is constructed with a fuzzy TS model as:

Rule j: If $\hat{\theta}$ is θ_j, then the reference signal has the form of:

$$\dot{r} = -\frac{1}{\tau_j} r + \frac{1}{\tau_j} r_o \,. \tag{7.59}$$

where r_o is the desired steady state value of r.

The maximal value of r_o depends on the capability of the system, which is calculated as:

Rule j: If $\hat{\theta}$ is θ_j, then the maximal value of r_o is:

$$\bar{r} = \bar{r}_j \,. \tag{7.60}$$

The reference signals therefore can be reconfigured with the fuzzy inference technique.

Remark 7.3: (7.59) is a first order system in the form of:

$$r = \frac{1}{\tau_j s + 1} r_o . \tag{7.61}$$

The reconfiguration in (7.59) is thus to adjust the time constant of the reference signal in (7.61). In the research, the objective of control is to drive the elevator to a required position. The response speed of the elevator is a combined function of the time constant in (7.61) and the gain of the controller. For the faulty elevator, tracking a reference signal that is faster than its limit might lead to damage since the actuators are working in the saturation zone. Therefore, a slower reference signal or a larger τ_j is required for the faulty elevator.

7.4 Active Fault Tolerant Control System

With the results from this and former chapters, an AFTC system as shown in Figure 1.1 is constructed. The system consists of Fault Detection and Estimation (FDE), a fault-free controller, and a reconfiguration mechanism:

FDE (as the magnitudes of faults are estimated, FDE is used here instead of FDI – Fault Detection and Isolation) consists of an Adaptive Unknown Input Observer and three $H_\infty/H\_$ adaptive observers for the fault detection and estimation. For fault detection, the output estimation errors of the observers are taken as

indicators of occurring faults; for fault estimation, the estimated values of parameters are taken as the magnitudes of faults;

A fuzzy controller is constructed in the form of (7.26) for the fault-free system to meet the stability and performance requirements;

The reconfiguration mechanism reconfigures the controller and the reference signal based on the fault information. At the detection of an occurring fault, the reference signal is reconfigured for the first time. Since detailed information of the occurring fault, namely the type and size of the fault, is not available, the worst situation is assumed so that the slowest reference signal is selected temporally. When the fault is identified and estimated, both the reference signal and the controller are reconfigured using the detail fault information. The reference signal is recalculated as shown in the rule of (7.59). The gains in the rule of the fuzzy controller are recalculated as shown in Equation (7.58).

7.5 The AFTC of the Elevator: Simulations

The AFTC system is applied to the elevator for the purpose of fault tolerant control. 5 faults described in Chapter 3 are applied to 5 simulations separately. The faults magnitudes and their occurring time in each simulation are listed in Table 7.1. The simulation on the fault of K_{sL} is not included here because, in the simulation, it is found that the change of K_{sL} has little effect on the performance of the elevator.

Table 7.1 Details of faults in the elevator

Parameters	Nominal Values	Fault Magnitudes	Occurring Time (sec)
k_{vL}	$0.00337(in/sec^2/mA)$	$-0.9\,k_{vL}$	8
H_m	8.6×10^3 $(lbf\text{-}in/rad)$	$+9H_m$	8
C_{12L}	3.208×10^{-4} $(in^3/sec/psi)$	$+9C_{12L}$	8
C_{1L}	$0\ (in^2/psi^{1/2})$	$+3.208\times10^{-3}$	8
C_{2L}	$0\ (in^2/psi^{1/2})$	$+3.208\times10^{-3}$	8

The objective of the control, as discussed in Chapter 3, is to move the two subsystems synchronously and follow the reference signal r under various fault conditions:

$$z=\begin{bmatrix}\dfrac{x_{7L}+x_{7R}}{2}\\ \dfrac{x_{7L}-x_{7R}}{2}\end{bmatrix}=\begin{bmatrix}r\\0\end{bmatrix}. \tag{7.62}$$

To show the performance of the elevator, the tracking error e_1, the position difference e_2 of two sub system, and the twisting torque T_r generated on the elevator are defined as:

$$e_1=\frac{x_{7L}+x_{7R}}{2}-r$$

$$e_2 = \frac{x_{7L} - x_{7R}}{2}$$

$$T_r = K_{Ps}\left(x_{7L} - x_{7R}\right). \tag{7.63}$$

7.5.1 The fault of k_{vL}

The simulation result of the elevator suffering k_{vL} fault is shown in the Figure 7.1. Three sub figures represent the tracking of reference signal r, the difference e_2 between two subsystems, and the twisting torque T_r generated on the joint of the elevator.

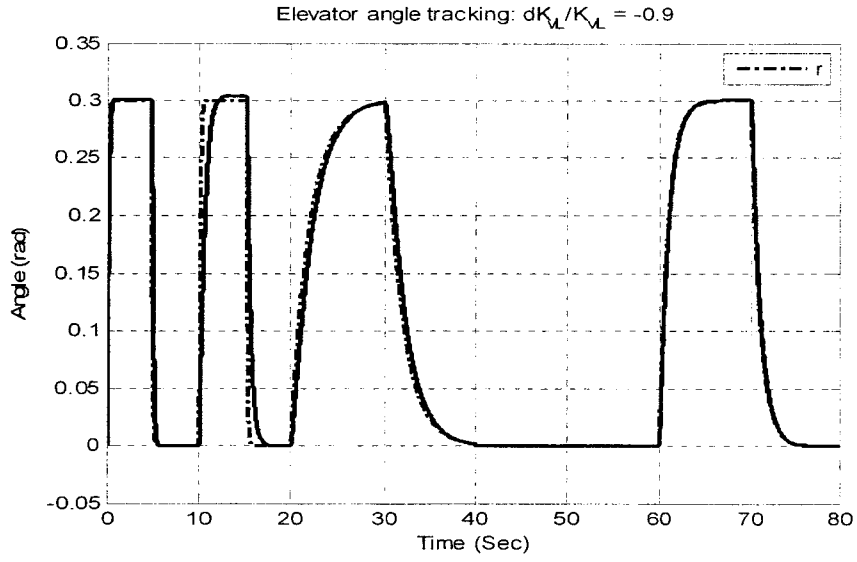

(a)

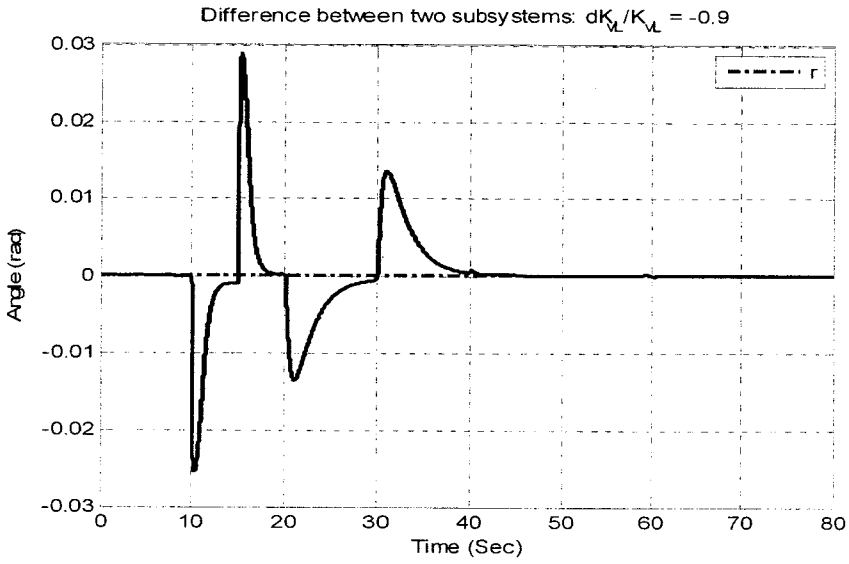

(b)

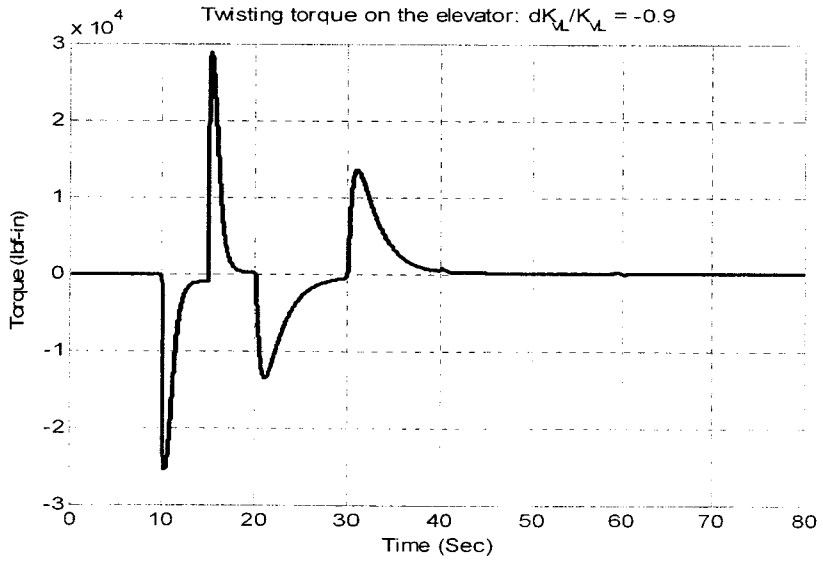

(c)

Figure 7.1 AFTC simulation on k_{VL} fault

To show the effect of the reconfiguration, the simulation is designed to run 80 seconds consisting of 4 periods:

1. In 0 – 10 seconds, the fault-free elevator is tracking a fast reference signal;

2. In 10 – 20 seconds, the faulty elevator is tracking the same reference signal as in 1;

3. In 20 - 60 seconds, the faulty elevator is tracking the slowest reference signal as discussed in Section 7.4. This is the first reconfiguration (at 20 second) of reference signal when a fault is detected;

4. In 60 – 80 seconds, the faulty elevator is tracking a reconfigured reference signal under the control of a new controller – this is the reconfiguration (at 60 second) of both the controller and the reference signal when the fault is estimated.

The performance difference of these 4 periods can also be seen in Table 7.2, where the steady-state errors of e_1, the maximal e_2 and the maximal T_r are shown.

From the simulation results, it can be seen that:

1. In the period 1, the elevator has full capability so that it can track a fast reference signal with small errors; meanwhile, the two subsystems are totally synchronized;

2. In the period 2 after the fault, the capability of the elevator is impaired so that following the same reference signal exceeds the limits of the elevator especially

for the left subsystem; as a result, a huge twisting torque is generated because of the discrepancy between the two subsystems;

3. In the period 3, the elevator is tracking the slowest reference signal; the twisting torque is reduced considerably; this is, however, a choice of safety over performance;

4. In the period 4, both the controller and the reference signal are reconfigured with the detail fault information; the performance of the system is recovered; the twisting torque is almost eliminated.

Table 7.2 Performance of the elevator – AFTC for k_{vL} fault

Period	Tracking Error e_1 (rad)	Maximal difference e_2 (rad)	Maximal Torque T_r (lbf-in)
1	*0.0009*	*0*	*0*
2	*0.0039*	*0.0288*	2.88×10^{-4}
3	*0.0015*	*0.0135*	1.35×10^{-4}
4	*0*	2.27×10^{-4}	*227*

7.5.2 The fault of H_m

The increase of the hinge stiffness H_m can restrict the travel range of the elevator. If the elevator is required to follow a reference signal that exceeds its limit, the difference

between the angle of the elevator and the reference signal cannot be eliminated. Due to the property of a PI controller, the control command to the EHSVs will keep increasing. In such a case, the hydraulic cylinders will eventually reach their limits and work in the saturation zone which may result in unexpected vibration and impact. In the long run, the elevator may be damaged.

The simulation also consists of 4 periods that are as the same as those in Section 7.5.1. The simulation results are shown in Figure 7.2 which consists of sub figures of elevator angle and the pressures in the cylinders. As the change of H_m will not influence the synchronization of the two subsystems, their difference and consequently the twisting torque are all zero.

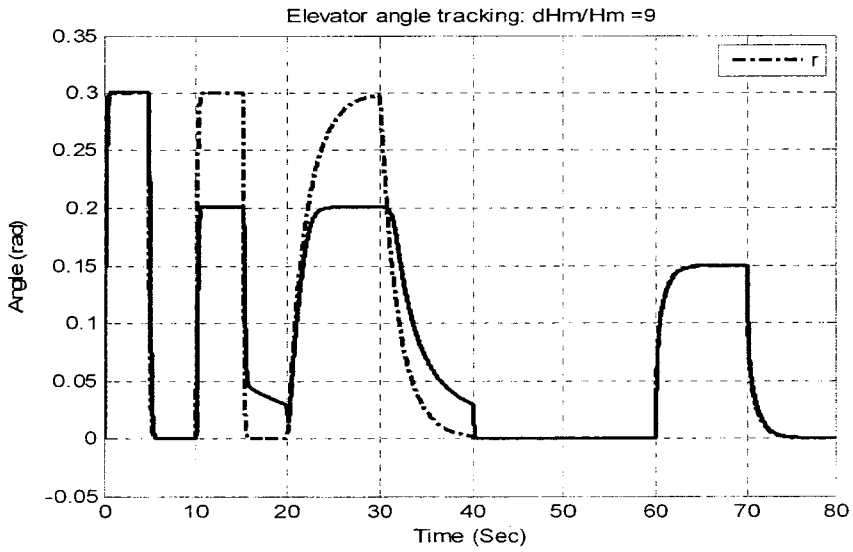

(a)

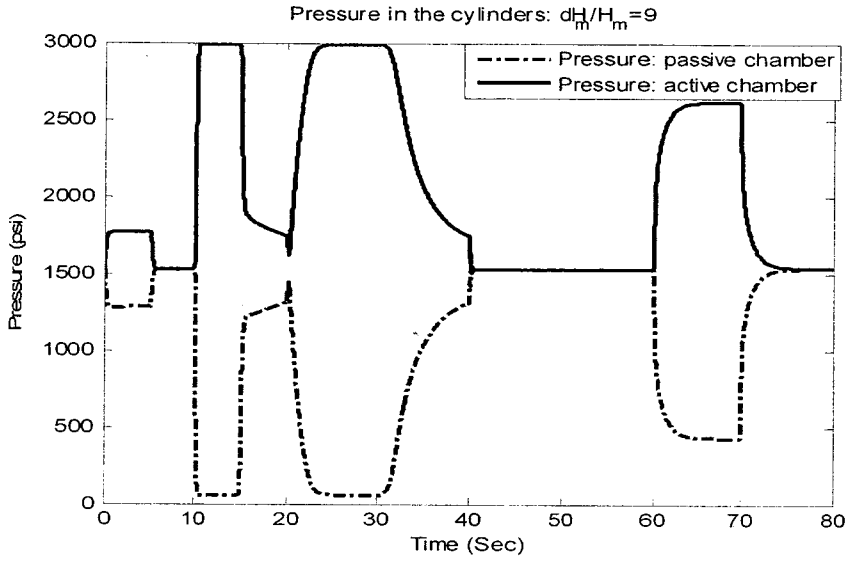

(b)

Figure 7.2 AFTC simulation on H_m fault

Table 7.3 Performance of the elevator – AFTC for H_m fault

Period	Tracking Error e_1 (rad)	Maximal difference e_2 (rad)	Maximal Torque T_r (lbf-in)
1	0.0009	0	0
2	0.103	0	0
3	0.10	0	0
4	0	0	0

From the pressure figure, it can be seen that, in the period 2 and 3, the pressures in the cylinders reach their limits: 3000psi (supply pressure) for the active chamber and 50psi (reservoir pressure) for the passive chamber. The elevator angle, however, still cannot follow the reference signal. After the second reconfiguration, a smaller reference signal is selected. The performance of the elevator is therefore restored partially. The tracking performance comparison of the 4 periods is also shown in Table 7.3.

7.5.3 The fault of C_{IL}

C_{IL} is the leaking from the active chamber to the environment. This is a severe fault as it not only impacts the performance of the elevator but also endangers the whole hydraulic system for the hydraulic fluid loss. A reasonable reaction is to shut down the faulty cylinder. The simulation results are shown in Figure 7.3. The simulation consists of 4 periods:

1. In 0 - 10 seconds, the fault-free elevator is tracking a fast reference signal;

2. In 10 - 20 seconds, the faulty elevator is tracking the same reference signal as in 1; the left cylinder, however, is shut down;

3. In 20 - 40 seconds, the faulty elevator is returning to its zero position;

4. In 40 - 80 seconds, the reference signal is reconfigured to the slowest one to reduce the twisting torque.

The performance comparison of the 4 periods can also be seen in Table 7.4.

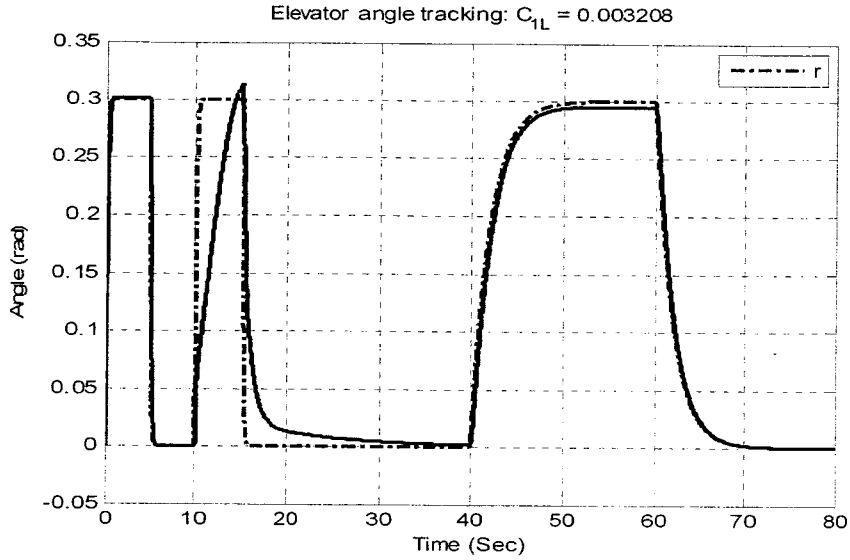
Elevator angle tracking: C_{1L} = 0.003208
r
Angle (rad)
Time (Sec)
0.35
0.3
0.25
0.2
0.15
0.1
0.05
0
-0.05
0
10
20
30
40
50
60
70
80

(a)

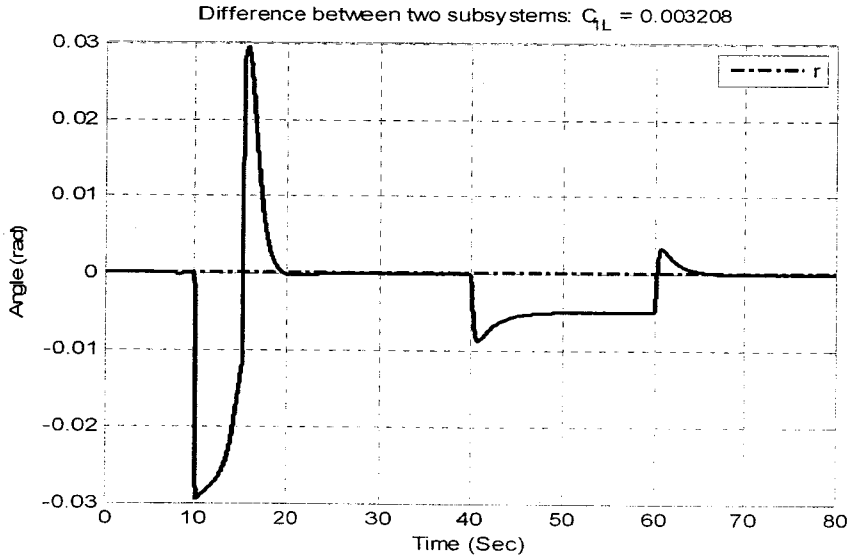
Difference between two subsystems: C_{1L} = 0.003208
r
Angle (rad)
Time (Sec)
0.03
0.02
0.01
0
-0.01
-0.02
-0.03
0
10
20
30
40
50
60
70
80

(b)

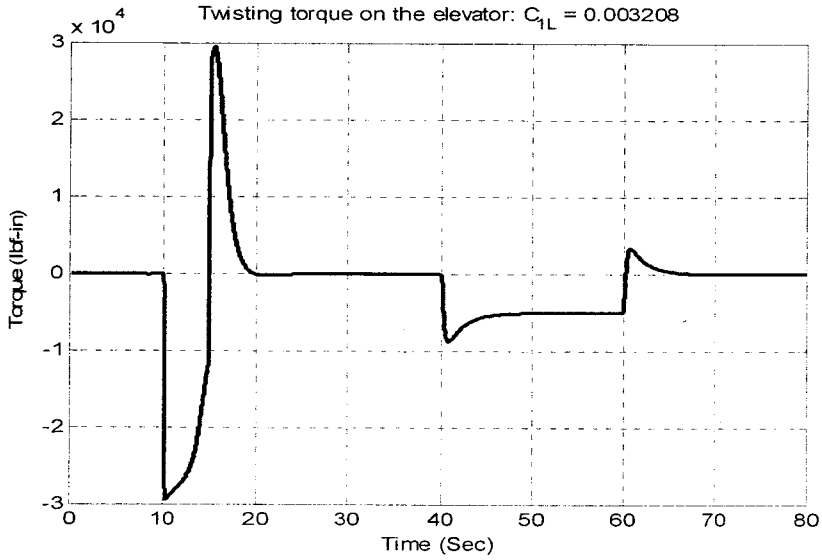

(c)

Figure 7.3 AFTC simulation on C_{IL} fault

Table 7.4 Performance of the elevator – AFTC for C_{IL} fault

Period	Tracking Error	Maximal difference	Maximal Torque
	e_1 (rad)	e_2 (rad)	T_r (lbf-in)
1	*0.0009*	*0*	*0*
2	-	*0.0295*	2.95×10^{4}
3	-	-	-
4	*0.0025*	*-0.0086*	-8.6×10^{3}

From the simulation results, it can be seen that, in the period 2, a huge twisting torque is generated because of the shutting down of the left cylinder. As the function of the left cylinder cannot be restored - to prevent the further failure of the hydraulic system, the reference signal is reconfigured so that the twisting torque is reduced to -8.6×10^{3} *lbf-in* from 2.95×10^{4} *lbf-in*.

7.5.4 The fault of C_{2L}

C_{2L} is the leaking from the passive chamber to the environment. The simulation results are shown in Figure 7.4. The simulation consists of 4 periods which are same as those in Section 7.5.4. The numerical comparison of the 4 periods is shown in Table 7.5.

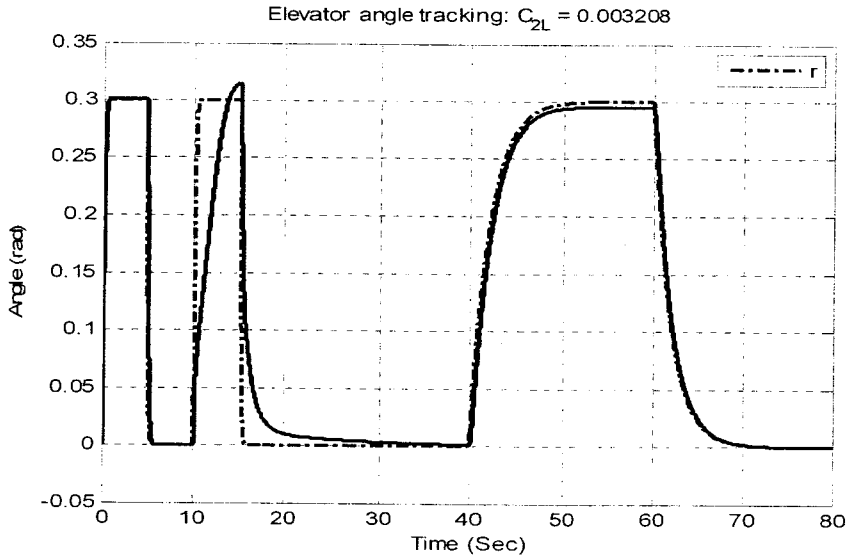

(a)

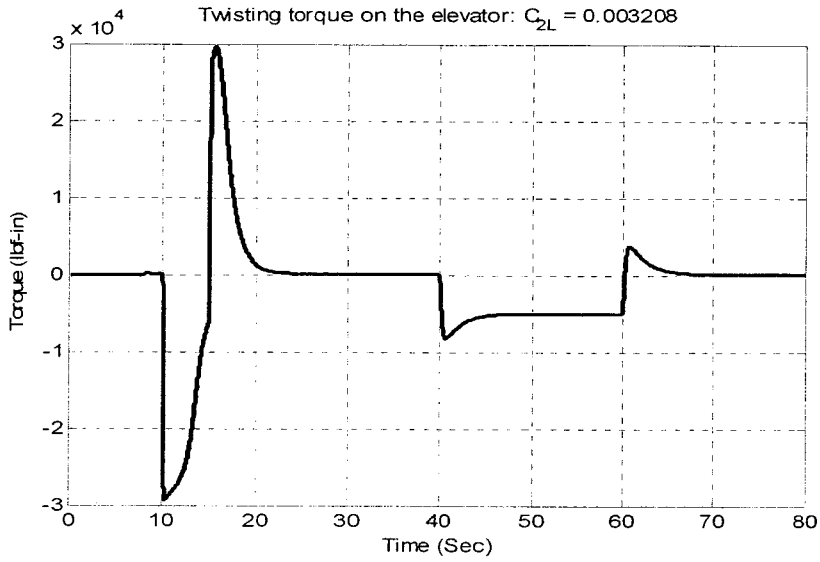

(b)

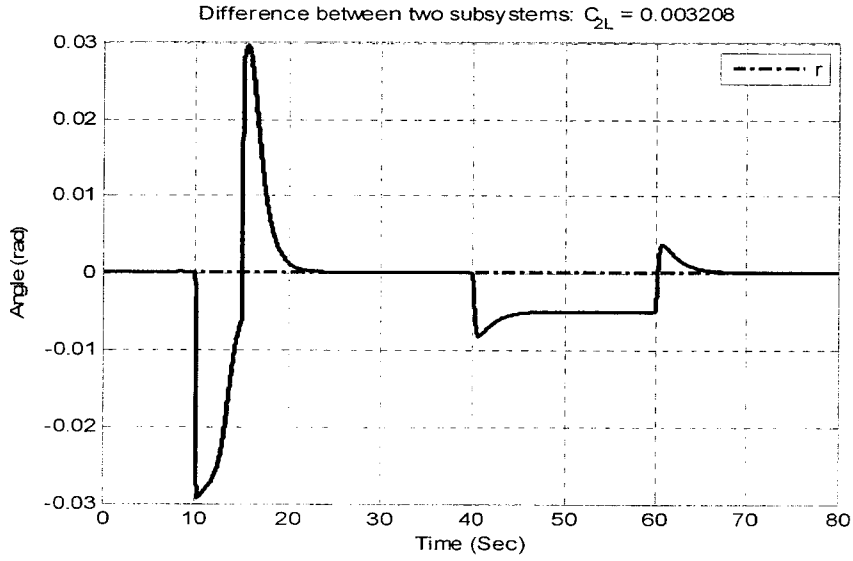

(c)

Figure 7.4 AFTC simulation on C_{2L} fault

Table 7.5 Performance of the elevator – AFTC for C_{2L} fault

Period	Tracking Error e_1 (rad)	Maximal difference e_2 (rad)	Maximal Torque T_r (lbf-in)
1	*0.0009*	*0*	*0*
2	-	*0.0298*	2.98×10^4
3	-	-	-
4	*0.0025*	*-0.008*	-8×10^3

From the simulation results, it can be seen that, in the period 2, a huge twisting torque is generated because of the shutting down of the left cylinder. As the function of the left cylinder cannot be restored - to prevent the further failure of the hydraulic system, the reference signal is reconfigured so that the twisting torque is reduced to -8×10^3 *lbf-in* from 2.98×10^4 *lbf-in*.

7.5.5 The fault of C_{12L}

C_{12L} is the leaking between the active and passive chambers. It is not as severe as the former two leaking since the hydraulic liquid will not leave the system. When a leaking fault is detected, however, the type and the magnitude of the fault cannot be decided. Therefore, the left elevator needs to be shut down for the time period before the fault is fully evaluated. The simulation consists of 4 periods:

1. In 0 - 10 seconds, the fault-free elevator is tracking a fast reference signal;

2. In 10 - 20 seconds, the faulty elevator is tracking the same reference signal as in 1; the left cylinder, however, is shut down;

3. In 20 -60 seconds, the faulty elevator is tracking the slowest reference signal; this is not a necessary reconfiguration; it is included in the simulation to show the effect of reference reconfiguration; the left elevator is still shut down;

4. In 60 - 80 seconds, both the controller and the reference signal are reconfigured using the available detail information of fault; the left cylinder is switched back to work.

The numerical comparison of the 4 periods is shown in Table 7.6.

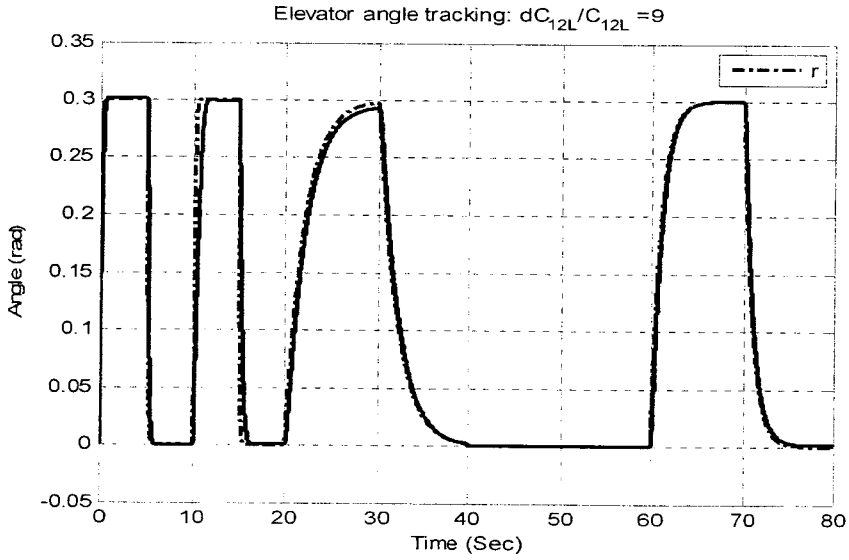

(a)

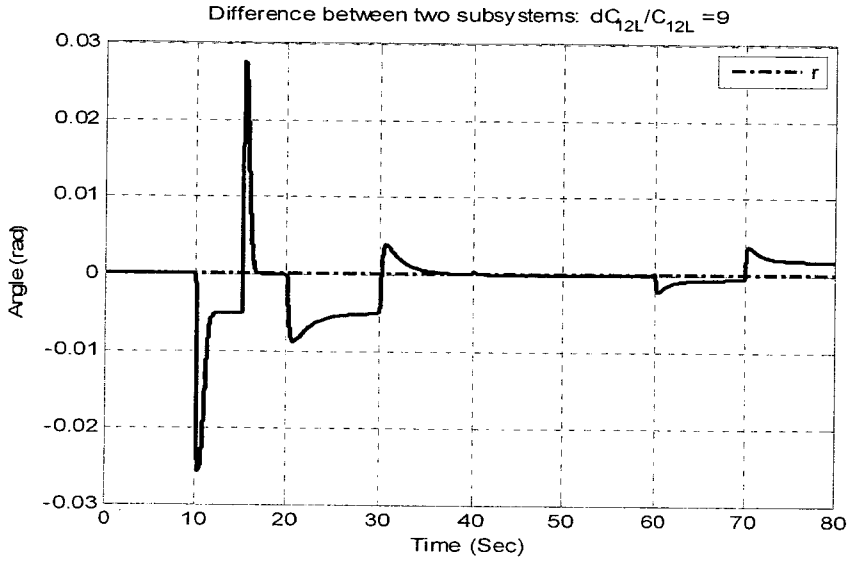

(b)

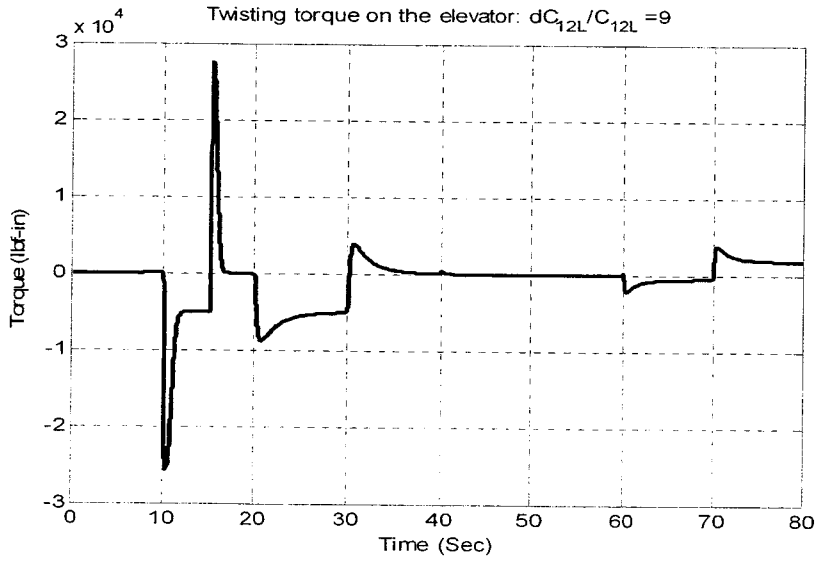

(c)

Figure 7.5 AFTC simulation on C_{12L} fault

Table 7.6 Performance of the elevator – AFTC for C_{12L} fault

Period	Tracking Error e_1 (rad)	Maximal difference e_2 (rad)	Maximal Torque T_r (lbf-in)
1	*0.0009*	*0*	*0*
2	*0.0009*	*0.0282*	2.828×10^{4}
3	-	*-0.0088*	-8.88×10^{3}
4	*0.0002*	*0.0034*	3.48×10^{3}

From the simulation results, it can be seen that, in the period 2 after the fault, a huge twisting torque is generated because of the shutting down of the left cylinder. In the period 3, the reference signal is reconfigured so that the twisting torque is reduced. In the period 4, the left cylinder is reconfigured and the twisting torque is further reduced.

From the Sections 7.5.1 to 7.5.5, the simulations on the fault tolerant control of the elevator show that the presented AFTC system is capable of:

1. Restoring the tracking performance of the post-fault elevator;

2. Preventing the further damage of the elevator by reducing the twisting torque.

7.6 Summary

A fuzzy PI controller is designed for the elevator with possible parameter faults. Different faults are modeled as different operating conditions of the system so that controllers addressing these faults can be constructed. Performance degradation due to occurring faults is considered explicitly in the controller design procedure as a change of decay rate. With the fault information available from FDI, the controller can be reconfigured easily with fuzzy inference technique. A reference reconfiguration method is also presented in the fuzzy inference form by formulating the reference signal into a fuzzy model. A complete Active Fault Tolerant Control system of the elevator, which integrates the results from Chapters 4 to 7, is proposed and then validated through the simulations.

CHAPTER 8

CONCLUDING REMARKS

8.1 Conclusions

Faults usually appear as tolerable performance deterioration of a system. In a safety critical environment, occurring faults need to be addressed properly to restore the performance of the system and, more importantly, to prevent faults from developing into severe failures. Active Fault Tolerant Control is an advanced control strategy to maintain the stability and performance of the post-fault system by reconfiguring the controller with the evaluated fault information. An AFTC system, therefore, consists of three components: a fault evaluation system, a reconfigurable controller and a reconfiguration mechanism. Beyond the common requirements of stability and performance, an AFTC system is also expected to have the features of prompt fault detection, accurate fault estimation, and proper post-fault reconfiguration.

This thesis studies the AFTC of an electro-hydraulic driven elevator. An AFTC system is constructed with the following components:

1. A Fault Detection and Estimation (FDE) component is built based on robust adaptive observers. The output estimation errors of the observers are taken as residuals for the purpose of fault detection. Once a fault occurs, the residuals deviate from zeros immediately so that the prompt detection of fault can be guaranteed. The location and magnitude of occurring fault are then estimated with

the parameter estimation part of the observer so that the accurate information of fault is available for the future reconfiguration;

2. A controller that can be easily reconfigured is designed in the fuzzy PI controller form. The controller is constructed based on the fuzzy TS model of a nonlinear system where the dynamics of the system - at different operating points and different fault scenarios - is modeled as linear models in the fuzzy rules. The stability and performance requirement is enforced in the form of matrix inequalities with the explicit consideration of performance degradation;

3. A reconfiguration mechanism is developed with fuzzy inference technique. The new controller can be reconfigured as the fuzzy blending of the pre-designed controllers. The reference signal of tracking is also reconfigured with fuzzy inference.

The main contributions of the thesis are the Fault Detection and Estimation (FDE) method based on robust adaptive observers and the reconfiguration method based on the fuzzy inference technique:

1. A disturbance-decoupled adaptive observer – Adaptive Unknown Input Observer (AUIO) – is constructed so that, if certain measurement redundancy requirement is satisfied, the estimation of fault is not affected by existing disturbance and other occurring faults. This is an excellent characteristic especially in a situation where the interacting faults may spoil the estimation of others. As shown in Chapter 6, three leaking faults in the hydraulic system are

interacting with each other so that false estimation might occur. To eliminate the effect of these false estimation on others, the dynamics and the faults in the hydraulic system are taken as disturbance to the AUIO in Chapter 4 so that the accurate estimations can be obtained;

2. Unitary System is defined as a system whose singular values of transfer function matrix are all equal. The method of constructing a closed-loop unitary system is developed. The benefit of a unitary system is that, for a fault detection system whose inputs are faults and outputs are residuals, all faults will appear in the residuals with the same intensity since, for different inputs with the same magnitude, the magnitude of the outputs is the same for a unitary system.

3. An H_∞/H_- adaptive observer is constructed based on the H_∞/H_- optimization, which is an integrated optimization of seeking the balanced robustness and sensitivity. In this thesis, the H_∞/H_- optimization for strictly proper systems, whose solution is not available before, is solved with Unitary System technique;

4. The controller design and reconfiguration methods based on fuzzy TS model are developed. Controller reconfiguration, performance degradation, and reference reconfiguration are not new concepts. However, to the best knowledge of the author, it is the first time all of these are considered in the framework of a single fuzzy inference system.

8.2 Future Work

The research in this thesis, which mainly focused on the fault detection and estimation component of AFTC, can be extended in the following areas:

1. Fault estimation with nonlinear adaptive observers. It is necessary to develop nonlinear adaptive observers since nonlinearity exists in most systems. Even for a linear system, nonlinear adaptive observers are required for the accurate estimation if certain information of the system, for example the signal matrix ϕ, is not available. In this thesis, the signal matrix ϕ consists of functions of known signals such as u and y so that the elements in ϕ are all known. In the case where a part of ϕ is unknown, the dynamics of the system becomes bilinear in ϕ and θ. A nonlinear adaptive observer is thus required for the estimation of θ. Although, for a system in certain forms, an extended Lungberger observer or extended Kalman filter can be applied for the parameter estimation, the disturbance rejection capability is to be investigated;

2. Unitary System. In this thesis, a closed-loop unitary system was constructed in a weighted observer form with static output feedback. The singular values of the closed-loop unitary system are equal to the magnitude response of a first order transfer function. With a dynamic output feedback, the singular values of a closed-loop unitary system might be assigned in a more complicated form such as the magnitude response of a second order transfer function. Moreover, the non-

singular requirement on CB of constructing a closed-loop unitary system needs to be relaxed.

REFERENCES

[1]. R. Isermann and P. Ball'e, "Trends in the application of model-based fault detection and diagnosis of technical processes", *Control Engineering Practice,* vol. 5, no. 5, pp. 709–719, 1997.

[2]. http://www.ntsb.gov/publictn/2004/AAR0401.pdf

[3]. Y. M. Zhang and J. Jiang, "Bibliographical review on reconfigurable fault-tolerant control systems", *Annual Reviews in Control*, vol. 32, pp. 229-252, Dec. 2008.

[4]. Y. M. Zhang and J. Jiang, "Fault tolerant control system design with explicit consideration of performance degradation", *IEEE Transactions on Aerospace and Electronic Systems,* vol. 39, pp. 838-848, Jul 2003.

[5]. V. Venkatasubramanian, R. Rengaswamy, K. Yin and S.N. Kavuri, "A review of process fault detection and diagnosis part I: quantitative model-based methods", *Computers and Chemical Engineering*, vol. 27, pp. 293-311, 2003.

[6]. V. Venkatasubramanian, R. Rengaswamy, K. Yin and S.N. Kavuri, "A review of process fault detection and diagnosis part II: qualitative models and search strategies", *Computers and Chemical Engineering*, vol. 27, pp. 313-326, 2003.

[7]. V. Venkatasubramanian, R. Rengaswamy, K. Yin and S.N. Kavuri, "A review of process fault detection and diagnosis part III: process history based methods", *Computers and Chemical Engineering*, vol. 27, pp. 227-346, 2003.

[8]. S. Simani, C. Fantuzzi and R.J. Patton, *Model-Based Fault Diagnosis in Dynamic Systems Using Identification Techniques*, Springer-Verlag, 2002.

[9]. S. Cholakkal, and X. Chen, "Fault tolerant control of electric power steering using kalman filter-simulation study", *Proceedings of 2009 IEEE International Conference on Electro/Information Technology*, pp. 128-133, 2009.

[10]. L. An, "Actuator leakage fault detection and isolation based on extended Kalman filtering scheme", *Ph.d thesis*, The University of Manitoba, 2006.

[11]. M. Sepasi and F. Sassani, "On-line fault diagnosis of hydraulic systems using Unscented Kalman Filter", *International Journal of Control Automation and Systems*, vol. 8, pp. 149-156, Feb 2010.

[12]. A. Saberi, A. Stoorvogel, P. Sannuti and H. Niemann, "Fundamental problems in fault detection and identification", *International Journal of Robust Nonlinear Control*, vol. 10, pp. 1209-1236, 2000.

[13]. H. Khan, S. C. Abou, and N. Sepehri, "Nonlinear observer-based fault detection technique for electro-hydraulic servo-positioning systems", *Mechatronics*, vol. 15, pp. 1037-1059, Nov. 2005.

[14]. R. Isermann, "Supervision, fault detection and fault diagnosis methods: an introduction", *Control Engineering Practice*, vol. 5, no. 5, pp. 639-652, 1997.

[15]. D. Yu, "Fault diagnosis for a hydraulic drive system using a parameter-estimation method", *Control Engineering Practice,* vol. 5, pp. 1283-1291, Sep. 1997.

[16]. R. Isermann, "Fault diagnosis of machines via parameter estimation and knowledge processing – tutorial paper", *Automatica*, vol. 29, no. 4, pp. 815-835, 1993.

[17]. Q. Zhang, "A new residual generation and evaluation method for detection and isolation of faults in nonlinear systems", *International Journal Adaptive Control and Signal Processing*, vol. 14, pp. 759-773, 2000.

[18]. H. Wang, Z. J. Huang, and S. Daley, "On the use of adaptive updating rules for actuator and sensor fault diagnosis", *Automatica*, vol. 33, pp. 217-225, 1997.

[19]. B. Jiang, M. Staroswiecki, and V. Cocquempot, "Fault diagnosis based on adaptive observer for a class of non-linear systems with unknown parameters", *International Journal of Control*, vol. 77, no. 4, pp. 415-426, 2004.

[20]. B. Jiang, M. Staroswiecki, "Adaptive observer design for robust fault estimation", *International Journal of Systems Science*, vol. 33, no. 9, pp. 767-775, 2002.

[21]. P. Garimella and B. Yao, "Model based fault detection of an electro-hydraulic cylinder", *ACC: Proceedings of the 2005 American Control Conference,* vols 1-7, pp. 484-489, 2005.

[22]. D. Wang and K. Y. Lum, "Adaptive Unknown Input Observer approach for aircraft actuator fault detection and isolation", *International Journal of Adaptive Control and Signal Processing*, vol. 21, pp. 31-48, 2007.

[23]. K. S. Narendra and A. M. Annaswam, *Stable Adaptive Systems*, Prentice Hall, New Jersey, 1989.

[24]. P. A. Ioannou and J. Sun, *Robust Adaptive Control*. Prentice Hall: New Jersey, 1996.

[25]. Q. Zhang, "Adaptive observer for Multiple-Input–Multiple-Output (MIMO) Linear Time-Varying systems", *IEEE Transactions on Automatic Control*, vol. 47, no. 3, pp. 525-529, 2002.

[26]. R. Marino and P. Tomei, "Global adaptive compensation of noises with unknown frequency", *39th IEEE Conference on Decision and Control*: Sydney, Australia, Dec. 2000.

[27]. G. R. Duan and R. J. Patton, "Robust fault detection using Luenberger-type Unknown Input Observers: a parametric approach", *International Journal of Systems Science*, vol. 32, no. 4, pp. 533- 540, 2001.

[28]. R. J. Patton and J. Chen, "On Eigenstructure Assignment for robust fault diagnosis", *International Journal of Robust Nonlinear Control*, vol. 10, pp. 1193-1208, 2000.

[29]. R. J. Patton and J. Chen, "Robust fault detection of jet engine sensor systems using Eigenstructure Assignment", *Journal of Guidance, Control, and Dynamics*, vol. 15, no. 6, pp. 1491-1497, 1992.

[30]. R. K. Douglas, and J. L. Speyer, "Robust fault detection filter design", *Journal of Guidance, Control, and Dynamics*, vol. 19, no. 1, pp. 214-218, 1996.

[31]. Y. Xiong and M. Saif, "Robust fault detection and isolation via a diagnostic observer", *International Journal of Robust Nonlinear Control*, vol. 10, pp. 1175-1192, 2000.

[32]. S. X. Ding, T. Jeinsch, P. M. Frank and E. L. Ding, "A unified approach to the optimization of fault detection systems", *International Journal of Adaptive Control and Signal Processing*, vol. 14, pp. 725-745, 2000.

[33]. E. G. Collins Jr. and T. L. Song, "Robust H_∞ estimation and fault detection of uncertain dynamic systems", *Journal of Guidance, Control, and Dynamics*, vol. 23, no. 5, pp. 857-864, 2000.

[34]. R. K. Douglas and J. L. Speyer, "H_∞ bounded fault detection filter", *Journal of Guidance, Control, and Dynamics*, vol. 22, no. 1, pp. 129-138, 1999.

[35]. S. Ibaraki, S. Suryanarayanan, and M. Tomizuka, "Design of Luenberger state observers using fixed-structure H_∞ optimization and its application to fault detection in lane-keeping control of automated vehicles", *IEEE/ASME Transactions on Mechatronics*, vol. 10, no. 1, pp. 34-42, 2005.

[36]. T. D. Curry and E. G. Collins Jr., "Robust fault detection and isolation using robust L_1 estimation", *Journal of Guidance, Control, and Dynamics*, vol. 28, no. 6, pp. 1131-1139, 2005.

[37]. D. Henry and A. Zolghadri, "Design of fault diagnosis filters: a multi-objective approach", *Journal of the Franklin Institute*, vol. 342, pp. 421 - 446, 2005.

[38]. W. H. Chung, "Game theoretic and decentralized estimation", *Ph. D dissertation*, University of California, Los Angeles, 1997.

[39]. R. H. Chen and J. L. Speyer, "A generalized least-squares fault detection filter", *International Journal of Adaptive Control and Signal Processing*, vol. 14, pp. 747-757, 2000.

[40]. Z.Y. Zhao, W.F. Xie and H. Hong, "Hybrid optimization method of Evoltionary Parallel Gradient Search", accepted by *International Journal of Artificial Intelligence*, 2009.

[41]. W. H. Chung and J. L. Speyer, "A game theoretic fault detection filter", *IEEE Transactions on Automatic Control*, vol. 43, no. 2, pp. 143-161, 1997.

[42]. M. Hou and R. J. Patton, "An LMI approach to H_-/H_∞ fault detection observers", *the UKACC International Conference on Control* 1996, pp. 305-310.

[43]. J. L. Wang, G. H. Yang, and J. Liu, "An LMI approach to H_ index and mixed H_/H_∞ fault detection observer design", *Automatica,* vol. 43, pp. 1656-1665, Sep. 2007.

[44]. M. L. Rank and H. Niemann, "Norm based design of fault detectors", *International Journal of Control,* vol. 72, pp. 773-783, 1999.

[45]. M. L. Rank and H. Niemann, "Norm based threshold selection for fault detectors", *Proceedings of the 1998 American Control Conference, vols 1-6,* pp. 2027-2031, 1998.

[46]. D. Henry and A. Zolghadri, "Norm-based design of robust FDI schemes for uncertain systems under feedback control: Comparison of two approaches", *Control Engineering Practice,* vol. 14, pp. 1081-1097, Sep. 2006.

[47]. J. Chen, R. J. Patton, and G. P. Liu, "Optimal residual design for fault-diagnosis using multiobjective optimization and genetic algorithms", *International Journal of Systems Science,* vol. 27, pp. 567-576, 1996.

[48]. F. Rambeaux, F. Hamelin, and D. Sauter, "Optimal thresholding for robust fault detection of uncertain systems", *International Journal of Robust and Nonlinear Control,* vol. 10, pp. 1155-1173, 2000.

[49]. I. M. Jaimoukha, Z. Li, and V. Papakos, "A matrix factorization solution to the H_/H_∞ fault detection problem", *Automatica,* vol. 42, pp. 1907-1912, Nov 2006.

[50]. K. Zhou, J. C. Doyle, and K. Glover, *Robust and Optimal Control*. Upper Saddle River, N.J.: Prentice Hall International, 1996.

[51]. D. Simon, *Optimal State Estimation : Kalman, H Infinity, and Nonlinear Approaches*. Hoboken, N.J. Wiley, 2006.

[52]. Y. M. Zhang and J. Jiang, "Active Fault-Tolerant Control System against partial actuator failures", *IEEE Transactions on Automatic Control*, vol. 49, no. 8, pp. 95-104, 2004.

[53]. M. Maki, J. Jiang and K. Hagino, "A stability guaranteed Active Fault-Tolerant Control System against actuator failures", *International Journal of Robust Nonlinear Control*, vol. 14, pp. 1061–1077, 2004.

[54]. F. Tao and Q. Zhao, "Design of stochastic fault tolerant control for H_2 performance", *International Journal of Robust Nonlinear Control*, vol. 17, pp. 1–24, 2007.

[55]. P. Mhaskar, A. Gani and P. D. Christofides, "Fault-tolerant control of nonlinear processes: performance-based reconfiguration and robustness", *International Journal of Robust Nonlinear Control*, vol. 16, pp. 91–111, 2006.

[56]. M. Karenko and N. Sepehri, "Fault-tolerant control of a servohydraulic positioning system with crossport leakage", *IEEE Transactions on Control Systems Technology*, vol. 13, pp. 155-121, 2005.

[57]. X. Zhang, T. Parisini and M. M. Polycarpou, "Adaptive fault-tolerant control of nonlinear uncertain systems: an information-based diagnostic approach", *IEEE Transactions on Automatic Control*, vol. 49, no. 8, pp. 1259-1274, 2004.

[58]. D. Ye and G. Yang, "Adaptive fault-tolerant tracking control against actuator faults with application to flight control", *IEEE Transactions on Control Systems Technology*, vol. 14, no. 6, pp. 1088-1096, Nov. 2006.

[59]. Z. Gao and P. Antsaklis, "On the stability of the Pseudo-Inverse method for reconfigurable control systems", *Proceedings of the IEEE 1989 National Aerospace and Electronics Conference*, pp. 333 – 337, 1989.

[60]. J. Jiang, "Design of reconfigurable control systems using Eigenstructure Assignments", *International Journal of Control*, vol. 59, pp. 395 - 410, 1994.

[61]. A. E. Ashari, A. K. Sedigh and M. J. Yazdanpanah, "Reconfigurable control system design using Eigenstructure Assignment: static, dynamic and robust approaches", *International Journal of Control*, vol. 78, no. 13, pp. 1005 - 1016, 2005.

[62]. K. S. Kim, K. J. Lee and Y. Kim, "Reconfigurable flight control system design using direct adaptive method", *Journal of Guidance, Control, and Dynamics*, vol. 26, no. 4, pp. 543-550, 2003.

[63]. L. F. Mendonc, S. M. Vieira, J. M. C. Sousa, J.M.C. and J. M. G. S´a da Costa, "Fault accommodation using fuzzy predictive control", *IEEE International Conference on Fuzzy Systems*, Vancouver, Canada, July 16-21, 2006.

[64]. J. Prakash, S. Narasimhan and S. C. Patwardhan, "Integrating model based fault diagnosis with model predictive control", *Industrial and Engineering Chemistry Research*, vol. 44, no. 12, pp. 4344-4360, 2001.

[65]. K. Astrom, P. Albertos, M. Blanke, A. Isidori, W. Schaufelberger and R. Sanz, *Control of Complex Systems*, Springer Verlag, 2001.

[66]. Y. M. Zhang and J. Jiang, "Integrated active fault-tolerant control using IMM approach", *IEEE Transactions on Aerospace and Electronic Systems*, vol. 37, no. 4, pp. 1221-1235, Oct. 2001.

[67]. H. N. Wu and M. Z. Bai, "Active fault-tolerant fuzzy control design of nonlinear model tracking with application to chaotic systems", *IET Control Theory and Application*, vol. 3, iss. 6, pp. 642 - 653, 2009.

[68]. H. N. Wu and M. Z. Bai, "H∞ fuzzy tracking control design for nonlinear Active Fault Tolerant Control Systems", *Journal of Dynamic Systems, Measurement, and Control*, vol. 130, 2008.

[69]. K. Zhang, B. Jiang, and M. Staroswiecki, "Dynamic output feedback fault tolerant controller design for Takagi–Sugeno fuzzy systems with actuator faults", *IEEE Transactions on Fuzzy Systems*, vol. 18, no. 1, Feb. 2010.

[70]. L. A. Zadeh, "Fuzzy sets", *Information and Control*, vol. 8, pp. 338-353, 1965.

[71]. L. A. Zadeh, "Fuzzy algorithms", *Information and Control*, vol. 12, pp. 94-102, 1968.

[72]. Z.Y. Zhao, W.F. Xie and H. Hong, "A fuzzy optimal controller for the mechatronic system with non-smooth nonlinearities", *International Journal of Advanced Mechatronic System*, vol. 1, no. 2, pp, 90-99, 2008.

[73]. Z.Y. Zhao, W.F. Xie and W.H. Zhu, "Fuzzy optimal control for harmonic drive system with friction variation with temperature", *Proceedings of IEEE International Conference on Mechatronics and Automation*, Harbin, China, Aug. 5-8, 2007.

[74]. Thales Avionics Canada Inc. *TPC_FBW_02_100A.mdl.*

[75]. Boeing 767 Systems Review – SmartCockpit.com, http://www.smartcockpit.com/data/pdfs/plane/boeing/B767/instructor/B767_Flight_Controls.pdf.

[76]. C. M. Close, D. K. Frederick, and J. C. Newell, *Modeling and Analysis of Dynamic Systems*, 3rd ed. New York: Wiley, 2002.

[77]. H. E. Merritt, *Hydraulic Control Systems*. New York , Chichester, Wiley, 1967.

[78]. Z.Y. Zhao, W. F. Xie, and H. Hong, "A disturbance decoupled adaptive observer and its application to faulty parameters estimation of a hydraulic driven elevator", *Proceedings of 2009 7th Asian Control Conference*, pp: 1120-1125, 2009.

[79]. Z.Y. Zhao, W. F. Xie, and H. Hong, "A disturbance decoupled adaptive observer and its application to faulty parameters estimation of a hydraulic driven elevator", submitted to *International Journal of Adaptive Control and Signal Processing*.

[80]. W. J. Rugh, *Linear System Theory*, Prentice Hall: New Jersey, 1996.

[81]. O. Gasparyan, *Linear and Nonlinear Multivariable Feedback Control : A Classical Approach*. Chichester, England ; Hoboken, NJ: Wiley, 2008.

[82]. D. S. Bernstein, *Matrix Mathematics : Theory, Facts, and Formulas*, 2nd ed. Princeton, NJ: Princeton University Press, 2009.

[83]. A. K. Sinha, *Linear Systems : Optimal and Robust Control*. Boca Raton: CRC Press, 2007.

[84]. A.G.J. MacFarlane and Y.S. Hung, "Analytic properties of the singular values of a rational matrix", *International Journal of Control*, vol. 37 pp. 221-234, 1983.

[85]. S. Boyd and V. Balakrishnan, "A regularity result for the singular values of a transfer matrix and a quadratically convergent algorithm for computing its L – norm", *System & Control Letters*, vol. 15, pp. 1-7, 1990.

[86]. Z. Y. Zhao, W. F. Xie, and H. Hong, "A Unitary System approach to the H∞/H_ optimization for fault detection observer design", submitted to *IEEE Transactions on Automatic Control.*

[87]. H. H. Rosenbrock, *State-Space and Multivariable Theory.* London: Nelson, 1970.

[88]. B. Kosko, "Fuzzy systems as universal approximators", *IEEE Transaction on Computers*, vol. 43, no. 11, pp. 1329-1334, 1994.

[89]. Z.Y. Zhao, W.F. Xie and H. Hong, "Identification of fuzzy Takagi-Sugeno (TS) model with Evolutionary Parallel Gradient Search", *Proceedings of North American Fuzzy Information Processing Society (NAFIPS 08) Conference 2008*, New York, USA, May 20 -22, 2008.

[90]. W.F. Xie, Y.Q. Zhu, Z.Y. Zhao and Y.K. Wong, "Nonlinear system identification using optimized dynamic Neural Network", *Neurocomputing*, vol. 72, iss. 13-15, pp. 3277-3287, Aug. 2009.

[91]. T. Takagi and M. Sugeno, "fuzzy identification of systems and its applications to modeling and control", *IEEE Transaction on System, Man,* and *Cyber*netics, vol. 15, pp. 116_132, 1985.

[92]. K. Tanaka and H. O. Wang, *Fuzzy Control Systems Design and Analysis*, New York, Wiley, 2001.

[93]. S. Boyd, L. El Ghaoui, E. Feron and V. Balakrishnan, "Linear Matrix Inequalities in system and control theory", *SIAM Studies in Applied Mathematics,* vol. 15, SIAM, Philadelphia, 1994.

[94]. PENOPT solver, http://www.penopt.com/

[95]. Y. Cao, J. Lam, and Y. Sun, "Static output feedback stabilization: an ILMI approach", *Automatica*, vol. 34, no. 12, pp. 1641-1645, 1998.

APPENDIX A

THE ILMI ALGORITHM

This appendix solves the following matrix inequality with Iterative Linear Matrix Inequality (ILMI) algorithm [95]:

$$P\left(A_i + BK_iC\right) + \left(A_i + BK_iC\right)^T P \le -2\gamma P \tag{A - 1}$$

$$P = P^T > 0 \tag{A - 2}$$

where $i = 1 \ldots n_r$.

The ILMI algorithm

Step 0. Select $Q > 0$, and solve P^o from the following Riccati equation:

$$A_1 P + PA_1^T - PBB^T P + Q = 0. \tag{A - 3}$$

Set $k = 1$ and $X^1 = P^o$.

Step 2. Minimize α subject to n_r following LMI constraints:

$$\begin{bmatrix} P^k A_i + A_i^T P^k - X^k BB^T P^k - P^k BB^T X^k \\ + X^k BB^T X^k - 2rP^k - \alpha P^k & \left(P^k B + C^T K_i^T\right) \\ \left(B^T P^k + K_i C\right) & -I \end{bmatrix} \le 0, \tag{A - 4}$$

and

$$P^k = \left(P^k\right)^T > 0 \tag{A - 5}$$

Denote α^k as the minimized value of α.

Step 3. If $\alpha^k \leq 0$, the solution is found as K_i for $i = 1 \ldots n_r$. Stop.

Step 4. Solve the following optimization problem for P^k and K_i

Op2: Minimize the $trace\left(P^k\right)$ subject to (A - 4) and (A - 5) with $\alpha = \alpha^k$. Denote P^* as the optimal value of P^k.

Step 5. If $\left\|X^k - P^*\right\| < \delta$, where δ is a predefined small constant of tolerance, then go to Step 6. Otherwise, set $k = k+1$ and $X^k = P^*$, then go to Step 2.

Step 6. The algorithm cannot find a solution. Stop.

APPENDIX B

MEMBERSHIP FUNCTIONS

1. Membership functions in the fuzzy TS model of the fault-free elevator

The premise variable of the fault-free elevator is

$$v = \begin{bmatrix} x_{3L} - x_{4L} \\ x_{5L} \\ x_{3R} - x_{4R} \\ x_{5R} \end{bmatrix}.$$

For each variable in v, there are two rules. The membership function regarding $(x_3 - x_4)$ and x_5 are shown in figures B.1 and B.2 respectively.

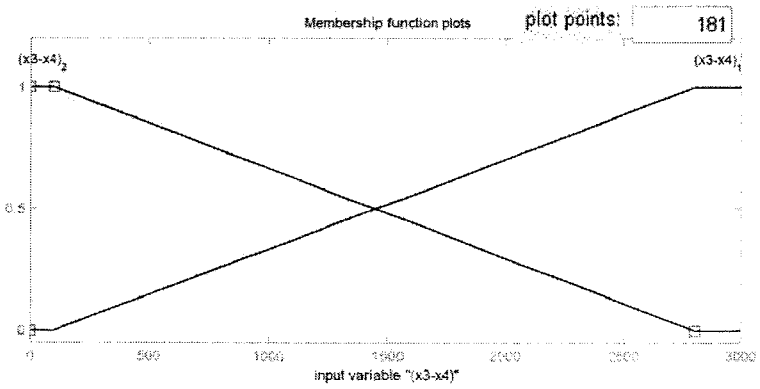

Figure B.1 Membership funcion of $(x_3 - x_4)$

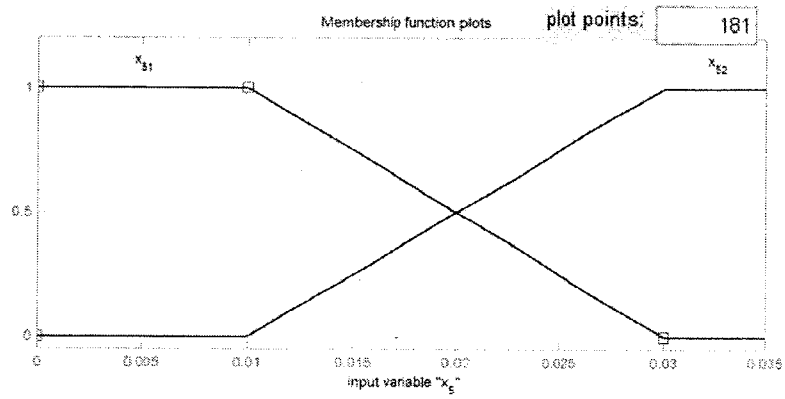

Figure B.2 Membership funcion of x_5

2. Membership functions in the fuzzy TS model of the fault elevator

Although 5 faults are considered in the ATFC simulation, there are no fuzzy rules for the two leaking faults to environment, C_{1L} and C_{2L}, since the corresponding actions to these faults are to shut down the left subsystem. Therefore the premise variables are

$$\theta = \begin{bmatrix} k_{vL} \\ H_m \\ C_{12L} \end{bmatrix}.$$

For each variable in θ, there are two rules. Their membership functions are shown in figures B.3 – B.5.

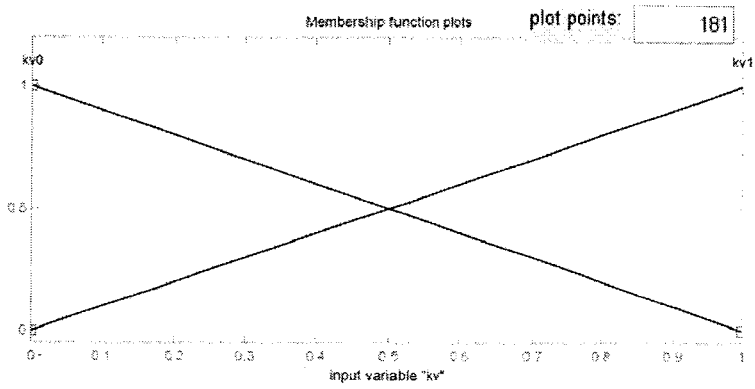

Figure B.3 Membership funcion of k_{vL}

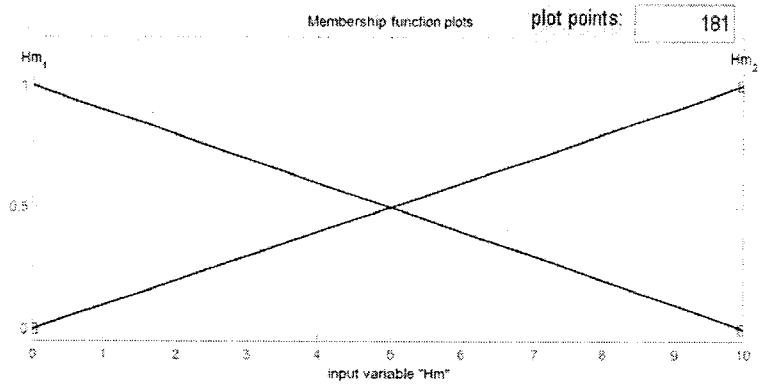

Figure B.4 Membership of H_m

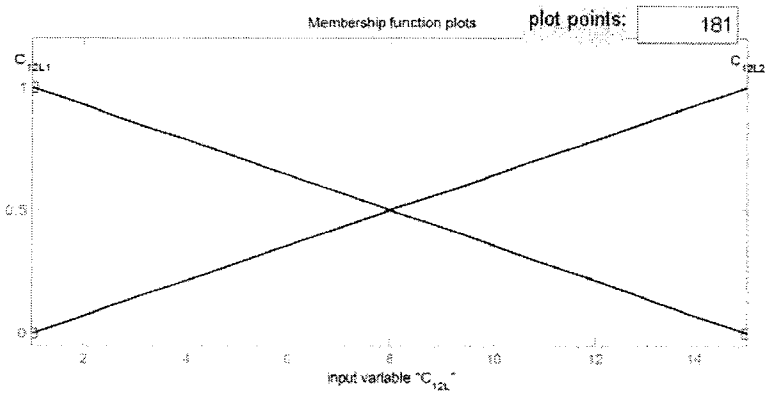

Figure B. 5 Membership of C_{12L}

APPENDIX C

LINEAR MODEL OF THE ELEVATOR

1. The program of constructing linear models:

```
%% Fuzzy model - nonlinear: linearized at (Xv, P_12) %%
%%

clear;

m=7.88e-3;     % Piston mass       - m
Ap=3.623;      % Piston area       - Ap
b=9.27;        % piston damping    - b
omega=817;     % Valve frequency   - omega
zeta=0.8;      % Valve damping     - zeta
k=omega^2*0.00337; % Valve gain - equaivelent    - kv*omega^2
beta=1e5;          % Volumn modulus - oil        - Beta
cl=3.208e-4;       % Valve flow coefficient      - C1
V=4.1;             % Cylinder chamber volumn - null position
As=250000;         % Stiffness - Piston          - Ks

J_of_surf=15/2;    % Inertia - elevator panel    - Js
B_of_surf=82;      % Damping - elevator panel    - Bs
l_of_arm=2.924;    % Leverage length - elevator panel  - l
Ps=500000;         % Stiffness - elevator panel        - Kps
HM=300;            % Hinge stiffness           - Hm
C_v=0.338/0.035;

P_sup=3000;
P_rev=50;
xv=[0.01 0.03];
P1_P2=[100 2800];

for i=1:2
    for j=1:2
        K_f=C_v*sqrt(P_sup-P1_P2(j));
        K_p=C_v/2/sqrt(Ps-P1_P2(j))*xv(i);
        K_leak=cl;
        K_tp=K_p+K_leak;

        denum=conv([m b As],[V beta*K_tp]);
        n_order=length(denum);
        denum(n_order-1)=denum(n_order-1)+1*beta*Ap^2;
        num=beta*Ap*K_f;

        sys_x5_2_x2=tf(num,denum);
        sys_x8_2_x2=tf([As*l_of_arm],[m b As]);
        sys_x5_x8_2_x2=[sys_x5_2_x2 sys_x8_2_x2];

        sys_L_1=ss(sys_x5_x8_2_x2);
```

```
n=size(sys_L_1.a,1);
sys_L=sys_L_1;


A_LL=[sys_L.a sys_L.b(:,1)*1 zeros(n,2) sys_L.b(:,2); ...
    zeros(1,n)   0         1        0         0 ; ...
    zeros(1,n)  -omega^2   -2*zeta*omega   0   0; ...
    As*l_of_arm*sys_L.c/J_of_surf 0   0  -B_of_surf/J_of_surf
-(As*l_of_arm^2+Ps+0.5*HM*57.29)/J_of_surf; ...
    zeros(1,n)         0         0         1         0];
A_RR=A_LL;
A_LR=zeros(n+4,n+4);
A_LR(n+3,n+4)=(Ps-0.5*HM*57.29)/J_of_surf;
A_Lin=[A_LL A_LR; A_LR A_RR];

B_Lin=zeros(2*n+8,2);
B_Lin(n+2,1)=k;
B_Lin(2*n+6,2)=k;
B_L=B_Lin(1:n+4,1);
B_R=B_L;

C_Lin=zeros(2,2*n+8);
C_Lin(1,n+4)=1;
C_Lin(2,2*n+8)=1;
C_L=C_Lin(1,1:n+4);
C_R=C_L;

C_Lin_Ps=zeros(2,2*n+8);
C_Lin_Ps(1,1:5)=sys_L.c;
C_Lin_Ps(2,10:14)=sys_L.c;

C_Lin_Xv=zeros(2,2*n+8);
C_Lin_Xv(1,6)=1;
C_Lin_Xv(2,15)=1;


A_LL_I=zeros(n+5,n+5);
A_LL_I(n+5,n+4)=1;
A_LL_I(1:n+4,1:n+4)=A_LL;
A_RR_I=A_LL_I;
A_LR_I=zeros(n+5,n+5);
A_LR_I(1:n+4,1:n+4)=A_LR;

A_I=[A_LL_I A_LR_I;A_LR_I A_RR_I];

B_I=zeros(2*n+10,2);
B_I(n+2,1)=k;
B_I(2*n+6+1,2)=k;

B_L_I=B_I(1:n+5,1);
B_R_I=B_L_I;

C_I=zeros(4, 2*n+10);
```

```
        C_I(1:2,9:10)=eye(2);
        C_I(3:4,19:20)=eye(2);
        C_L_I=C_I(1:2,1:n+5);
        C_R_I=C_L_I;

        A{(i-1)*2+j}=A_I;
        B{(i-1)*2+j}=B_I;
        C{(i-1)*2+j}=C_I;

    end
end
```

2. The linear model linearized at
$\left(x_{3L}-x_{4L},\quad x_{5L}\quad x_{3R}-x_{4R}\quad x_{5R}\right)_o=\left(100\quad 0.01\quad 100\quad 0.01\right)$:

```
A{1}=
[-1185.88601571233,-8833.63769554799,-
143.566661468527,0,0,64,0,0,0,0,0,0,0,0,0,0,0,0,0,0;
    8192,0,0,0,0,0,0,0,0,0,0,0,0,0,0,0,0,0,0,0;
    0,256,0,0,0,0,0,0,0,0,0,0,0,0,0,0,0,0,0,0;
    0,0,0,-1176.39593908629,-
7745.57820431472,0,0,0,128,0,0,0,0,0,0,0,0,0,0,0;
    0,0,0,4096,0,0,0,0,0,0,0,0,0,0,0,0,0,0,0,0;
    0,0,0,0,0,0,1,0,0,0,0,0,0,0,0,0,0,0,0,0;
    0,0,0,0,0,-667489,-1307.20,0,0,0,0,0,0,0,0,0,0,0,0,0;
    0,0,4234987.62225222,0,17245562.1451492,0,0,-10.9333333333333,-
352805,0,0,0,0,0,0,0,0,0,0,65520.8666666667,0;
    0,0,0,0,0,0,0,0,1,0,0,0,0,0,0,0,0,0,0,0;
    0,0,0,0,0,0,0,0,1,0,0,0,0,0,0,0,0,0,0,0;
    0,0,0,0,0,0,0,0,0,0,-1185.88601571233,-8833.63769554799,-
143.566661468527,0,0,64,0,0,0,0;
    0,0,0,0,0,0,0,0,0,0,8192,0,0,0,0,0,0,0,0,0;
    0,0,0,0,0,0,0,0,0,0,0,256,0,0,0,0,0,0,0,0;
    0,0,0,0,0,0,0,0,0,0,0,0,0,-1176.39593908629,-
7745.57820431472,0,0,0,128,0;
    0,0,0,0,0,0,0,0,0,0,0,0,0,4096,0,0,0,0,0,0;
    0,0,0,0,0,0,0,0,0,0,0,0,0,0,0,0,0,1,0,0;
    0,0,0,0,0,0,0,0,0,0,0,0,0,0,0,0,-667489,-1307.20000000000,0,0,0;
0,0,0,0,0,0,0,0,65520.8666666667,0,0,0,4234987.62225222,0,17245562.1451
492,0,0,-10.9333333333333,-352805,0;
    0,0,0,0,0,0,0,0,0,0,0,0,0,0,0,0,0,0,1,0,0;
    0,0,0,0,0,0,0,0,0,0,0,0,0,0,0,0,0,0,0,1,0;]


B{1}
=[0,0;
  0,0;
  0,0;
  0,0;
  0,0;
  0,0;
  2249.43793000000,0;
  0,0;
```

```
  0,0;
  0,0;
  0,0;
  0,0;
  0,0;
  0,0;
  0,0;
  0,0;
  0,2249.43793000000;
  0,0;
  0,0;
  0,0;]


C{1}
=[0,0,0,0,0,0,0,0,1,0,0,0,0,0,0,0,0,0,0,0;
  0,0,0,0,0,0,0,0,0,1,0,0,0,0,0,0,0,0,0,0;
  0,0,0,0,0,0,0,0,0,0,0,0,0,0,0,0,0,1,0;
  0,0,0,0,0,0,0,0,0,0,0,0,0,0,0,0,0,0,1;]
```